Serotonergic Modulation and its Influence on Signal Processing at Cellular Level in Deep Cerebellar Nuclei Neurons

Dissertation

Zur Erlangung des Grades eines Doktors
der Naturwissenschaften

der Fakultät für Biologie
und
der Medizinischen Fakultät
der Eberhard-Karls-Universität Tübingen

presented by

Meng-Larn Lee

from Nantou, Taiwan

11-2006

Tag der mündlichen Prüfung:	23 - 03 - 2007
Dekan der Fakultät für Biologie:	Prof. Dr. F. Schöffl
Dekan der Medizinischen Fakultät:	Prof. Dr. I.B. Autenrieth
1. Berichterstatter:	Prof. Dr. H.P. Thier.
2. Berichterstatter:	Prof. Dr. B. Antkowiak
Prüfungskommission:	Prof. Dr. H.P. Thier
	Prof. Dr. B. Antkowiak
	Prof. Dr. E. Günther
	Prof. Dr. U. Ilg
	Prof. Dr. W. Schmidt

Contents

Abbrievation

5-HT	serotonin (5-hydroxytryptamine)
BK	big conductance calcium-dependent potassium current
DCN	deep cerebellar nuclei
GABA	γ-aminobutyric acid
EPSC	excitatory postsynaptic current
IPSC	inhibitory postsynaptic current
STA	spike trigger average

I declare that I have produced the work entitled "**Serotonergic Modulation and Its Influence on Signal Processing at Cellular Level in Deep Cerebellar Nuclei Neurons**", submitted for the award of a doctorate, on my own (without external help), have used only the sourced and aids indicated and have marked passages included from other works, whether verbatim or in content, as such. I swear upon oath that these statements are true and that I have not concealed anything. I am aware that making a false declaration under oath is punished by a term of imprisonment of up to three years or by a fine.

Meng-Larn Lee

30 Nov, Tübingen

Abstract

Deep cerebellar nuclei (DCN) neurons generate the final output of cerebellum and receive abundant modulatory serotonergic inputs from brainstem neurons. The aim of this present study was to elucidate the influence of serotonin on signal processing performed by DCN neurons. Since signal processing is determined by the interplay between intrinsic and synaptic properties, the impact of serotonin on intrinsic as well as synaptic properties was investigated. To this end whole-cell patch clamp recordings were performed in rat cerebellar slices.

Serotonin caused a persistent membrane depolarization at current clamp recordings, which was mediated by an increase of tonic cationic currents and a concomitant decrease of tonic potassium currents. At the same time, serotonin influenced the waveform of action potentials that showed a reduced depolarization slope and peak amplitude, both indicating a reduced availability of voltage-gated sodium channels. However, serotonin showed a complicated effect at dynamic clamp recordings where the neuronal response depended on the average activity level before drug application. Spike rate was reduced by serotonin for depolarized high activity states and unaltered or slightly increased for hyperpolarized low activity states. The spike timing precision was not altered, showing that the response of DCN neurons to input transients was not affected by serotonin. The overall synaptic shunting level of the simulated synaptic inputs had also an impact as it shifted the degree of depolarization induced by serotonin. Therefore, the effect of serotonin on DCN activity was influenced twofold by background synaptic activity, first via its impact on the mean activity level and second via its shunting strength.

Due to the functional relevance of inhibitory transmission between Purkinje cells and DCN neurons, its modulation by serotonin was the second focus of this study. Two previous studies have described frequency dependent short-term depression of this synapse in response to repetitive activation with multiple spike trains. Using dynamic clamp in the present study revealed that short-term depression might stabilize the membrane potential close to the activation threshold thereby significantly extended the working range of DCN neurons into regimes of high inhibitory input activity. Short-term depression did not change spike timing precision showing that responses to input transients were unaltered. Serotonin

reduced the amplitude of evoked inhibitory postsynaptic currents potentially by reducing the release probability of presynaptic $GABA_A$ vesicles. However, short-term depression was not altered by serotonin at all tested frequencies, neither for the initial nor the steady-state phase. The time course of recovery from depression was not influenced by serotonin either.

Overall these results indicate that serotonin altered the input-output transfer function of DCN neurons. Therefore, serotonin might act in concert with short-term depression as a high-pass filter, making the response of DCN neurons less dependent on the mean level of inhibitory input while retaining their sensitivity to transient changes in input activity and synchronized input.

1. Introduction

The signal processing performed by a nervous system like the mammalian brain is determined by its network connectivity and by the properties of its neurons, especially their intrinsic and their synaptic properties. These properties are often plastic, a term by which we refer to the well known fact that they can be altered either in response to their own activation history or in response to a particular class of modulating inputs. Those neuromodulatory inputs are found in all brain structures and one factor hampering our understanding of brain function is our limited knowledge about the effects of modulatory inputs on information processing. Due to the large diversity of neuron types and the corresponding diversity of modulating mechanisms there is no simple answer to the question how neuronal signal processing is altered by modulating inputs. Instead, this question has to be studied for each neuron type separately and the insights gained this way need to be combined in network models to arrive at a quantitative and mechanistically founded description of information processing.

The main question addressed in the present project is the modulation of signal processing in neurons of the deep cerebellar nuclei (DCN) by serotonin (5-hydroxytryptamine, 5-HT). To this end, whole cell patch-clamp recordings were performed in rat cerebellar slices. Current clamp and voltage clamp recordings were used to characterize the effects of 5-HT on intrinsic and synaptic properties. The impact of 5-HT on the signal processing by DCN neurons was studied using dynamic current clamp. In these experiments, DCN neurons were stimulated with simulated synaptic inputs that represented the activity of a large population of excitatory and inhibitory input neurons. This way the impact of background synaptic activity was taken into consideration, that recently has been shown to play an important role for the signal processing in many neuron types (Desai and Walcott, 2006; Reig et al., 2006; Crochet et al., 2005; Wolfart et al., 2005; Zsiros and Hestrin, 2005; Destexhe et al., 2003; Mitchell and Silver, 2003; Shu et al., 2003; Chance et al., 2002).

The results section is organized in two parts. In the first part, the effect of 5-HT on the intrinsic properties of DCN neurons and the resulting consequences for the processing of given synaptic inputs are addressed. In the second part, the effect of 5-HT on inhibitory postsynaptic currents and the impact of short-term synaptic plasticity on DCN activity were investigated (Fig. 1). The results presented here might contribute to a better understanding

of cerebellar signal processing as a whole if they are taken into consideration within the framework of large scale cerebellar network simulations.

In the following introduction I will provide some background information to enable readers not especially familiar with the topics addressed here to follow the present study. In the first part the connectivity and physiology of DCN neurons are addressed, that represent the output neurons of the whole cerebellum. The second part gives a brief overview about synaptic short-term plasticity that is relevant for the inhibitory synapses between Purkinje cells and DCN neurons. The third part reviews some recent findings about the functional relevance of background synaptic activity that turned out to be crucial in my dynamic clamp experiments. And the last part, number four, will provide an overview of the serotonergic system as far as it is related to the cerebellum.

Besides questions of basic scientific interest that represent the main focus of the present study, its results might also be of practical interest within the context of clinical studies that related the treatment of cerebellar ataxia to the cerebellar serotonergic system (Takei et al., 2005; Trouillas et al., 1997; Trouillas, 1993). In those studies, two agonists of 5-HT1_A receptors, tandospirone and buspirone, helped to reduce symptoms of some certain subtypes of cerebellar ataxia (Takei et al., 2005; Trouillas et al., 1997), and a precursor of 5-HT, L-5-HTP, had some value for the treatment of cerebellar ataxia (Trouillas, 1993). Knowing not only the mediating receptor subtypes but also their effects on signal processing might facilitate the success of goal-directed approaches in clinical therapy.

1.1. the Deep Cerebellar Nuclei (DCN)

DCN neurons integrate the excitatory input to the cerebellum that originates from various brain regions and inhibitory inputs that originates from the cerebellar cortex. The result of this processing represents the final output of the whole cerebellum. Despite the obvious relevance of the DCN for cerebellar information processing, their specific functional role is still under debate (Mauk, 1997). For example, the DCN have been viewed either as sequential locations for information storage or as active manipulators in motor learning behaviour, i.e. classically conditioned eyeblink response.

No matter what their specific role is, all signals that reach the cerebellum are finally processed within the DCN and transferred from there. Therefore, a better understanding of the signal processing within the DCN is likely to facilitate our understanding of cerebellar function in general.

1.1.1. intrinsic connection in cerebellar nuclei

The connectivity between the cerebellar nuclei, extra cerebellar brain regions and the cerebellar cortex is naturally crucial for the signal processing performed within the DCN. Based on gross anatomical criteria, cerebellar nuclei are divided into three regions: the dentate nucleus, the interposed nucleus (composed of emboliform and globose nuclei), and the fastigial nucleus (Fig. 2A). Each of these nuclei receives inputs from specific regions of the cerebellar cortex and project to specific brain areas related to motor function.

The dentate is the most lateral of all nuclei. It receives inputs from lateral cerebellar cortex and projects to motor, premotor and prefrontal cerebral cortical areas. The interposed, which is located between the dentate and the fastigial, receives inputs from paravermis and projects to lateral corticospinal and rubrospinal systems, controlling lateral descending motor systems. The fastigial, the most medial nucleus, receives inputs from midline cerebellar cortex and projects to cerebral cortex and brainstem regions, controlling medial descending motor systems (Ghez and Thach, 1991).

The DCN receive the majority of their synaptic input from Purkinje cells as suggested by quantitative electronmicrosopic studies of synapses. This $GABA_A$-type input accounts for ~ 70 % of all synapses in all three cerebellar nuclei for excitatory as well as inhibitory DCN neurons (Palkovits et al., 1977; De Zeeuw and Berrebi, 1995). This number illustrates already the dominant role of this inhibitory input in the control of DCN activity. Another ~16% of synapses are also GABAergic but do not originate from Purkinje cells. This input has been assigned to local inhibitory interneurons and to collaterals of inhibitory projection neurons (De Zeeuw and Berrebi, 1995). Besides inhibitory input, DCN receive excitatory input from climbing fibers and mossy fibers. Climbing fibers originate exclusively from the inferior olive. Mossy fibers in contrast originate from various brain regions including the spinal cord, the pontine nuclei that relay input from the cerebral cortex and several brain stem nuclei that receive input from spinal cord as well as higher brain centers including the cerebral cortex (Ghez and Thach, 1991). Altogether, these excitatory inputs contribute only about 10 % of all input synapses on DCN neurons (De Zeeuw and Berrebi, 1995).

1.1.2. properties of DCN neurons

Excitatory and inhibitory projecting neurons are diffusely distributed in DCN (De Zeeuw and Berrebi, 1995; Chen and Hillman, 1993; Batini et al., 1992). Excitatory glutamatergic DCN neurons have soma diameters between 15 and 25 μm and project to premotor areas

such as thalamus, red nucleus and other brainstem nuclei. Inhibitory GABAergic neurons have smaller soma diameter between 5 and 15 µm and project exclusively to the inferior olive (De Zeeuw and Berrebi, 1995; Batini et al., 1992). Small DCN neurons with diameters of about 5 µm are GABAergic as well as glycinergic and represent supposedly local inhibitory interneurons (Chen and Hillman, 1993; Chan-Palay, 1977). Despite some overlap between the soma sizes of these neuron types, soma size can serve as a first criterion to judge the projection type.

Three physiological properties of DCN neurons have been described in detail in the literature based on current clamp experiments because they are suspected to be of functional relevance. First, DCN neurons are continuously active *in vivo* (Aksenov et al., 2005; Holdefer et al., 2005; Rowland and Jaeger, 2005) despite ongoing inhibition from Purkinje cells, and are spontaneously active *in vitro* in the presence of synaptic blockers, indicating the existence of intrinsic pacemaking currents. Whether the continuous *in vivo* DCN activity is due to intrinsic depolarizing currents or due to a baseline of excitatory input or both is still unknown. Second, a depolarizing sag (Fig. 2C, bottom arrow) is developing after the onset of hyperpolarizing current injection. The hyperpolarization-activated inward rectifying I_h current is responsible for the sag (Aizeman and Linden, 1999). Third, a robust rebound depolarization accounted by T-type calcium current is elicited after the offset of hyperpolarizing current injection, often leading to a brief sodium spike burst and depolarization (Fig. 2C, upper arrow). Rebound depolarization can be induced by brief inhibitory inputs from Purkinje cells so that it provides the mechanism by which inhibitory Purkinje cells can drive postsynaptic excitation and calcium entry (Aizeman and Linden, 1999; Aizeman et al., 1998).

1.1.3. ionic currents in DCN neurons

As in almost all neurons, a fast TTX-sensitive sodium current is responsible for the generation of action potentials in DCN neurons (Raman et al., 2000). The action potential upstroke is in general dominated by the activation of sodium channels because potassium channels that contribute to the repolarization are activated with some delay. Therefore, it has been suggested that rate of depolarization of action potentials might serve as a reliable measure of the availability of voltage-gated sodium channels under experimental conditions where a direct measurement is not feasible (Azouz and Gray, 2000). Spike amplitude and threshold are also suggested as indicators of sodium channel availability (Miles et al., 2005;

Azouz and Gray, 2000). The action potential repolarization is mediated by several potassium currents. These currents comprise the ubiquitous rectified potassium current, an A-type potassium current, and a big-conductance calcium-activated potassium (BK) current (Sausbier et al., 2004; Kang et al., 2000). An interesting and functionally most likely important property of sodium channels is that only about 25% are available at the average membrane potentials of DCN neurons while the rest is already inactivated (Raman et al., 2000). Therefore, it is reasonable to assume that slight depolarization or hyperpolarization might have strong effects on DCN activity by altering the percentage of available sodium current.

What current type is responsible for the depolarizing drive that mediates spontaneous spiking activity of DCN neurons *in vitro*? Besides the voltage-gated currents just mentioned, DCN neurons have been reported to contain a persistent mixed cationic current with a reversal potential close to -34 mV. This current has been suggested to depolarize the membrane potential of DCN neurons during interspike intervals above spiking threshold (Raman et al., 2000). Together with an apamin-sensitive calcium dependent small conductance potassium current (SK), it results in a pacemaker activity that is responsible for the spontaneous *in vitro* spiking (Aizenman and Linden, 1999).

Blocking calcium currents with cobalt and thereby indirectly all calcium-dependent potassium channels abolished membrane potential repolarization and spiking completely (Raman et al., 2000). This illustrates the functional relevance of calcium-dependent potassium channels (BK, SK, and potentially others) for the ongoing activity of DCN neurons. Blocking only particular subsets of calcium-dependent potassium channels using BAPTA or apamin switched the spiking pattern of DCN neurons from regular firing to bursting (Aizenman and Linden, 1999), further illustrating the functional relevance of calcium-dependent potassium channels.

1.2. Synaptic Transmission

Information is transmitted between neurons via electrical or chemical synapses. The functional properties of chemical synapses are one crucial component for the processing of information in neuronal networks. This is illustrated by the fact that these properties are highly plastic meaning that the strength and duration of synaptic signal transduction depends in almost all synapses heavily on their activation history and on modulatory inputs that originate usually from other brain regions. The basic mechanisms of chemical synaptic transduction are standard textbook knowledge. Briefly, an action potential invading the presynaptic terminal triggers calcium entry into the terminal resulting in the fusion of neurotransmitter vesicles with the plasma membrane and subsequent transmitter release into the synaptic cleft. The released neurotransmitter molecules cross the synaptic cleft by diffusion, and bind to specific receptors on the membrane of the postsynaptic neuron. Depending on the nature of those receptors this results in a direct gating of ionotropic ion channels and a fast electric response and/or in a much slower response mediated via metabotropic receptors that influence the activity of various ion channels only indirectly via second messenger cascades. Each of the steps just described can be subject to modulation thereby altering the properties of synaptic transmission and subsequently information processing.

As just implied, two groups of ligand-gated transmitter receptors are distinguished, ionotropic and metabotropic. Ionotropic receptors are fast gating ion channels that alter their gating state in response to transmitter binding causing an alteration of the current flow across the postsynaptic membrane. This in turn results either in depolarization or hyperpolarization depending on the electric charge of the ions and the direction of flow. Metabotropic receptors act indirectly via second messenger cascades on the activity of ion channels. The targets of those signalling cascades can be transmitter-gated receptors but also intrinsic channels that are ion channels gated by voltage, calcium, and so forth or persistent channels that are permanently open. Furthermore, metabotropic receptors are not only located at the post-synaptic side of synapses but often also at the presynaptic side. Therefore, they can alter the properties of the transmission machinery on both sides of the synapse.

The most frequent neurotransmitters in the central nervous system are the amino acids GABA (γ-aminobutyric acid) and glutamate. Both act on ionotropic receptors. Glutamate causes postsynaptic depolarization via AMPA, NMDA, and kainate receptors. GABA

causes postsynaptic hyperpolarization binding to $GABA_A$ and $GABA_C$ receptors. However, metabotropic receptors are known for both transmitter molecules. For glutamate, 8 metabotropic receptors ($mGluR_{1-8}$) have been described, and for GABA one metabotropic receptor ($GABA_B$-R) is known. Despite these metabotropic effects glutamate and GABA are considered classical neurotransmitters because of the abundance of their ionotropic receptors within the central nervous system. Serotonin (5-HT), acetylcholine (ACh), noradrenaline (NA), dopamine (DA), and histamine (HA) in contrast are considered as neuromodulatory transmitter substances because they act either exclusively via metabotropic receptors within the central nervous system (NA, DA, HA) or metabotropic receptors outnumber ionotropic ones (5-HT, ACh). For 5-HT only one ($5\text{-}HT_3$) out of 15 receptor subtypes is ionotropic.

1.2.1. mechanism of short-term depression

As mentioned above, the strength of almost all synapses investigated so far is altered in a use-dependent fashion depending on their activation history. This phenomenon is referred to as synaptic plasticity. The strength of synapses can be increased (facilitation or potentiation), it can be decreased (depression) or complex mixed combinations of both might occur. Depending on the time scale of their development and duration, synaptic plasticity is classified as short-term (lasts from milliseconds to minutes) or long-term (lasts from hours to maybe a live time).

One question addressed in my thesis is whether 5-HT has an effect on the short-term depression that has been described for the synapse between Purkinje cells and DCN neurons (Peroarena and Schwarz, 2003; Telgkamp and Raman, 2002). Therefore, I will provide some background about short-term depression in the following. The exact molecular mechanisms underlying short-term plasticity, facilitation or depression, are not completely understood. Mostly presynaptic events are responsible for short-term plasticity in general. The calcium level within the presynaptic terminal, the so called residual calcium, is known as one of the most important factors (Zucker and Regehr, 2002). Changes in synaptic strength during trains of synaptic stimulation are primarily attributable to changes of the presynaptic calcium level. For example, changes of residual calcium were found to alter synaptic strength in rat cerebellar parallel-Purkinje synapses (Kreitzer and Regehr, 2000) and in rat neocortical neurons (Tsodyks and Markram, 1997). In the case of depression, postsynaptic events like receptor desensitization might contribute in some

synapses besides presynaptic events (Zucker and Regehr, 2002). On the presynaptic side, the number of vesicles at the release side might actually be reduced, depletion of the readily releasable pool (Zucker and Regehr, 2002; Brenowitz and Trussell, 2001), and/or the probability of vesicles of this pool to be released might be reduced (Malinina et al., 2005; Fuhrmann et al., 2004; Zucker and Regehr, 2002; Wu and Borst, 1999; Tsodyks and Markram, 1997). Fortunately for modelling purposes both cases are mathematically equivalent. These reductions are activity-dependent, meaning that higher synaptic stimulation frequencies result in stronger depression (Peroarena and Schwarz, 2003; Telgkamp and Raman, 2002; Wang and Kaczmarek, 1998; Tsodyks and Markram, 1997).

A reduction of stimulation frequency results in a recovery from depression. The molecular mechanisms underlying recovery are mostly unknown but the residual calcium level is also here crucial (Fuhrmann et al., 2004; Sakaba and Neher, 2001; Wang and Kaczmarek, 1998). An elevated presynaptic calcium level accelerated recovery from depression. This finding was supported *in vitro* at the calyx of held in rat medial nucleus of trapezoid body (MNTB), where calcium facilitated refilling of the depleted readily releasable vesicle pool. Calmodulin, a calcium binding protein, was identified as the calcium sensor there (Sakada and Neher, 2001). In the same structure of the mouse the presence of EGTA, a calcium chelator, blocked the replenishment of the readily releasable vesicle pool (Wang and Kaczmarek, 1998), confirming the role of residual calcium.

Not only the rate of depression but also that of recovery has been reported to increase with increasing synaptic stimulation frequencies (Sakaba and Neher, 2001; Wang and Kaczmarek, 1998). Also here, an increased presynaptic calcium level was important. Presynaptic calcium currents did not inactivate significantly in response to high frequency stimulation (Wang and Kaczmarek, 1998), and therefore an accumulation of presynaptic residual calcium was suggested as the most important parameter (Kreitzer and Regehr, 2000). However, such a calcium-dependence of recovery from depression might not be a general feature of all synapses as suggested by studies with conflicting results from different synapses. In rat cortical synapses replenishment did not depend on residual calcium *in vitro* (Wu and Borst, 1999). Furthermore, recovery from depression at the calyx of held was unchanged when calcium homeostasis was altered by adding fura-2, a calcium buffer (Weis et al., 1999). Impacts of neuromodulatory transmitters on recovery from depression have not been reported yet.

1.2.2. functional role of short-term depression

The functional role of short-term depression can be characterized as a temporal filter or a dynamic gain modulator within a mathematical framework of description (Chung et al., 2002; Chance et al., 1998; Abbott et al., 1997). In rat cortical neurons, short-term depression of excitatory transmission has been described as a dynamic, input-specific gain control mechanism that amplified the response of low frequency inputs in comparison to high frequency inputs (Abbott et al., 1997). Based on single cell modelling studies, it has been suggested that short-term depression might provide a mechanism to phase-shift in the input-output relation of neurons (Chance et al., 1998). Intracellular recordings performed *in vivo* in rats showed that short-term depression in excitatory inputs to thalamocortical synapses contributed to sensory adaptation without altering main intrinsic properties of neurons (Chung et al., 2002). Furthermore, short-term depression improved coincidence-detection of chick auditory neurons in nucleus laminaris by reducing inter-EPSC interval duration (Cook et al., 2003), which might improve sound localization that requires precise temporal processing of binaural inputs.

1.2.3. modulation of serotonin on synaptic efficacy

5-HT modulates the strength of synaptic transmission in various brain regions, often by altering the probability of transmitter release presynaptically. In rat dorsolateral septal nucleus, 5-HT enhanced excitatory transmission by increasing glutamate release via 5-HT_{2A} receptor (Hasuo et al., 2002). In rat medial preoptic nucleus, 5-HT reduced both excitatory and inhibitory fast transmission by reducing transmitter release (Malinina et al., 2005).

Manifold interactions between 5-HT and other metabotropic receptors have been reported. In rat prefrontal cortex, an agonist of mGluR-2 suppressed the enhancement of excitatory transmission in layer V pyramidal neurons that can be induced by DOI, an agonist of the 5-HT2_A receptor (Marek et al., 2000). In rat midbrain slices, 5-HT attenuated the inhibitory effect caused by $GABA_B$ receptor activation in dopamine-containing neurons via presynaptic 1_B receptors (Johnson et al., 1992). Such interactions of modulatory systems might open a way for new therapeutic approaches. Due to their complexity, the goal directed design of therapeutic approaches, however, will require an understanding of the related mechanisms not only on the pharmacological level but also on the signal processing level.

5-HT has been reported to modulate short-term plasticity in many synapse types, in most

cases via presynaptic mechanisms. In cultured sensorimotor neurons of the marine snail aplysia, homosynaptically released 5-HT influenced short-term depression and recovery from depression of excitatory synapses both indirectly, by altering the coupling between pre-synaptic action potentials and transmitter release, and directly, by changing the transmitter available for release (Zhao and Klein, 2006). In rat layer IV cortical neurons, 5-HT reduced presynaptic glutamate release and thereby the strength of excitatory synaptic via 1_B receptors (Laurent et al., 2002).

1.2.4. synaptic transmission in DCN neurons

As already mentioned, DCN neurons receive inhibitory inputs from Purkinje cells and excitatory inputs from mossy fibers and climbing fibers. Both can control DCN spiking precisely in time. Considering the massive inhibitory input from Purkinje cells to DCN neurons it is of particular interest that DCN spiking might be triggered by populations of Purkinje cells that pause in synchrony for brief time periods (≥ 20 ms) (Gauck and Jaeger, 2000, 2003). It is important to note that such a type of disinhibition is distinct from the one associated with rebound spiking because rebound spiking involves the activation of T-type calcium channels which are not involved here. The depolarizing drive could be provided instead either by persistent intrinsic inward currents and/or by a baseline of excitatory background synaptic activity (Gauck and Jaeger, 2003). Therefore, information might be transmitted very efficiently from the cerebellar cortex to the DCN via pauses of Purkinje cell activity (Gauck and Jaeger, 2003).

A study of paired pulse depression suggested that the synaptic connections between individual Purkinje cells and DCN neurons have many release sites (Pedroarena and Schwarz, 2003), something that was proposed earlier based on quantitative anatomical data (Palkovitz et al., 1977). The same paired pulse study implied that short-term depression is independent of release probability and of presynaptic origin (Pedroarena and Schwarz, 2003). Furthermore, repetitive stimulation showed that short-term depression of the inhibitory postsynaptic currents (IPSCs) is frequency-dependent (Pedroarena and Schwarz, 2003; Telgkamp and Raman, 2002). The level of depression increased with an increasing stimulating frequency (Telgkamp and Raman, 2002), indicating the high sensitivity to temporal information at this synapse.

The synaptic strength during steady-state depression was found to be comparatively high at the Purkinje-DCN synapse even for high stimulating frequencies (Peroarena and Schwarz,

2003; Telgkamp and Raman, 2002). These results were interpreted such that a mechanism might exist capable of limiting synaptic failure and thereby depression. Based on morphological and kinetic data it has been suggested that synaptic spillover might represent such a mechanism. According to electron microscopic reconstructions, the boutons of Purkinje terminals have multiple independent active zones. Statistics predicts that the probability for synchronous failure at all those zones decreases with an increasing number of zones. Therefore, the overall probability of synaptic failure should be low and a high response probability could be maintained even at high presynaptic firing rates (Telgkamp et al., 2004). Spillover between neighbouring zones could further reduce the level of depression. In contrast to Pedroarena and Schwarz (2003), Pugh and Raman (2006) showed that not only presynaptic but also postsynaptic mechanism are likely to contribute to short-term depression because $GABA_A$ receptors at Purkinje terminals were found to desensitize and deactivate rapidly (Pugh and Raman, 2006). Such a postsynaptic desensitization might further limit the extend of depression at high frequencies.

Comparatively little is known about excitatory inputs to DCN neurons. Excitatory post-synaptic currents (EPSCs) in DCN neurons comprise three components: AMPA, fast-NMDA and slow-NMDA (Anchisi et al., 2001). The total NMDA component is about 83 % of the AMPA component at a membrane potential of -60 mV. The amplitudes of fast and slow NMDA components are about equal at positive potentials (> 0 mV) but the fast NMDA is larger at physiologically relevant hyperpolarized potentials (Anchisi et al., 2001). The functional role of excitation is still debated. *In vivo* studies are controversial in that excitatory inputs might provide an important drive for limb-movement regulation (Holdefer et al., 2004) but play only an accessory role for the classically conditioned eyeblink response (Aksenov et al., 2005).

Besides ionotropic neurotransmitter receptors, $GABA_B$ and metabotropic glutamate receptors exist in DCN neurons and at Purkinje terminals (Anchisi et al., 2001; Mouginot and Gähwiler, 1996; Morishita and Sastry, 1995). The reported effects of $GABA_B$ receptor activation at the Purkinje-DCN synapse *in vitro* are conflicting: in one pharmacological study $GABA_B$ autoreceptors were not activated neither by electrical stimulation of Purkinje cells nor by endogenous GABA release (Morishita and Sastry, 1995), however, pharmacological activation of the presynaptic $GABA_B$ receptors by the agonist baclofen reduced the amplitude of evoked IPSCs (Morishita and Sastry, 1995) and the amplitude and frequency of spontaneous IPSCs (Mouginot and Gähwiler, 1996). However, $GABA_B$ and

metabotropic glutamate receptors appear not to contribute to short-term depression as the application of their antagonists did not alter depression patterns induced by multiple stimulation of Purkinje-DCN synapses in cerebellar slices (Peroarena and Schwarz, 2003; Telgkamp and Raman, 2002).

Several neuromodulatory substances were found within the DCN, including serotonin (Geurts, 2002; Kitzman and Bishop, 1994), norepinephrine, acetylcholine and histamine (Schweighofer et al., 2004). Interactions between the serotonergic and the cholinergic systems have been reported in rat hippocampus (Izumi et al., 1994), cortex (Giovannini et al., 1998) and spinal cord (Cordero-Erausquin and Changuex, 2000). No such interactions are known in the DCN so far.

1.3. Synaptic Integration

There exists a large gap between our understanding of single neurons based on classical *in vitro* current clamp and voltage clamp studies and our understanding of their performance under natural conditions *in vivo*. One major reason is that most neurons are subjected to high levels of background synaptic activity *in vivo* that might fundamentally modify their properties such that their actual performance might not only deviate from but even contradict our expectations drawn from *in vitro* current clamp and voltage clamp experiments. One experimental approach to bridge this gap, at least to a particular degree, is the use of dynamic current clamp that allows one to stimulate neurons *in vitro* with simulated synaptic input in a way similar to the input they might experience under *in vivo* conditions. One major limitation of dynamic current clamp is that it necessarily provides a point source of input at the soma via the recording electrode thereby neglecting the fact that synaptic input is distributed all over the cell. How crucial this mismatch is for the validity of the results will depend on the electrotonic compactness of the neurons under study (see discussion). Therefore, some fundamentals about electrotonic compactness and high levels of background synaptic activity are addressed in the following paragraphs.

1.3.1. cable equation and electrically passive neuron models

Based on their passive electrical properties, neurons can be considered to act as low-pass filters. These properties are the starting point to estimate the electrical compactness of neurons. Passive electrical models can be constructed knowing the morphology and some basic electrical parameters like input resistance, membrane capacitance, membrane resistance and axial resistance. Passive models allow one to predict the propagation of e.g. synaptic inputs from the dendrites to the soma. On their way to the soma the input amplitude drops because current leaks out of the membrane and because the membrane capacitance is continuously charged and discharged. Solutions of the cable equation are one way to describe the signal amplitude V(x) as a function of location x in the unit of electrical length λ. For a tube of membrane with a sealed-end, corresponding e.g. to the dendritic branch of a neuron, the appropriate solution provides the following description of the signal amplitude as a function of length (x):

$$V(x) = V_0 \cosh(x_{end}/\lambda - x/\lambda)/\cosh(x_{end}) \; .$$

1.3.2. impact of 'high conductance state' on firing activity

Different from the quiescent environment *in vitro*, neurons *in vivo* are subjected to an intense bombardment by a barrage of ongoing excitatory and inhibitory synaptic input activity. This background synaptic activity will influence neuronal responses by increasing the membrane conductance, increasing the depolarization, increasing the amplitude of membrane potential fluctuation and reducing the input resistance compared to conditions *in vitro* and in anesthesia (Destexhe et al., 2003; Steriade et al., 2001; Matsumura et al., 1988), resulting in a 'high conductance state'. It also makes neuronal responses more stochastic to external stimuli.

A number of *in vitro* and computational studies showed that background synaptic activity has a strong influence on the input-output transfer function of neurons (Wolfart et al., 2005; Fellous et al., 2003; Shu et al., 2003; Mitchell and Silver, 2003; Chance et al., 2002). According to those studies, background synaptic activity could modulate the overall gain of neuronal transmission, generate an input-output phase shift (Mitchell and Silver, 2003; Chance et al., 2002), alter the slope or offset of input-output relation (Wolfart et al., 2005; Mitchell and Silver, 2003; Chance et al., 2002), increase spike timing precision (Shu et al., 2003, Zsiros and Hestrin, 2005), enhance the sensitivity to small signal amplitudes (Shu et al., 2003) and modify the effects of neurotransmitters (Desai and Walcott, 2006). An *in vitro* study by Wolfart et al. (2005) demonstrated furthermore the complex interaction between intrinsic properties and background synaptic activity by showing how synaptic input switched firing patterns of thalamocortical neurons.

Intracellular recordings *in vivo* showed that even synaptic plasticity was modulated by the level of background synaptic activity (Crochet et al., 2005; Reig et al., 2006). An increased level of background synaptic activity decreased the amplitude of plastic changes but increased the probability to induce potentiation rather than depression. A low background level, in contrast, increased the amplitude of plastic changes but reduced the probability to induce potentiation rather than depression (Crochet et al., 2005). The degree of short-term synaptic depression was lower *in vivo* than *in vitro* (Reig et al., 2006).

The examples above illustrate the functional relevance of background synaptic activity. Many of these *in vitro* studies used dynamic current clamp approaches illustrating the additional insight into signal processing of neurons that conventional current clamp and voltage clamp experiments would not have provided. The question might come up,

especially to people exclusively working *in vivo*, whether experiments like that could be done right away *in vivo*? *In vivo* systems have of course the big advantage of an intact synaptic network. This advantage, however, has the downside that the time course and strength of most synaptic inputs is unknown and it can not be inferred from the neuron's response. Therefore, provided that an understanding of neuronal signal processing is the scientific goal, a satisfactory analysis of those *in vivo* data would be impossible. Taken together, using dynamic current clamp *in vitro* offers several advantages over other *in vitro* and *in vivo* approaches. Therefore, I investigated the signal processing of DCN neurons and its modulation by 5-HT in cerebellar slices applying *in-vivo*-like synaptic input patterns with dynamic current clamp.

1.3.3. advantage of dynamic current clamp

As already mentioned, dynamic current clamp can be used to stimulate neurons in an *in-vivo*-like fashion with simulated synaptic activity *in vitro*. To this end, a current is injected via the patch clamp pipette into the neuron that is updated in real time for each step of data acquisition and current injection. The injected synaptic current (I_{syn}) is calculated based on a conductance model (G(t)) of the synaptic input within the computer. According to Ohm's law the injected current is calculated as the product of G(t) and the synaptic driving force (V_m - E_{rev}), that is the difference between the momentary membrane potential (V_m) and the reversal potential of the simulated synapse type (E_{rev}):

$$I_{syn} = G(t)*(E_{rev}-V_m) .$$

The difference between a current clamp experiment and a dynamic current clamp experiment becomes obvious reflecting on this equation. In current clamp a fixed current waveform would be injected into the neuron independent from the neuronal response. In dynamic current clamp, the injected current depends on the neuron's response that is its membrane potential. If the membrane potential is identical to the reversal potential the injected current is actually zero despite a large synaptic conductance. This is exactly how real synapses function *in vivo*. The simulated synaptic activity could represent the activity of one input neuron, the population activity of inputs of one kind, or the activity of several distinct input populations.

1.4. Serotonin

The serotonergic system originates in the brainstem raphe nuclei from two main cell groups, rostral (superior) and caudal (inferior). The rostral group is located mainly in the midbrain, it comprises three nuclei, dorsal raphe, median raphe, and centralis superior and its axons project to telecephalon, diencephalon, forebrain and cerebellum. The caudal group is located mainly in the medulla, it comprises three nuclei, raphe magnus, raphe obscurus and raphe pallidas and it projects to the spinal cord (Cooper et al., 2003; Jacobs and Fornal, 1995). Therefore, the serotonergic system reaches large parts of the central nervous system, where it modifies numerous synaptic and intrinsic neuronal properties.

1.4.1. multiple and heterogeneity effects of serotonin

5-HT is the neuromodulator studied most but understood least for the following reasons. First, there exists a large number of different 5-HT receptor subtypes and their effects are highly heterogeneous (Aghajanian, 2000; Glennon et al., 2000). 5-HT acts on intrinsic as well as synaptic properties of neurons. Second, few highly specific receptor agonists and antagonists are known for these receptors. The wide range of receptor subtypes and overlapping responses to drugs add to the fairly humble understanding of the serotonergic system (Glennon et al., 2000). A third reason is that multiple effects of 5-HT are to be expected at single nerve cells and none of the classical pharmacological studies ever tried to analyse the combined effects that 5-HT might have on signal processing.

So far 14 different 5-HT receptor subtypes distributed over 7 distinct families have been identified. This receptor diversity and their complex cellular distribution account for the multiple electrophysiological effects that 5-HT exerts in the central nervous system (Aghajanian, 2000; Glennon et al., 2000; Andrade, 1998). Of all receptors, only the 5-HT3 receptor is ionotropic, while all others are G-protein coupled metabotropic receptors. The 5-HT3 receptor has a mixed cationic permeability with a reversal potential of 0 mV.

The effect of 5-HT does not only depend on the set of activated receptor subtypes but also on the release and reuptake systems for 5-HT. 5-HT is released from neurons and therefore its release is supposed to be calcium-dependent and TTX-sensitive (Beas-Zarate et a., 1984, Mendlin et al., 1996). Besides typical synapses, 5-HT is also released by ‘volume trans-mission’. In volume transmission the release site is not part of a typical synaptic junction with postsynaptic specialisations but the neurotransmitter has to diffuse over longer distances to receptors that are often diffusely distributed over the surface of

potential postsynaptic targets. Through this mechanism, the affective field of one presynaptic active zone is extended. The non-junctional serotonergic terminals described in the cerebellum (Chan-Palay, 1977) suggest this kind of transmission. For volume transmission the distribution, activity and affinity of reuptake systems and transporters on neighbouring cells, neurons and glia alike, becomes especially relevant for the action of a neuromodulator like 5-HT. Blocking those transporters is expected to increase the extracellular concentration and thereby the amplitude and duration of 5-HT action.

1.4.2. interaction between serotonin and other neurotransmitter systems

Besides its effect via 5-HT receptors, *in vivo* and *in vitro* studies showed that 5-HT interacts with multiple neurotransmitter systems such as GABA (Malinina et al., 2005; Tan et al., 2004; Monckton and McCormick, 2002; Mitoma and Konishi, 1999; Kitzman and Bishop, 1997; Mitoma et al., 1994; Cumming-Hood et al., 1993; Johnson et al., 1992; Strahlendorf et al., 1989), glutamate (Malinina et al., 2005; Hasuo et al., 2002; Laurent et al., 2002; Marek et al., 2000; Thellung et al., 1993; Gardette et al., 1987; Lee et al., 1985), dopamine (Di Matteo et al., 2002) and acetylcholine (Cordero-Erausquin and Changuex, 2000; Giovannini et al., 1998; Izumi et al., 1994). Interactions like that raise the complexity of serotonergic actions and are likely to limit our understanding of the serotonergic system even further.

In case of the dopaminergic system, 5-HT has been reported to cause inhibitory effects by activation of 5-HT2_C receptors (Di Matteo et al., 2002). A moderate to dense localization of 5-HT2_A and 2_C receptor mRNAs and proteins was found in substantia nigra and ventral tegmental area as well in the regions of their axon terminals (Esposito, 2006).

For the acetylcholinergic system, an immunocytochemical study showed that 5-HT1_A receptors are localized on cholinergic neurons in the medial septum and diagonal band of Broca that project to the hippocampus in rats (Kia et al., 1996). In a microdialysis study in freely behaving rats, 5-HT increased hippocampus acetylcholine level via 5-HT1_A receptors and reduced it via 5-HT1_B receptor (Izumi et al., 1994). Potassium-evoked release of cerebral acetylcholine, however, was reduced by 5-HT via 5-HT3 receptors (Giovannini et al., 1998). In addition, three nicotinic acetylcholine receptor populations reduced 5-HT release tonically or non-tonically in rat spinal cord, suggesting a cholinergic regulation in descending serotonergic pathways (Cordero-Erausquin and Changuex, 2000).

In addition, application of corticotropin-releasing factor as well as acute stress were reported to prolong the enhancement of GABAergic transmission by 5-HT in rat prefrontal cortex *in vitro* (Tan et al., 2004). This interaction supports a role of the serotonergic system for psychiatric disorders.

Because other neuromodulatory systems are present in the DCN, an interaction between the serotonergic system and those systems might be possible. Such interactions, however, have not been investigated yet.

1.4.3. relation between serotonin and motor activity

In the following I will give a brief overview about the functional role of the serotonergic system as it has been inferred from *in vivo* recordings. The topic of my thesis is the effect of 5-HT on DCN activity but this is part of the larger question how the serotonergic and the cerebellar systems might interact. Defying considerable research efforts, it is still difficult to assign specific functions to the cerebellum. On a more general level, however, it is undisputed that the cerebellum is involved in motor control, motor learning, and the integration of motor commands with sensory information.

What is the function of the serotonergic system? In general, a close relation was found between the activity of serotonergic neurons and motor behaviour. Brain stem serotonergic neurons increased their firing rate during increased motor activity (Jacobs and Fornal, 1999; Veasey et al., 1995). *In vivo* microdialysis studies revealed elevated 5-HT levels in cat cerebellum (Mendlin et al., 1996) and in rat forebrain (Rueter and Jacobs, 1996) during periods of increased overall motor activity. Serotonergic neurons in pontine and medullar cell groups were generally unresponsive to physiological stressors, like heat, pain, food and water deprivation, and so forth, but their activity was elevated during periods of increased muscle tone or tonic motor activity (Jacobs and Fornal, 1999). Therefore it has been suggested that the primary function of the brainstem serotonergic system might be to facilitate motor output on a gross behavioural level.

1.4.4. serotonergic modulation in the cerebellum

All regions of the cerebellum receive serotonergic innervation, mainly from the medullary and pontine reticular formation (Schweighofer et al., 2004; Kitzman and Bishop, 1994; Kerr and Bishop, 1991). This implies an important modulatory role of 5-HT on cerebellar function.

At the cerebellar input level, pontine nuclei and inferior olive are highly innervated by serotonergic fibers (Schweighofer et al., 2004; Möck et al., 2002; Placantonakis et al., 2000). The pontine nuclei receive serotonergic input from medullary raphe and reticular nuclei. The effect of this input is a membrane depolarization and a reduction of synaptic strength (Möck et al., 2002). The serotonergic input to the inferior olive originates from praragigantocellular reticular nucleus, raphe obscurus and pallidus. It results in membrane depolarization, enhanced firing rates and abolished subthreshold rhythmic oscillation of inferior olive neurons *in vivo* and *in vitro* (Placantonakis et al., 2000; Sugihara et al., 1995). Overall 5-HT appears to increase the level of activity at cerebellar afferents.

Various effects of 5-HT have been described in the cerebellar cortex. The serotonergic innervation of the cerebellar cortex originates from the reticular nucleus and the lateral tegmental nucleus (Kerr and Bishop, 1991). It was reported to reset the firing rate of Purkinje cells to a preferred state *in vivo*: the spike rate was increased for slow-firing neurons and was increased for high-firing neurons (Strahlendorf et al., 1984). A change in excitability might be caused by an inhibitory effect on the I_h current via $5\text{-}HT_{2/1C}$ receptors (Li et al., 1993).

Several effects of 5-HT on the synaptic efficacy of cerebellar Purkinje cells have been described. *In vivo* recordings suggest that 5-HT is reducing glutamate-induced excitation (Lee et al., 1985) and at the same time it is decreasing GABA-mediated inhibition (Strahlendorf et al., 1989). Recordings from Purkinje cells *in vitro* found an increase of the IPSC amplitude by 5-HT but no effect on EPSCs (Mitoma et al., 1994). 5-HT has also been reported to reinforce the inhibitory transmission on to Purkinje cells by enhancing the GABAergic transmission from cerebellar interneurons to Purkinje cells (Mitoma and Konishi, 1999). Furthermore, 5-HT enhanced the inhibitory input to Golgi cells most likely by activating Lugaro cells, an inhibitory interneuron of the cerebellar cortex (Dieudonné and Dumoulin, 2000). 5-HT has also been reported to reduce excitatory transmission between mossy fibers and granule cells *in vitro* (Thellung et al., 1993). Effects of 5-HT on other synapses in the cerebellar cortex have not been reported yet.

The focus of my study is the question how 5-HT modulates DCN activity and thereby signal processing. The effects of 5-HT on DCN activity described so far are ambiguous. Dense 5-HT positive varicosities are found in all cerebellar nuclei that are distinct from climbing and mossy fibers (Kerr and Bishop, 1991). These serotonergic afferents to DCN neurons originate from dorsal raphe nuclei, locus coeruleus, and dorsal tegmental nucleus

(Kitzman and Bishop, 1994). The serotonergic fibers projecting to the DCN are distinct from those projecting to the cerebellar cortex. This implies that cerebellar cortex and DCN are modulated differently by the serotonergic system. *In vitro* studies reported either an increased DCN activity after iontophoretic 5-HT application (Gardette et al., 1987) or both, a decrease and an increase of DCN activity (Cumming-Hood et al., 1993). In contrast, *in vivo* studies reported either a reduced activity in the interposed nucleus by iontophoretic 5-HT application (Kitzman and Bishop, 1997) or various effects including inhibition, excitation and biphasic activity changes, in the dentate and the interposed nuclei (Di Mauro et al., 2003).

Several effects of 5-HT on synaptic transmission in DCN neurons have been described. *In vitro*, the strength of excitatory synaptic transmission was reduced after iontophoretic 5-HT application in the DCN (Gardette et al., 1987). *In vivo*, 5-HT reduced the effect of excitatory amino acid application and potentiated the effect of GABA application in the cat interposed nucleus (Kitzman and Bishop, 1997). Together these studies suggest that the overall effect of 5-HT mediated synaptic actions is to reduce DCN activity.

In consideration of those contradictory 5-HT effects, one important result of my study is that the level of background synaptic activity is likely to act as an important boundary condition that can influence the effect of 5-HT on DCN activity.

2. Material and Methods

2.1. Electrophysiology

2.1.1. slice preparation

Sprague-Dawley rats (10-15 days old) were anesthetized with isofluran and decapitated. Parasagittal cerebellar slices were cut in 275 µm on a vibratome (Leica, Germany) in ice-cold slicing solution containing (in mM): 85 NaCl, 75 saccharose, 3 KCl, 4 $MgSO_4$, 1.2 KH_2PO_4, 26 $NaHCO_3$, 0.5 $CaCl_2$, 20 glucose, 0.5 ascorbic acid. Ascorbic acid is an anti-oxidative compound which helps neurons to survive oxidative stress caused by free radicals during the slice preparation; the reduced NaCl and $CaCl_2$ concentrations were intended to reduce stress by a reduction of spike activity and calcium influx. After cutting, slices were stored at room temperature for one hour before the experiment started while the solution was slowly replaced by ACSF containing (in mM): 125 NaCl, 3 KCl, 1.9 $MgSO_4$, 1.2 KH_2PO_4, 26 $NaHCO_3$, 2 $CaCl_2$, 20 Glucose. Slices were incubated for 1-6 hours at room temperature before being transferred to the recording chamber. Slice and recording solutions were continuously oxygenated with 95% O_2 and 5% CO_2. The recording temperature was 33°C.

For unknown reasons, the success rates of DCN recordings from animals older than 16 days were so low that it was unfeasible for the present project. This difficulty is testified by the lack of any *in vitro* DCN studies with a notable number of older animals also from other studies (Pugh and Raman, 2005; Telgkamp et al., 2004; Telgkamp and Raman, 2002; Anchisi et al., 2001; Gauck and Jaeger, 2000; Aizenman and Linden, 1999; Aizenman et al., 1998). Since no difference in response properties was found for neurons recorded from 10 to 15 day-old animals, all animals of this range were pooled.

2.1.2. data acquisition

Data were recorded with SEC-05LX amplifier (npi, Germany), in discontinuous sampling mode with a switching frequency of 30 kHz and a duty cycle of ¼. Data acquisition and current injection was done at a sampling frequency of 10 kHz (DAQ board: PCI-6052E, National Instruments) in all experiments.

2.1.3. general electrophysiology

Whole-cell patch clamp recording were made from DCN neurons located mainly in the dentate nuclei, rarely in the interposed. Excitatory inputs were blocked either by 1 mM kynurenic acid or by 100 µM D-AP5 (Tocris, USA) and 25 µM DNQX, while inhibitory inputs were blocked by 10 µM bicuculline or 40 µM picrotoxin. In some experiments, serotonin reuptake receptors were blocked by 20 µM clomipramine (Tocris, USA), a selective 5-HT reuptake inhibitor. Electrodes were filled with the intracellular solution containing (in mM): 10 EGTA, 10 K-Hepes, 0.5 $CaCl_2$, 4 NaCl, 2 $MgC1_2$, 4 K_2-ATP, 0.4 Na_2-GTP, 10 Na-phosphocreatine, adjusted pH to 7.3 with KOH.

For voltage clamp recordings of 5-HT activated intrinsic currents, all voltage-gated sodium, potassium and calcium currents were blocked extracellularly using broad range blockers in regular recording solution (in mM): 10 TEA, 2 4-AP, 2 $CoCl_2$, 10 Hepes, 1 µM TTX, buffered to pH 7.4 with HCl. This was done to make neurons electrotonically as compact as possible and to isolate the 5-HT target currents, which were not blocked by these substances (see results).

2.1.4. synaptic recordings

For the measurement of postsynaptic currents, neurons were made electrotonically as compact as possible by blocking postsynaptic voltage-gated sodium, potassium and calcium currents by a modified intracellular solution containing (in mM): 112.5 CsF, 4 CsCl, 10 EGTA, 10 K-Hepes, 0.5 $CaCl_2$, 4 NaCl, 2 $MgC1_2$, 1 QX-314, 4 K_2-ATP, 0.4 Na_2-GTP, 10 Na-phosphocreatine, adjusted pH value to 7.3 with CsOH. Intracellular floride ions inactivate calcium currents thereby suppressed any calcium-mediated activity (Kay et al., 1986). Besides its electrotonic effect, this avoided an interference of long-term plasticity that might be induced otherwise by repetitive long lasting synaptic stimulation (Ouardouz and Sastry, 2000). Cells were held at 0 mV to achieve a sufficient driving force of about 70 mV for inhibitory synapse. All drugs were purchased from Sigma-Aldrich.

Postsynaptic currents were evoked by activation of input axons with 1, 10, 20, 50, 100 Hz with a 100-µsec width pulse, delivered through concentric bipolar stimulating electrodes placed in the surrounding nucleus region. A stimulation train of 1 Hz lasting for 10 seconds was applied 3 times to check the stability of the synaptic currents. The stimulus trains were applied at an intertrain interval of 5 seconds. The response current traces were averaged over 6 to 10 identical stimulus presentations.

2.2. Stimulus Construction

2.2.1. current clamp

Current clamp experiments were performed to determine the spike frequency-current relationship of DCN neurons as one measure of input-output characteristics. To this end, constant currents of 2-second duration with ±25, ±50, ±75, ±100 pA amplitude was injected and the corresponding membrane potentials 1 second before, during and 2 seconds after current injection was recorded. All these 5-second lasting current clamp traces were applied 2-3 times and were separated by pauses of 2 seconds from each other. The current pulses, as well as the dynamic clamp stimuli mentioned below, were applied before, during and after 5-HT perfusion, in the presence of both excitatory and inhibitory synaptic blockers.

2.2.2. voltage clamp

Voltage clamp experiments were performed to characterize currents underlying the intrinsic effects of 5-HT. The recorded neurons were held at a particular holding potential and the corresponding injected current to keep this voltage value was recorded, namely the holding current. The opening of an ion channel causes a current flux type that would bring the membrane potential closer to its reversal potential. The voltage clamp electronics, however, detects even slight deviations between the holding potential and the membrane potential and injects a counteracting current that prevents those deviations almost completely. The involved current types can then be identified by the kinetics and the pharmacology of this holding current that is a mirror image of the activated intrinsic currents.

The potential of -50 mV was selected as the baseline holding potential. The holding current was minimum at -50 mV, indicating that most intrinsic currents are closed at this potential. From -50 mV, voltage clamp commands to potentials ranging from -110 to +30 mV were applied. The voltage step lasted for 2 seconds, and the corresponding holding current was recorded from 1 second before until 2 seconds after these steps. The voltage command was performed before, during and after 5-HT application, in the presence of broad range blockers of voltage-gated channels.

2.2.3. dynamic current clamp

Dynamic current clamp was used to investigate the impact of 5-HT on signal processing in DCN neurons. In general, at dynamic current clamp experiments a conductance is

simulated using a computer that represents the activity of synaptic or intrinsic ion channel populations. This conductance is used to stimulate real neurons in whole-cell patch clamp mode (Robinson and Kawai, 1993; Sharp et al., 1993). To this end, a current is injected via the recording electrode that is calculated from the simulated conductance and the driving force, which is the difference between momentary membrane potential and reversal potential of the tested ion channel type. Therefore, a dynamic interaction between real neurons and simulated synaptic inputs is established in dynamic current clamp (Fig. 3A).

In the dynamic clamp experiments, an *in-vivo* like synaptic current (I_{syn}) was injected into the patched neuron. It was calculated based on the instantaneously recorded membrane potential (V_m) and the time-dependent excitatory ($G_{ex}(t)$) and inhibitory ($G_{in}(t)$) conductances, according to this equation:

$$I_{syn} = G_{ex}(t)*(E_{ex}-V_m) + G_{in}(t)* (E_{in}-V_m) .$$

The underlying calculation and current injection were done by computer for each sampling point during the recording. The sampling frequency was 10 kHz. The excitatory (E_{ex}) and inhibitory (E_{in}) reversal potentials were 0 mV and -70 mV, respectively. All excitatory and inhibitory input elements were simulated as poisson elements that generated spikes with an absolute refractory period of 3 ms and a given mean firing frequency. Each spike caused a simulated unitary conductance change (g_{ex} or g_{in}) in the recorded neuron. $G_{ex}(t)$ and $G_{in}(t)$ represent the temporal linear sum of all unitary excitatory and inhibitory conductance changes (Fig. 3B):

$$G_{ex}(t) = \Sigma g_{ex} , G_{in}(t) = \Sigma g_{in} .$$

The activity of 100 inhibitory input elements was simulated. They were either independently active (unsynchronized) or organized in 10 independently active groups of 10 synchronized elements per group (synchronized). Their input frequency ranged from 10 to 75 Hz for different stimuli. Unitary inhibitory conductance changes were calculated by a dual-exponential function with a rise time constant (τ_{rise}) of 0.93 ms and a decay time constant (τ_{decay}) of 13.6 ms (Anchisi et al., 2001):

$$g_{in} = 1/(\tau_{decay} - \tau_{rise})*(e^{-(t/\tau decay)} - e^{-(t/\tau rise)}).$$

Summation all those unitary inhibitory conductances resulted in an average value of 16 nS for a mean input frequency of 35 Hz.

To isolate the effect of inhibitory input, excitatory input was not amplitude modulated and consequently no unitary excitatory conductance changes were simulated. The impact of amplitude modulated excitatory input was addressed in an earlier study by Gauck and Jaeger (2003). Only the impact of one excitatory input parameter was addressed here, its voltage dependence. Therefore, excitatory input was simulated as a voltage dependent and a voltage independent version that were otherwise identical. The voltage independent version had always a constant conductance of 12 nS. The voltage dependent version was normalized such that it had a conductance of 12 nS for a membrane potential of -40 mV. The voltage dependent excitatory input was composed of a voltage independent AMPA component and two voltage dependent NMDA components, fast and slow (Anchisi et al., 2001). $G_{ex}(t)$ was calculated by the equation:

$$G_{ex}(t) = G_{AMPA}(\text{constant}) + G_{fastNMDA}(\text{constant})* f_{fast}(V_m) + G_{slowNMDA}(\text{constant})*f_{slow}(V_m) .$$

The voltage dependence of NMDA component was introduced by a voltage-dependent multiplication factor calculated by this equation:

$$f(V_m) = 1/[1 + P_1*\exp(-P_2* V_m)] .$$

The best fit to the experimentally reported voltage-dependence of NMDA current was achieved by setting P_1 and P_2 to 0.002 and 0.109 for the fast NMDA component, and to 0.25 and 0.057 for the slow NMDA component (Anchisi et al., 2001; Gauck and Jaeger, 2003).

All stimuli were calculated off-line in advance and stored on hard disk. All dynamic clamp stimuli lasted 10 seconds. They were applied 3-5 times in an interface fashion and separated by 1-sec pauses.

To investigate the effect of 5-HT on the firing activity of DCN neurons under *in-vivo* like synaptic inputs, a series of dynamic clamp stimuli was applied that contained always one inhibitory (G_{in}) and one excitatory (G_{ex}) conductance. The simulated inhibitory input was either synchronized or unsynchronized with input frequency of 10, 20, 35, 50 or 75 Hz. The simulated NMDA input was either constant or voltage-dependent. To address the impact of synaptic shunting, G_{in} and G_{ex} were multiplied with different gain factors: 0.5, 1, 1.5. The inhibitory input used here was synchronized and the tested frequencies were 20, 27.5, 35, 42.5 or 50 Hz. The gain factor alters neither the time course of simulated conductance nor the combined reversal potential (V_{syn}), but the injected synaptic current (I_{syn}) for a given driving force ($V_{syn} - V_m$) according to the equation:

$$I_{syn} = \text{gain}*(G_{ex} + G_{in})(V_{syn} - V_m) .$$

2.2.4. simulation of short-term depression

The inhibitory synapses between Purkinje cells and DCN neurons express short-term depression if activated repeatedly. The impact of short-term depression on the firing activity of DCN neurons was tested in the absence and presence of 5-HT. To this end a series of dynamic clamp stimuli was constructed that extended the tested stimulus parameters described above (voltage dependence of NMDA excitation, inhibitory synchronization, and inhibitory input frequency) by short-term depression. To simulate short-term depression, a model by Varela et al (1997) was adopted. In this model, the response amplitude (A) was calculated as the product of the initial amplitude (A_0) and various dynamic variables for facilitation (F) and depression (D):

$$A = A_0F_1F_2....F_nD_1D_{2....}D_n .$$

The parameters describing the dynamics of F and D were fitted to data by Telgkamp and Raman (2002). Model construction and parameter fit was done by my supervisor Dr. V. Gauck and is not subject of my thesis. Nevertheless I will provide some information regarding these parameters in the following. A_0 was normalized such that the resulting average value of A was equal for poisson stimuli with and without short-term depression at an inhibitory input frequency of 35 Hz. Facilitation variables (F) were not required and set to 1. Two depression variables, one with a fast kinetic (D_1) and the other with a slow kinetic (D_2), were sufficient to fit the data by Telgkamp and Raman (2002). The dynamics of D_1 and D_2 are determined by two parameters each, called d and τ, according to the following equations that describe the change of D for successive time steps:

$$D \rightarrow D*d ,$$

$$\tau_D \, (dD/dt) = 1 - D .$$

The parameter d (≤ 1) can be interpreted physiologically such that the releasable vesicle pool is depleted by a fixed ratio for each synaptic activation. The time constant τ describes the speed of recovery from depletion that proceeds exponentially towards a maximally loaded vesicle pool during the subsequent inter-stimulus time. The parameters d, τ of D_1 and D_2 were fitted to the data by Telgkamp and Raman (2002) employing a genetic algorithm.

2.3. Data Analysis

Long lasting recordings of around 3 hours were required because extensive stimulus sets were applied before, during and after 5-HT application to each DCN neuron. Such long lasting recordings turned out to be demanding and often frustrating, especially in the DCN. Many neurons that showed initially a perfect response developed a run down before the recording end and had to be excluded from analysis. Furthermore, a complete washout of 5-HT induced effects was rarely achieved even for neurons where an exceptional long washout time ($\geq$ 90 min) was possible. Therefore, criterions to identify cells acceptable for data analysis had to be formulated regarding recording stability and partial washout of 5-HT. Cells with an overall drift $< \pm$ 5 mV in membrane potential were accepted for analysis. Among them, only cells with a partial recovery from 5-HT effect in membrane potential after 20-minute washout were included in the analysis.

Pooled data were analyzed using custom made software written in Matlab (MathWorks, USA) and Origin (Microcal Software, USA), and reported as mean ± SE. The analyzed parameters were mean firing rate (for current clamp and dynamic clamp), the spike timing precision (for dynamic clamp) and the holding current (for voltage clamp). The first 500 msec of the recording at dynamic clamp was were discarded to exclude response transients from the analysis that were occasionally caused by voltage steps at stimulus onset.

The calculation of spike timing precision was based on spikes elicited in response to repetitive applications of identical stimuli. Each spike determined a time window of ± 5 msec. The number of spikes falling into this time window but elicited by the other presentations of the same stimulus was determined. Calculating the average of this number for all spikes in all stimulus presentations and dividing it by the number of stimuli minus one resulted in a preliminary precision value. The precision value expected by chance had to be subtracted from this value to determine the final or shuffle corrected (see below) precision value. The precision level expected by chance was determined in the same way from the same data as the preliminary precision after randomly rearranging the interspike intervals (shuffling) within each response trace. Subtracting the chance level from the preliminary precision resulted in the final shuffle corrected precision.

Several parameters were used to determine the effect of 5-HT on action potential waveform. Cells that responded with a depolarization block to current injection amplitudes between +20 and +75 pA were excluded from this analysis. The depolarizing slope of action potential was characterized as the slope from 20 - 80 % of the action potential

amplitude. Spike amplitude was determined as spike peak minus spike threshold. Spike threshold in turn, was determined as the potential with maximal change in slope for an interval of 2 ms preceding each spike. The mean membrane potential was simply calculated as the averaged potential of the whole response. For a few cases the mean voltage was also calculated after excluding action potentials from the voltage traces. The deviation between both measures was negligible.

To analyze the effect of 5-HT on postsynaptic currents, the amplitude of evoked IPSC was calculated as the difference between IPSC peak current either to the holding current preceding each train or to the synaptic current preceding each stimulation. Spontaneous IPSCs were analyzed with Minianalysis Software (Jaelin Software, Leonia, NJ) by a detection threshold of 5 pA. The short-term depression that elicited by repetitive synaptic stimulation was characterized by steady-state amplitude which was calculated as the average of the IPSCs following the first 5 evoked events of each train.

Statistical analysis were made with pair-t test if not indicated otherwise, and $p < 0.05$ level was accepted to be statistical significant.

3. Results

The averaged soma size of all recorded neurons was 20.83 ± 0.67 μm (n = 42). Although recorded cell types could not be distinguished based on positional information, because excitatory and inhibitory neurons were diffusely distributed in cerebellar nuclei (De Zeeuw and Berrebi, 1995; Batini et al., 1992), the averaged diameter exceeding 15 μm indicates that mainly gluta-matergic neurons were recorded (De Zeeuw and Berrebi, 1995; Batini et al., 1992).

Several difficulties turned out to make data collection in the present project an unfortunate inefficient endeavour. The two most relevant ones are briefly mentioned here. DCN slices are well known for being an extremely difficult preparation. The reasons are not known, but maybe DCN neurons are particularly vulnerable to the mechanical stress caused by the preparation because the large number of axonal fibers running through this structure might transduce shear forces during slicing on the tissue and cells. The long recording time (> 3 hours in each session) required in the experiments made the task even more difficult because a large proportion of the data had to be excluded from analysis based on the criteria formulated in the methods part. Therefore, the overall success rate was actually as low as 42 accepted recordings out of 393 preparations, and was even worse for postsynaptic experiments.

3.1. Effects of Serotonin on Intrinsic Properties

3.1.1. serotonin caused a depolarizing current

The recorded DCN neurons had a mean membrane potential of -47.11 ± 1.04 mV and fired spontaneously on average with a frequency of 4.44 ± 0.5 Hz (n =25) in the presence of 10 μM kynurenic acid and 40 μM picrotoxin. In 2 out of 25 cells, 5-HT had no effect in current clamp recordings. After application of 10 μM 5-HT for 5-10 minutes, the membrane potential of DCN neurons was significantly depolarized by 7.99 ± 0.92 mV (n = 23, $p < 0.01$) and the spike rate was increased by 6.63 ± 1.11 Hz (n = 23, $p < 0.01$).

To confirm a complete block of all synaptic inputs, kynurenic acid was replaced to 100 μM D-AP5 and 25 μM DNQX. The recorded cells had a mean membrane potential of -44.45 ± 1.2 mV (n = 7) and fired spontaneously at the frequency of 7.99 ± 0.92 Hz (n = 6, excluding 1 silent neurons). After 10 μM 5-HT application for 5-10 minutes, the membrane potential was significantly depolarized by 5.38 ± 0.95 mV (n = 7, $p < 0.01$), but the change

in spike rate differed from cell to cell: 2 out of 6 cells had no evident change in firing rate (an decrease of 0.69 ± 0.45 Hz), and the rest 4 cells showed an increase by 4.41 ± 1.77 Hz. These two groups of excitatory blockers showed no significant difference in the recorded DCN neurons in mean membrane potential ($p = 0.58$), spontaneous firing rate ($p = 0.91$) and the magnitude of depolarization by 5-HT ($p = 0.15$) therefore all cells were pooled. The effects of 5-HT were long-lasting (up to 30 minutes) and could be washed away only partially (Fig. 4A).

Was the observed inter-cell variability of 5-HT effect cell type specific? All recorded neurons at current clamp were categorized by soma size and response to 5-HT to address this question in Table 1. 2 out of 32 neurons were insensitive to 5-HT at current clamp, and one of them is with soma diameter smaller than 15 μm while the other one is between 15 - 20 μm. For the rest 30 cells, no cells with soma size smaller than 15 μm were recorded. The majority of neurons with soma sizes between 15 - 20 μm responded to 5-HT with a clear depolarization and increased spike rate ($n = 14$), while 2 of these neurons were only slightly depolarized: one did not change the spike rate and the other one entered a depolarization block. All neurons larger than 20 μm responded to 5-HT with a significant depolarization and enhanced spike rate ($n = 13$). These data might indicate that smaller presumably inhibitory DCN neurons are rather insensitive to 5-HT. However, more data and an immunohistochemical identification of inhibitory neurons would be required to substantiate this hint. Overall, no correlation between soma size and 5-HT effect can be inferred from these data.

5-HT caused a parallel upward shift of the spike rate over a wide range of current injection amplitudes at current clamp (Fig. 4B), indicating a recruitment of a persistent depolarizing current. The firing rate during 5-HT application was reduced below the control level for large current values due to depolarization block (Fig. 4C).

The current underlying the depolarization by 5-HT was further examined by voltage clamp. Starting from a baseline holding potential of -50 mV, various voltage steps were applied and the additional currents required holding these target voltages were recorded. 5-HT (10 μM) always caused a net increase of a persistent inward current by 59.39 ± 9.4 pA ($n = 7$) at -50 mV, even in the presence of the blockers for the majority of voltage-gated sodium, potassium and calcium currents (Fig. 5A-B), indicating that these currents did not contribute to this effect. Therefore, the current types that could have contributed to the 5-

HT effect was restricted to an increase of persistent sodium current, a decrease of persistent potassium current, and a change of I_h current. However, specific blockers are not available for most persistent current types. Blocking the I_h current in DCN neurons with ZD-7288 for unknown reasons always resulted in a slow but substantial run down possibly because the ionic homeostasis was distorted. Therefore, the data had to be analyzed in a different way. IV-curves were constructed by plotting the holding current at the final 50 msec of each voltage step. This was done before and during 5-HT treatment and the resulting IV-curves were compared. Assuming that not just one but two persistent current types are activated by 5-HT the induced current ($\Delta I_{5\text{-}HT}$) is described by Ohm's law:

$$I + \Delta I_{5\text{-}HT} = (G_{Na} + \Delta G_{Na})^* (V_m - E_{Na}) + (G_K + \Delta G_K)^*(V_m - E_K).$$

According to this equation, only an opposite conductance change of equal strength in G_{Na} and G_K ($\Delta G_{Na} = -\Delta G_K$) would result in a parallel shift of the I-V curve, while any imbalance between ΔG_{Na} and ΔG_K would lead to an intersecting point. If only one conductance type, either G_{Na} or G_{Na}, were modulated by 5-HT, then one would expect an intersecting point at the reversal potential of the target channel. In the case that 5-HT modulated two currents, the IV-curve intersection would be more depolarized than E_{Na} for $\Delta G_{Na} > -\Delta G_K$, while it would be more hyperpolarized than E_K for $\Delta G_{Na} < -\Delta G_K$.

The voltage clamp experiments actually revealed two patterns: a parallel shift of the I-V curve (Fig. 5C, n = 3) and an intersecting point at about +5 to +10 mV (Fig. 5D, n = 4). There is no intrinsic current type known with a reversal potential between +5 and +10 mV. This suggests that 5-HT activated two or more current types in an unbalanced way as just described. The finding of parallel IV-curves suggests also the concerted but balanced activation of several current types.

The I_h current of DCN neurons (Raman et al., 2000) had also to be considered as a potential target of 5-HT, because 5-HT is known to act on I_h in various neuron types (Bickmeyer et al., 2002; Li et al., 1993) including Purkinje cells of the cerebellum (Li et al., 1993). Testing such an impact experimentally turned out to be difficult due to the instability of DCN neurons after I_h block, as already mentioned. A careful analysis of the voltage clamp data, however, suggested that the I_h current was not altered by 5-HT in DCN neurons as described in the following. The gradual decline of the current traces in Figure 5B during the voltage steps was caused by the slow activation of the I_h current. A baseline shift of these traces in Figure 5B resulted in an almost perfect match (not shown) indicating that I_h was not altered by 5-HT. To quantify this, the IV-curves were not calculated by the last 50

ms (Fig 5B, squares) but by the initial current (Fig 5B, triangles) that was determined fitting an exponential to the I_h and extrapolating it back to the start time of the voltage command. Therefore, these initial current amplitudes are devoid of an I_h component. The corresponding IV-curves (Fig. 5E, F) show the same pattern as the ones including I_h (Fig. 5C, D), an intersection at +5 mV (Fig. 5C, E) or a parallel shift (Fig. 5D, F). Taken together, the depolarization of DCN neurons by 5-HT was most likely mediated by the activation of a persitent depolarizing cation current and the concomitant reduction of a persistent potassium current.

Like for the current clamp data, the question was addressed whether the effect of 5-HT might correlate with soma size to infer any potential neuron type specific 5-HT action. The relevant voltage clamp data are listed in Table 2 and did not reveal any relation between cell type and 5-HT action.

3.1.2. serotonin reduced sodium channel availability

The analysis provided so far focused on persistent effects of 5-HT. The available literatures, however, provide abundant examples for 5-HT effects on transient voltage-gated currents (Aghajanian, 2000; Melena et al., 2000; Placantonakis et al., 2000; Andrade, 1998). To address a potential 5-HT effect on such currents in DCN neurons, the spike triggered average (STA) of the voltage trace was calculated and the action potential waveform was analysed in current clamp.

The STA at spontaneous spiking (Fig. 6A) revealed that 5-HT (10 μM) caused a significant reduction in the depolarizing slope by 39.95 ± 5.53 % ($n = 22$, $p < 0.01$), a reduced action potential amplitude by 12.28 ± 1.83 mV ($n = 22$, $p < 0.01$) and an increased spike threshold by 4.5 ± 1.2 mV ($n = 22$, $p < 0.01$). These findings suggested a reduction of voltage-gated sodium channel availability (Miles et al., 2005; Azouz and Gray, 2000) by 5-HT.

However, the membrane potential is not controlled in the current clamp experiments and depolarization by itself will cause the same phenomena. Therefore, the action potential parameters were plotted as a function of mean potential (Fig. 6B). After having eliminated the impact of depolarization, 5-HT significantly reduced action potential slope by 19.3 ± 6.7 % ($n = 9$, $p < 0.05$) and action potential amplitude by 6.12 ± 1.6 mV ($n = 9$, $p < 0.01$), respectively. The spike threshold was slightly but insignificantly increased by 1.32 ± 0.84 mV ($n = 9$, $p = 0.16$).

Furthermore, 5-HT reduced the amplitude of fast-afterhyperpolarization (AHP) and shifted slow-AHP upwards (Fig. 6A, arrows). Slow-AHP was partially recovered after long-time washout but fast-AHP not. This effect further reduced the de-inactivation of voltage-gated sodium channels and speeded depolarization block by 5-HT. Taken together, these results show that 5-HT did affect not only persistent current types but also transient voltage- dependent currents that contributed to the action potential waveform.

3.1.3. activity-dependent effect of serotonin under simulated synaptic inputs

Next, we investigated the alteration of firing activity after intrinsic properties were changed by 5-HT. Dynamic current clamp was used to introduce simulated synaptic inputs into the recorded neurons. First, we applied voltage dependent and independent NMDA components combined with synchronized and unsynchronized inhibitory inputs at 35 Hz, the mean firing frequency of Purkinje cells *in vivo* (Stratton et al., 1988; Savio and Tempia, 1985). The spike response and raster plot for a short time segment from one typical neuron is shown in Figure 7A. However, no significant difference in firing activity was found during application of 5-HT (10 μM) in all testing conditions (Fig. 7B) even though 5-HT increased spontaneous spike rate in the same neurons (Fig. 7B, spontaneous spiking).

For further elucidation, stimuli of identical excitatory component but with an extended range of inhibitory input frequency, from 10 to 75 Hz, were applied. Surprisingly, the effect of 5-HT was activity dependent, different from the results in current clamp. The input-output functions before and during 5-HT treatment intersected at the inhibitory frequency of around 35 Hz, in accordance to our former results. The spike rate was reduced by 5-HT at more depolarized potentials, where the inhibitory input frequency was lower, but left unchanged or slightly increased at more hyperpolarized potentials in all tested conditions (Fig. 8A). This can be characterized as a normalizing effect on the input-output characteristic of DCN neurons that was found to be significant mainly at depolarized activity states (Fig. 8A, 10 Hz). Take the response to synchronized inhibitory and voltage-dependent excitatory inputs as an example (Fig. 8A, top left). During application of 10 μM 5-HT the spike rate was significantly reduced by 9.36 ± 2.97 Hz at an inhibitory input frequency of 10 Hz ($n = 8$, $p < 0.05$), by 5.49 ± 2.49 Hz at 20 Hz ($n = 8$, $p = 0.06$), and significantly decreased by 1.8 ± 0.55 Hz at 50 Hz ($n = 8$, $p < 0.05$), by 46.76 ± 27.79 % at 75 Hz ($n = 8$, $p = 0.14$).

The effect of 5-HT on spike timing precision was also analysed because this parameter and the spike rate together determine the amount of information that a neuron can possibly transmit. In contrast to the spike rate, there was basically no change in spike timing precision by 5-HT (Fig. 8B), indicating a generally unaltered signal reliability in the tested frequency range. The only exception was a significant decrease of precision at unsynchronized inhibitory inputs of 10 Hz and voltage-dependent excitatory inputs by 13.75 ± 6.8 % (Fig. 8B, third, $n = 8$, $p < 0.01$).

Increased depolarization and reduced sodium channel availability represent opponent influences on the excitability of DCN neurons. Therefore, the question arises what their combined effect was on cell activity. In the following it will be shown that their concerted action resulted in the activity-dependent effect of 5-HT described above. This conclusion will be tested experimentally by altering the strength of the synaptic shunting effect. I will start with an explanation of synaptic shunting in the context of the present dynamic current clamp experiments.

Each ion channel type, whether synaptic or intrinsic, has a partial voltage clamp effect. If a channel is activated, it will generate a current (I_{ion}) that is given as the product of its conductance (G_{ion}) and the driving force that is the difference (E_{ion}-V_m) between its reversal potential and the membrane potential:

$$I_{ion} = G_{ion} * (E_{ion}-V_m) .$$

If only one channel would be open at a time, I_{ion} would flow until V_m reached E_{ion} and I_{ion} would cease not because the channel closed but because the driving force vanished. In this respect each channel or current type exerts a partial weak voltage clamp effect on the membrane potential of a neuron. Most of the time not only one but many ion channel types are active, and each of them pulling V_m towards its own reversal potential. The combined action of these ion channels, however, can be characterised by the combined reversal potential (V_{syn}) that lies in between the reversal potentials of all active ion channels. The combined reversal potential corresponds to a weighted sum of the individual reversal potentials and is given for the synaptic conductances simulated in the present study by the following equation:

$$V_{syn} = (E_{ex}*G_{ex} + E_{in}*G_{in})/(G_{ex} + G_{in}) .$$

The corresponding injected current (I_{inj}) is given by this equation:

$$I_{inj} = (G_{ex} + G_{in})*(V_{syn} - V_m) .$$

The voltage change that the activation of a single presynaptic input (excitatory (g_{ex}) or inhibitory (g_{in})) might induce ($E_{ex}*g_{ex}$ or $E_{in}*g_{in}$) is divided by the total of all synaptic inputs ($G_{ex} + G_{in}$). Therefore, it is immediately clear that its impact will become smaller and smaller with an increasing number of other active input elements, corresponding to what is commonly referred to as synaptic shunting.

Hence, V_{syn} provides a very efficient way to describe the simulated synaptic current I_{syn} as it allows one to collapse all synaptic equilibrium potentials into one potential (V_{syn}) and all simulated conductances into one conductance ($G_{ex}+G_{in}$). Note that not only G_{ex} and G_{in} but also V_{syn} are now functions of time.

The interaction between 5-HT action and synaptic shunting is illustrated in Figure 9. In current clamp 5-HT increased the net inward current thereby depolarizing the cell. In dynamic current clamp the synaptic current was shifted after 5-HT application such that its hyperpolarizing component was increased (Fig. 9B). This shift corresponds to a synaptic outward current that shunted the 5-HT induced inward current at least partially. As a result the depolarizing effect of 5-HT was either reduced or even totally abolished like for the neuron shown in Figure 9A.

From these considerations it is clear that we can manipulate the amount of 5-HT induced depolarization in dynamic clamp experiments by changing the absolute strength of the simulated synaptic input simply by multiplication of ($G_{ex} + G_{in}$) with a particular factor that I will call 'gain' in the following. Note that such a gain factor will not alter the combined reversal potential as it cancels out of the equation for V_{syn}. The central idea behind the subsequent experiments was to manipulate the 5-HT induced depolarization via the synaptic gain and to see whether the balance between the opponent 5-HT effects on excitability could be shifted this way.

To this end, a series of stimuli with inhibitory input frequencies of 20, 27.5, 35, 42.5 and 50 Hz, was applied for gain factors of 0.5, 1 and 1.5. The strength of the synaptic shunting current at gain factor 0.5 is just half that at gain factor of 1 for a given driving force, as described by the equation:

$$I_{syn} = gain*(G_{ex} + G_{in})(V_{syn} - V_m).$$

The results of Figure 10 showed that the effect of 5-HT on DCN activity did indeed depend on the strength of synaptic shunting that is represented by the gain factor. DCN activity was increased by 5-HT at gain 0.5, unaltered at gain 1 and decreased at a gain 1.5

(Fig. 10A, top panel). To fully appreciate this result, especially the fact that activity was reduced at gain 1.5, it is important to note that the membrane potential was depolarized by 5-HT for all gain factors (Fig. 10A, middle panel). Obviously, an activity reduction can not be caused by a depolarization on its own. An explanation is provided by the finding that the spike slope, which represents a sensitive measure for sodium channel availability, was reduced for all gain factors (Fig. 10A, bottom panel). Therefore these data strongly support the interpretation that the relative impact of two opponent influences on excitability, namely depolarization and sodium channel availability, was shifted by changing the gain factor. At gain 0.5 the effect of depolarization dominated and net excitability was increased, at gain 1.5 the reduced sodium channel availability is dominated and net excitability was reduced, and at gain 1 both effects just cancelled each other. This shift of relative impact can be understood mechanistically by observing carefully membrane potential and spike slope. The spike slope during 5-HT application was almost identical for all gain factors (Fig. 10A, bottom panel). Therefore it can not account for the shift in activity. The 5-HT induced depolarization however, that is the difference between both curves, decreased continuously with increasing gain (Fig. 10A, middle panel). Therefore, by increasing the strength of synaptic shunting via the gain factor, the positive influence of depolarization on excitability was gradually reduced resulting in a reversal of the 5-HT action from increasing to decreasing.

The impact of synaptic shunting on the 5-HT induced activity change just described allows one to make a prediction that is tested in the following. The model states that two opponent excitability effects, depolarization and sodium channel inactivation, cancel each other exactly where the input-output curves before and during 5-HT application cross each other. Increasing synaptic shunting should reduce the impact of depolarization and shift the balance in favour of reduced sodium channel availability. This in turn should result in a shift of the crossing point of the input-output curves towards more hyperpolarized membrane potentials that correspond to higher inhibitory input activities. Figure 10B shows the result of a re-presentative experiment where this prediction was tested. The result corresponds exactly to the model predicting. The crossing point between input-output curves is shifted towards larger inhibitory input frequencies for an increasing strength of synaptic shunting.

Taken together, the activity dependent effect that 5-HT exerted in DCN neurons in dynamic current clamp experiments can be understood based on its opponent excitability

effects, i.e. an increased net inward current with resulting depolarization and a reduced sodium channel availability

3.2. Effects of Serotonin on Inhibitory Postsynaptic Currents

In the experiments described so far, the effect of 5-HT on intrinsic properties and its consequences for the processing of given synaptic input activity were investigated. The next question was whether 5-HT might also directly influence synaptic input in DCN neurons. Such an effect comes was suggested by numerous studies that reports effects of 5-HT on synaptic effects in other neuron types (Monckton and McCormick, 2002; Möck et al., 2002; Mitoma and Konishi, 1999; Andrade, 1994; Mitoma et al., 1994; Thellung et al., 1993; Strahlendorf et al., 1989; Lee et al., 1985). Furthermore, 5-HT receptors have been reported to play a presynaptically modulatory role in various brain areas (Zhao and Klein, 2006; Malinina et al., 2005; Hasuo et al., 2002; Laurent et al., 2002; Andrade, 1994). Due to the functional relevance of inhibitory input to DCN neurons (Gauck and Jaeger, 2000), the effect of 5-HT on inhibitory input was the focus of this part.

Serotonergic modulation of inhibitory transmission between Purkinje cells and DCN neurons was studied by voltage clamp recordings in the presence of AP-5 (100 µM) and DNQX (25 µM) to block excitatory synaptic input. Postsynaptic currents were evoked by repetitive extracellular electrical stimulation with frequencies of 1, 10, 20, 50 and 100 Hz. The 1-Hz stimuli lasted 10 seconds, while the remaining stimuli lasted as long as 100 repetitive stimulations of that frequency.

Since the stimulating electrodes were placed in the DCN in vicinity to the recorded neurons, it could not be ruled out that collaterals of local inhibitory neurons were activated besides Purkinje cell axons. However, given the predominance that synapses from Purkinje cells on DCN neurons, 85 % of somatic and 50 % for dendritic synapses (Chan-Palay, 1977), it is likely that mostly Purkinje terminals were activated in the experiments.

3.2.1. effect of serotonin on IPSCs and short-term depression

All recorded neurons responded to trains of repetitive stimulation with short-term depression for all tested stimulating frequencies (Fig. 11A, left). The magnitude of depression was frequency-dependent as described earlier by Telgkamp and Raman (2002) and Pedroarena and Schwarz (2003). At 50 and 100 Hz, individual postsynaptic currents did not decay back to prestimulus baseline, but a substantial steady-state baseline was observed (Fig. 11A, left, 50 and 100 Hz). Synaptic failures were absent at stimulus frequencies ≤ 20 Hz, but they were present for stimulation frequencies ≥ 50 Hz. The percentage of failures was not analysed separately, instead they were implicitly taken into

account averaging current traces in response to repeated identical stimulus presentations. Facilitation of postsynaptic current was never seen. Bicuculline (10 μM) abolished the amplitude of evoked IPSCs to 3.9 ± 1.3 % of control amplitude (n = 5), revealing their GABAergic origin. One out of 5 neurons was excluded from analysis due to its insensitivity to 5-HT.

The waveform parameters of evoked IPSCs were fitted by a dual-exponential function. At stimulating frequency of 1 Hz and holding potential at 0 mV, the time constants were 1.69 ± 0.3 ms for rising and 20.16 ± 1.8 ms for decay under control conditions, and 1.81 ± 0.29 ms for rising and 19.96 ± 1.9 ms for decay after 10 μM 5-HT application (n = 5). The corresponding p-values revealed that there was no significant difference between control and 5-HT (p = 0.89 for rising time constant, 0.19 for decay time constant).

5-HT (10 μM) reduced the amplitude of evoked IPSCs over all tested input frequencies (Fig. 11A, right) but did not alter the activity-dependence of short-term depression. This was revealed by the normalization of IPSC amplitudes before and during 5-HT application by the amplitude of the first corresponding IPSC (Fig. 11B, n = 3).

The impact of 5-HT on short-term depression was further analysed by dividing the response traces into an initial and a steady-state response. The initial response was calculated as the average amplitude of second to fifth IPSCs, while the steady-state was calculated as the average amplitude following the first 5 IPSCs. Naturally, the amplitude of the first IPSC (P_1) within traces did not depend on stimulation frequency (Fig. 11C, top left). Therefore P_1-amplitudes was taken as an activity independent measure of 5-HT on IPSC amplitude. 5-HT (10 μM) reduced P_1 amplitude by 34.91 ± 10 % at 1 Hz (n = 5, p = 0.06), 44.71 ± 11.7 % at 10 Hz (n = 5, p = 0.07), 43.16 ± 10.2 % at 20 Hz (n = 5, $p < 0.05$), 40.15 ± 8.6 % at 50 Hz (n = 5, $p < 0.05$), and 38.28 ± 7.5 % at 100 Hz (n = 5, $p < 0.05$). The average reduction of P_1 by 5-HT is 40.24 ± 1.74 % with no significant difference between stimulus frequencies. Second, 5-HT reduced the amplitude of the second to fifth IPSCs ($P_{2\text{-}5}$, Fig. 11C, top middle) by 45.67 ± 12.2 % at 1 Hz (n = 5, p = 0.08), 40.55 ± 16 % at 10 Hz (n = 5, p = 0.14), 33.93 ± 11.5 % at 20 Hz (n = 5, p = 0.07), 35.77 ± 8 % at 50 Hz (n = 5, $p < 0.05$). A significant reduction of $P_{2\text{-}5}$-amplitudes was found with increasing frequencies. The steady-state amplitude of IPSCs (P_{ss}, Fig. 11C, top right) was reduced by 5-HT by 47.11 ± 12.44 % at 1 Hz (n = 5, p = 0.08), 44.01 ± 11.1 % at 10 Hz (n = 5, p = 0.15), 27.71 ± 11.6 % at 20 Hz (n = 5, p = 0.07), and 10.22 ± 18.9 % at 50 Hz (n = 5, p = 0.1).

This reduction degree did depend significantly on the stimulus frequency. The reduction of initial IPSC amplitude ($P_{2\text{-}5}/P_1$) during short-term depression showed no significant difference (Fig 11C, middle bottom): 17.59 ± 14.0 % at 10 Hz (n = 5, p = 0.6), 20.87 ± 0.9 % at 20 Hz (n = 5, p = 0.33), 8.6 ± 22.35 % at 50 Hz (n = 5, p = 0.11). The steady-state reduction during short-term depression (P_{SS}/P_1) was also slightly less pronounced after 5-HT application but the corresponding differences between control and 5-HT were also here insignificant (Fig. 11C, right bottom): 10.24 ± 5.6 % at 10 Hz (n = 5, p = 0.21), 30.62 ± 15.38 % at 20 Hz (n = 5, p = 0.1), and 57.72 ± 16.3 % at 50 Hz (n = 5, p = 0.18).

Taken together, 5-HT reduced the overall IPSC amplitude by about 40 % but did not alter the activity dependence of IPSC amplitudes as seen during stimulus conditions in which short-term depression was induced.

3.2.2. effect of serotonin on spontaneous IPSCs

Spontaneous presynaptic activity results in spontaneous postsynaptic events, the analysis of which can provide some information about the underlying mechanisms. DCN neurons held at 0 mV displayed outward spontaneous IPSCs (sIPSCs) with peak amplitude ranging from 5 to 170 pA (Fig. 12A, top trace), with an average amplitude of 16.6 ± 12.9 pA and inter-event interval of 61.86 ± 108.14 ms (from 6100 events). 5-HT application reduced both amplitude and frequency of sIPSCs (Fig. 12A, middle trace). All events were completely blocked in the presence of 10 μM bicuculline (Fig. 12A, bottom trace).

During 10 μM 5-HT application, mean inter-event interval was 73.85 ± 137.76 ms (from 5118 events, $p < 0.001$) and amplitude 14.62 ± 8.86 pA ($p < 0.001$). The cumulative curve of inter-event interval was shifted to right (Fig. 12B), showing an increased proportion of longer inter-event intervals after 5-HT. The cumulative curve of amplitude was shifted to left, indicating an increased proportion of smaller sIPSC amplitudes after 5-HT (Fig. 12C). A reduction in sIPSC amplitude by itself does not allow yet a definite distinction between pre- and postsynaptic mechanisms because it could be due to reduced transmitter release and/or due to receptor desensitization. The reduced sIPSC frequency, however, can only be of presynaptic origin, indicating that a reduced release probability is at least one part of the synaptic 5-HT effect.

3.2.3. effect of serotonin on recovery from depression

An important aspect of short-term depression not addressed yet is the recovery from depression. To study whether 5-HT would modulate recovery, stimulus spike trains were split in two parts with a step-like transition from high (depression train) to low stimulating frequencies (recovery train). During recovery IPSC amplitudes increased from the depression to 50 - 70 % of the first IPSC in depression train (Fig. 13A-B). Before this level was reached, transiently increased IPSC amplitude was observed (Fig. 13A). This transient was unlikely caused by the time constant that determined the depression because it was much slower.

The rate of recovery in both initial and steady-state phases was positively correlated to the preceding depression frequency, in both control and 5-HT conditions (Fig. 13A-C). As a measure for recovery, the first IPSC amplitude and the average IPSCs amplitudes following the first 5 IPSCs in recovery train were divided by the first IPSC amplitude in depression train (Fig. 13B-C). The recovery ratio at initial and steady-state phases over all tested frequencies was listed in Table 3. Based on these data presented here, no significant influence of 5-HT on recovery from depression can be inferred (Fig. 13D). It can not be excluded, however, that a larger sampling base might reveal such a difference.

3.2.4. impact of short-term depression in inhibitory inputs on spiking

The dynamic clamp experiments presented so far did not take short-term depression at the Purkinje cell to DCN synapses into consideration. Therefore, the dynamic clamp experiments described above were extended taking into account short-term depression. See the methods part for a description of its implementation. The experiments just described revealed that 5-HT did not alter the dynamic properties of short-term depression. Therefore, the parameters extracted from Raman et al. (2002) were suitable to simulate short-term depression not only for control conditions but also for 5-HT application. Since the absolute IPSC amplitude, however, was altered by 5-HT, the inhibitory input conductance had to be normalized to make results comparable. The normalization was chosen such that the mean inhibitory conductance with and without short-term depression was identical for an inhibitory input frequency of 35 Hz. This value was preferable since DCN showed identical frequency responses before and during 5-HT application at this level of inhibitory input. This way matched reference points were established for the effects of 5-HT and short-term

depression. As before, excitatory input was identical for all conditions and the frequency of inhibitory inputs was varied.

Short-term depression increased the output frequency of DCN neurons at high (> 35 Hz) inhibitory input frequencies thereby extending their working range to more hyperpolarized potentials (Fig. 14, left, filled gray circle). There was almost no change of output frequency for low (< 35 Hz) inhibitory input frequencies. The responses to synchronized inhibitory inputs and voltage-dependent excitatory inputs (Fig. 14A, right, black and gray filled columns) were significantly increased by 3.19 ± 0.27 Hz at 50 Hz input ($n = 5$, $p < 0.001$), by 3.93 ± 0.64 at 75 Hz input ($n = 5$, $p < 0.01$), but insignificantly reduced at depolarization range by 0.87 ± 1.76 at 10 Hz input ($n = 5$, $p = 0.64$) and by 1.73 ± 0.8 at 20 Hz input ($n = 5$, $p = 0.09$). This effect of short-term depression can be characterized as a normalization of the output spike rate for high inhibitory input frequency.

This normalization effect of short-term depression was further enhanced after 5-HT application (Fig. 14A, left, gray open circles). The spike rate was increased by 1.74 ± 0.76 Hz at 50 Hz input ($n = 5$, $p = 0.08$), by 0.67 ± 0.39 Hz at 75 Hz input ($n = 5$, $p = 0.16$). For low inhibitory input activity, 5-HT caused a reduction of input spike rate by 5.52 ± 3.08 Hz at 10 Hz ($n = 5$, $p = 0.14$), 2.05 ± 2.48 Hz at 20 Hz ($n = 5$, $p = 0.45$; Fig. 14A, right, gray filled and open columns). These effects did not reach significance levels of $p \leq 0.05$ due to variability between cells. Similar effects were found for synchronized inhibitory input and constant excitatory input (Fig. 14B). For unsynchronized inhibitory inputs these effects were much less pronounced (Fig. 14C-D).

The combined effect of short-term depression and 5-HT was further analysed by calculating the mean membrane potential (Fig. 15). Short-term depression caused a depolari-zation of the mean membrane potential at high inhibitory input frequencies (>35 Hz) for all stimulus conditions. Thereby, further hyperpolarization with increasing inhibitory input was almost completely prevented. At low inhibitory input frequencies, in contrast, short-term depression caused only a slight hyperpolarization (Fig. 15, left, gray filled circle). 5-HT caused an additional depolarization for all stimulus conditions (Fig. 15, left, open black and gray circles).

For synchronized inhibition and voltage-dependent excitation (Fig. 15A, right, black and gray filled columns), short-term depression depolarized the mean membrane potential value

from -58.1 ± 0.36 to -45.82 ± 0.61 mV at 75 Hz inputs ($n = 5$, $p < 0.001$), from -50.98 ± 0.52 to -45.77 ± 0.64 mV at 50 Hz inputs ($n = 5$, $p < 0.001$); while membrane potential was hyperpolarized from -32.47± 1.61 to -35.76 ± 1.45 mV at 20 Hz inputs ($n = 5$, $p < 0.001$), from -25.56 ± 2.09 to -28.89 ± 1.95 mV at 10 Hz ($n = 5$, $p < 0.001$). With short-term depression, application of 5-HT depolarized membrane potential overall insignificantly (Fig. 15A, right, gray filled and open columns). The effects of short-term depression were highly significant for all stimulus conditions (Fig. 15A, right, gray filled and open columns), while the additional depolarization caused by 5-HT was significant only for high inhibitory input without short-term depression (Fig. 15A, right, black filled and open columns). The mean membrane potential was depolarized by 5-HT from -50.98 ± 0.52 to -48.61 ± 1.18 mV at 50 Hz input ($n = 5$, $p < 0.05$), from -58.1 ± 0.36 to -56.23 ± 0.75 mV at 75 Hz input ($n = 5$, $p < 0.05$). Taken together, the effects of short-term depression and 5-HT on membrane potential extended the operation range of DCN neurons for high inhibitory input activity.

Information transmission is not only determined by spike rate but also by spike timing precision the analysis of which is presented in the following. Overall, spike timing precision was neither altered by short-term depression nor by 5-HT significantly (Fig. 16, left). Two exceptions were found for the trivial reason that neurons did not spike without short-term depression. Shot-term depression increased precision from 0 % to 59.55 ± 3.85 % at 75 Hz input of synchronized inhibition and voltage-dependent excitation (Fig. 16A, right, gray filled column, $n = 5$, $p < 0.001$) and from 0 % to 14.51 ± 4.88 % at 50 Hz input of unsynchronized inhibition and voltage-dependent excitation (Fig. 16C, right, gray filled column, $n = 5$, $p < 0.05$). Spike precision was also enhanced from 12.13 ± 6.2% to 27.57 ± 3.87 % at 10 Hz input of unsynchronized inhibition and constant excitation (Fig. 16D, right, black and gray filled columns, $n = 5$, $p < 0.05$). In this case precision might have been increased because short-term depression hyperpolarized the strongly depolarized membrane potential thereby increasing sodium channel availability. Taken together, these results suggest that information transmission is unlikely to be altered via effects of short-term depression or 5-HT on spike timing precision.

3.3. Pharmacological Consideration

Although the pharmacology of 5-HT was not the topic of the present study, some experiments were performed to address the question of which 5-HT receptor subtypes might mediate its effect on intrinsic DCN properties. To this end, specific agonists and antagonists for each receptor subtype were bath applied under current clamp. From immunohistochemical studies, it's known that 5-HT1, 2, 3, 5 receptor subtypes are expressed in rat cerebellar nuclei (Guerts, 2002). A broad range of 5-HT concentration (in μM: 0.1, 0.2, 0.5, 1, 2, 10) was tested, and identical effects was found from 1 μM to 10 μM (n = 2). The 5-HT_1 receptor agonist RU-24969 (0.5 μM, n = 2) and 5-CT, a 5-HT_5 agonist (5 μM, n = 3) caused effects identical to 10 μM 5-HT (Fig. 17A-B).

The effect of antagonists was dose-dependent. Application of 5-HT_1 receptor antagonist of Cyanopindolol (20 μM) prevented the depolarization by 1 μM 5-HT (n = 2), but failed to block that by 10 μM 5-HT (n = 2). Application of SB-266970 (20 μM), an antagonist of 5-HT_5 receptor, blocked the depolarization by 5 μM 5-CT (n = 1) but failed to prevent that by 10 μM (n = 3). In contrast, cinanserin (20 μM, n = 1), an antagonist of 5-HT_2 receptors, and Y-250 (20 μM, n = 3), an antagonist of 5-HT_3 receptors, failed to block the effects by 1 μM 5-HT. Overall, these results indicate that 5-HT_1 and 5-HT_5 receptors are the most likely candidates mediating the effects of 5-HT on the intrinsic properties of DCN neurons.

4. Discussion

How serotonin alters the signal processing of DCN neurons is the main question of my PhD project. The current clamp and voltage clamp experiments showed that 5-HT has an influence on intrinsic as well as synaptic properties of DCN neurons. First, 5-HT caused two opposing effects on excitability: it depolarized the membrane potential and it reduced the availability of voltage-gated sodium channels. The resulting impact of 5-HT on the firing activity of DCN neurons was determined with dynamic clamp and depended crucially on the interplay of these intrinsic effects and synaptic background activity. An activity-dependent effect of 5-HT was found, where the firing rate was reduced for depolarized pre-drug activity states but unaltered or slightly increased for hyperpolarized pre-drug states. Second, 5-HT reduced the strength of inhibitory input to DCN neurons without changing synaptic short-term depression significantly. Altogether the effect of 5-HT can be described as a change in the input-output transfer function that shifts the working range of DCN neurons to more hyperpolarized activity regimes reducing at the same time its slope.

4.1. Methodological Argumentations

Dynamic current clamp and its results represent an important part of this work. Therefore, two methodological aspects of dynamic current clamp are discussed in the following. Both aspects deal in different ways with the question how close a dynamic clamp experiment might be to the *in vivo* situation. The dynamic clamp method itself is described briefly in the introduction and detailed in the methods part.

The synaptic current representing the activity of whole populations of simulated input elements is usually injected via the patch clamp pipette into the soma of the recorded neuron. Therefore, the applied synaptic input is provided as a point source neglecting that synaptic input is distributed all over the cell *in vivo*. If everything else were identical to the *in vivo* situation how sever would the error be that one introduces this way? The following will show that the answer to this question depends on the neuron type, e.g. on the electrotonic compactness of a neuron. The voltage at the end of a sealed end core conductor like a dendrite is described by the equation:

$$V_{dendrite} = V_{soma}/\cosh(x_{dendrite}/\lambda),$$

where λ represents the electrical length of its semi-infinite counterpart. The electrotonic length of DCN dendrites is maximally 0.5 λ (Steuber et al., 2004). Therefore, the amplitude

difference between somatic and dendritic voltage signals is less then 12 % in DCN neurons ($(1-V_{dendrite}/V_{soma})*100$). Pyramidal cells in contrast have a dendritic length of about 2 λ (Ulrich and Strick, 2000) and consequently the voltage difference between soma and dendritic tip will be 73 %. This clearly illustrates that the error introduced by simulating a point source of synaptic input will crucially depend on the electrotonic properties of the recorded neurons and that it is comparatively low for the compact DCN neurons. The same is true for the shunting effect that is affected only half as strong by distance as the amplitude of voltage signals (Williams, 2004).

Another aspect of the dynamic clamp approach is actually not specific but applies to all simulation methods. That is the question how well the properties of the simulated activity match that *in vivo*. In the present study this applies to the properties of the simulated synaptic activity. Relevant parameters are for example the number of input elements, their mean frequency, their activity patterns, and the amplitude, time course and voltage dependence of postsynaptic conductances. Some of these parameters are known quite accurate, some are known approximately and others are completely unknown. The time course and the voltage dependence of postsynaptic conductance changes are known quite precisely (Pedroarena and Schwarz, 2003; Telgkamp and Raman, 2002, Anchisi et al., 2001). The amplitude of postsynaptic conductances are either unknown (AMPA and NMDA components) or their estimates vary over a wide range (Pedroarena and Schwarz, 2003; Telgkamp and Raman, 2002). The same is true for the number of input elements were the estimates range from 30 to 800 (Palkovitz et al., 1977). The activity patterns of individual input elements, excitatory and inhibitory, might be available, but the population activity of the input elements of individual DCN neurons is completely unknown. Therefore, assumptions have to be made for those partly or completely unknown parameters. With respect to the total mean inhibitory and total mean excitatory input for example, two parameters also completely unknown but of utter importance, it turns out that the number of input elements and the amplitude of individual inputs are interchangeable. 100 inputs of amplitude 1 (here arbitrary unit) provide the same mean input as 400 inputs of amplitude 0.25. What changes are statistical properties of the input, e.g. the amplitude fluctuation of the total input will drop from 100 to 400 elements. Because of this commutability, the stimulus design started out with the assumption that the overall input has to be in a kind of equilibrium that allows the neurons to spike with reasonable, that is *in vivo*-like, rates. This determined the balance between excitatory versus inhibitory inputs

and due to the interdependence just described also the input amplitude as soon as a particular input number was chosen. Starting out with such a consideration about equilibrium might seem a bit unusual. But it makes perfect sense taking into consideration that many of the processes that physiologists studied in the past, including synaptic and intrinsic plasticity, are serving actually the goal to maintain homeostasis which is required to keep neurons in an operational regime where they can respond best to incoming signals.

The amplitude of the simulated inhibitory inputs was actually lower then the lowest of the widely ranging estimates (Peroarena and Schwarz, 2003; Telgkamp and Raman, 2002), therefore the dynamic clamp stimuli under rather then overestimated the impact of synaptic shunting that was crucial for the results. For excitatory input only two aspects were simulated: its overall mean and its voltage dependence. The amplitude fluctuation caused by unitary excitatory events was neglected. This does not impose any limitation since inhibitory inputs can trigger action potentials via brief disinhibition (Gauck and Jaeger, 2000) just as reliable and frequent as excitatory inputs as described in Gauck and Jaeger (2003). With respect to the pattern of inhibitory input activity randomly spiking input elements were chosen. On the one hand, because information about population input activity is not available on the other hand because this approach is akin to the white noise approach from systems theory. The basic idea behind that is to probe a system with a wide range of input patterns to evaluate its dynamic response properties. The simulated input was not white noise of course, because the postsynaptic conductances act as low pass filters. But otherwise, e.g. because of the random Poisson-like input activity, the DCN neurons were activated with a large range of input dynamics likely to cover the physiologically relevant one. This range was further extended by testing two levels of input synchronization resulting in two levels of input fluctuation around identical means and various inhibitory input frequencies. Therefore, the dynamic clamp stimuli probed DCN neurons with a wide range of potentially occurring stimulus properties.

4.2. Effects of Serotonin on Intrinsic Properties

5-HT had multiple effects on intrinsic DCN properties. In current clamp, it depolarized the membrane potential and reduced the availability of voltage-gated sodium channels. Both 5-HT actions are expected to influence DCN excitability but in opposite directions. Depolarization was caused by an increase of a tonic cationic current as well as a reduction of a tonic potassium current most likely via the activation of 5-HT_1 or/and 5-HT_5 receptors. At dynamic current clamp, 5-HT caused an activity-dependent effect on firing performance. This activity dependence was due to background synaptic activity that influenced the state of the neuron and thereby indirectly the effect of 5-HT. Therefore, the effect of 5-HT is likely to depend also on the state of the network comprising the input elements of DCN neurons.

4.2.1. regulation of firing by serotonergic effect and background synaptic activity

Based on the results from the current clamp and dynamic clamp experiments, a model (Fig. 18) was developed to explain the activity-dependent effect of 5-HT. The question this model is supposed to explain is why 5-HT did not alter DCN activity always in the same manner but instead caused a slight increase for low and a reduction for high pre-drug activity levels? The brief answer is that background synaptic activity determined the relative impact of two 5-HT actions, depolarization and sodium channel reduction. Membrane depolarization is usually addressed as an increase in neuronal excitability (Perrier et al., 2003; Möck et al., 2002; Monckton and McCormick, 2002; Andrade, 1998). Reduced sodium channel availability, in contrast, is addressed as a reduced excitability as it will reduce the probability for a given input to trigger an action potential. The third player in this game is synaptic shunting that depends linearly on the strength of background synaptic activity. Synaptic shunting has been reported to decrease the slope of neuronal input-output transfer functions (Mitchell and Silver, 2003; Chance et al., 2002). Figure 18 illustrates how these three factors are thought to interact in the control of DCN activity.

The voltage and current clamp experiments showed that the 5-HT induced an inward current and the resulting depolarization depended little on the DCN membrane potential. The availability of sodium channels however dropped with an increasing depolarization. If 5-HT is depolarizing DCN neurons while reducing their sodium channel availability, it is difficult to predict whether the spike rate should rise or fall. The relative impact between these 5-HT effects is obviously decisive here. At hyperpolarized potentials sodium channel

availability is high enough such that the additional recruitment of sodium channels by depolarization will outnumber the reduced availability by 5-HT. Consequently, 5-HT will increase the spike rate. At depolarized potentials sodium channel availability is already low and a further reduction by 5-HT will outnumber an additional recruitment by depolarization. The net effect is a reduced spike rate after 5-HT application. Therefore, the input-output curves before and after 5-HT application should cross each other at an intermediate activity level. This exactly was observed experimentally. If the model where correct, one should be able to predict the results of new experiments. This was done. Background synaptic activity determined the DCN activity level to a considerable degree via its shunting effect. Therefore, it should be possible to manipulate the 5-HT induced depolarization by changing the strength of synaptic shunting. A reduced shunting magnitude should allow more depolarization and shift the crossing point to more depolarized potentials. An increased shunting, in contrast, should reduce 5-HT induced depolarization and shift the crossing point to more hyperpolarized potentials.

These predictions were actually confirmed in two kinds of experiments. This was an important support for the interpretation of the data. Furthermore it nicely demonstrates how the effect of a given neuromodulatory input might depend on the functional context as it is set by the network activity of non-modulatory inputs. Interestingly, a similar activity-dependent effect of 5-HT has been described *in vivo* where the spiking activity of Purkinje cells was reduced for high pre-drug activity and enhanced for low predrug-activity (Strahlendorf et al., 1984).

4.2.2. ionic channels modulated by serotonin

The effects of 5-HT on the intrinsic properties of DCN neurons that were crucial for the activity dependence just described were a reduction of voltage-gated sodium channel availability, an enhancement of tonic cationic current and a reduction of tonic potassium current. This was concluded indirectly based on an evaluation of the action potential slopes and the IV-curves. The underlying channel types, however, were not identified pharmacologically. On the one hand, this was not the focus of the present study; on the other hand, this would have extended its time frame tremendously. Potential candidates for involved current types, however, are known from other preparations. 5-HT has been reported to depolarize rat spinal motoneurons by inhibiting a TASK-1-like potassium current (Perrier et al., 2003) and in mouse PFC neurons it reduced the availability of a slow-inactivated

sodium current (Carr et al., 2003). In mice DCN neurons, a voltage-independent tonic cationic current is responsible for the depolarization during the interspike interval period (Raman et al., 2000). This current might be a candidate to be modulated by 5-HT via type 1 and/or 5 receptors. However, it was not possible to test this experimentally because this current has not been characterized pharmacologically yet.

A reduction in sodium channel availability by 5-HT was inferred from a reduced uprising action potential slope. This is supposed to be a highly sensitive measure because no other channel type alters its activation stronger during the uprising AP slope than sodium channels (Azouz and Gray, 2000). The slope reduction was partially washed out, like the other 5-HT effects, ruling out the possibility that it was caused by a reduction in recording quality over time. Other criterions, like spike amplitude and spike threshold, are also used to estimate the sodium channel availability. Those parameters were not presented here but they were analysed as they underlie the calculation of AP slope. The spike amplitude was also reduced by 5-HT, but spike threshold was not if plotted against the mean membrane potential even so the spike rate was. One possible reason might be that potassium channels that contribute to the spike threshold were also reduced by 5-HT such that its effects on sodium and potassium channels cancelled each other regarding spike threshold. The discrepancy between this criterion and the others is nevertheless puzzling. Because of the dominant role of sodium channel activation for action potential upstroke, however, the slope criterion appears to be the most reliable one. Therefore the reduced depolarizing slope was taken as an indicator of reduced sodium channel availability by 5-HT.

Are other intrinsic currents of DCN neurons also possible targets of 5-HT? The spike triggered averages of the voltage trace suggest that 5-HT reduced a fast afterhyperpolarizing current in DCN neurons. This could either be an A-type potassium current or a BK current (Kang et al., 2000). Since the availability of voltage-gated sodium channels is about 25 % for the spontaneous activity level of DCN neurons (Raman et al., 2000), a reduced after-hyperpolarization is likely to further reduce the sodium channel availability reducing their de-inactivation after spikes. Therefore, the overall intrinsic effects of 5-HT depolarized DCN neurons but at the same time it reduced their spike generation ability.

According to the current clamp and voltage clamp recordings, two groups of DCN neurons might have been recorded. DCN neurons differed with respect to the IV-curves and with respect to their propensity to enter a depolarizing block after 5-HT application.

However, no correlation was found between these properties and the soma size of DCN neurons that can serve as a criterion to separate small, intermediate sized and large DCN neurons (Czubayko et al., 2001; Chan-Palay, 1977). However, it can not be excluded that various neuron types were recorded that more elaborate anatomical and immunohistochemical methods would have allowed identifying. The long recording times, however, made such an anatomical analysis unfeasible because a reciprocal correlation exists between the success of anatomical reconstructions and recording time (personal experience communicated by Dr. V. Gauck, Dr. F. Sultan, and Dr. D. Jaeger).

Agonists of 5-HT1 and 5-HT5 receptors had the same effect as 5-HT on the availability of sodium channels. A similar action of 5-HT is known from rat cortical neurons, where the activation of 5-$HT1_A$ receptor blocked voltage-sensitive sodium channels (Melena et al., 2000). The finding that different receptor subtypes mediated identical effects is in contradiction to the classical suggestion that each 5-HT receptor subtype should have its unique specific action. One possible reason for such a result might be that the actions of the serotonergic drugs used were not specific enough (Glennon et al., 2000). Another possibility, however, is that various receptor subtypes use actually a common final path of signaling cascades (Andrade, 1998). Examples are known also from other preparations like the mouse subthalamic nucleus where 5-HT increased the membrane excitability via 5-$HT2_C$ as well as 5-HT4 receptors while activation of 5-HT1 receptor resulted in a reduction (Stanford et al., 2005). Furthermore, in mouse hippocampus CA1 neurons, activation of 5-HT4 as well as 7 receptors increased I_h and shifted its activation curve (Bickmeyer et al., 2002). Therefore, the 5-HT1 and 5 receptor triggered signaling cascades might converge onto a common final signaling path in DCN neurons.

The results presented here differed with respect to the effect of 5-HT on spontaneous activity of DCN neurons from two former *in vitro* studies where 5-HT was applied iontophoretically and different effects on spontaneous activity of rat DCN neurons were observed (Cumming-Hood et al., 1993; Gardette et al., 1987). However, these two studies are even conflicting with each other, in which either excitation or inhibition as well as excitation or no impact was reported. Different experimental procedures might be responsible for these differences.

4.3. Effects of Serotonin on Synaptic Transmission

Besides intrinsic properties I tested also the effect of 5-HT on the synaptic properties of DCN neurons and focused on inhibitory input because of the prominent functional role that it likely has for DCN neurons. 5-HT reduced the strength of inhibitory synapses to DCN neurons over a wide range of presynaptic firing frequencies. Within this frequency range, however, neither short-term depression nor recovery from depression were altered by 5-HT. Therefore, 5-HT reduced the strength of inhibitory synaptic transmission but did not alter short-term plasticity.

4.3.1. mechanism of serotonin action

Recording spontaneous IPSCs revealed a reduced frequency and reduced postsynaptic amplitude after 5-HT application. The first observation would result from a reduced release probability for vesicles while the second result could result from reduced sensitivity of postsynaptic $GABA_A$ receptors but also from a reduced presynaptic vesicle release probability. Therefore, the results indicate that presynaptic as well as postsynaptic mechanisms are responsible for the effect of serotonin on inhibitory synaptic transmission to DCN neurons. The recording of miniature IPSCs combined with a statistical analysis and/or single channel recordings might reveal the contribution of pre- and postsynaptic mechanisms to the synaptic 5-HT effect. Those experiments, however, were beyond the scope of the present project.

The present results seem to be in conflict with an *in vivo* study by Kitzman and Bishop (1997), where 5-HT potentiated the inhibitory effect of GABA in the interposed nuclei. However, more complicated uncontrolled effects of 5-HT on local networks in the study by Kitzman and Bishop might account for the difference.

4.3.2. functional role of short-term depression in DCN activity

Short-term depression can be addressed in general as a temporal filter of synaptic transduction (Chung et al., 2002; Chance et al., 1998; Abbott et al., 1997). Therefore, short-term depression adds a dynamic property to the signal transduction between Purkinje cells and DCN neurons that is likely to be of functional importance (Telgkamp and Raman, 2002; Pedroarena and Schwarz, 2003). Its functional role, however, has not been studied yet. In the present work some of these functional aspects were addressed using dynamic current clamp. Inhibitory conductance traces were generated taking into consideration the dynamics

of short-term depression. To this end the parameters of a model by Varela et al. (1997) were fitted to match the data published by Telgkamp and Raman (2002). Model development, fitting procedure and stimulus generation were all done by my supervisor Dr. V. Gauck and are therefore not extensively described here. A brief description of the model by Varela et al. (1997) and the other procedures is provided in the methods part. 5-HT and short-term depression both influence the signal processing in DCN neurons and therefore the question was how each of these factors acts in isolation and what their combined action might be. For low and intermediate frequencies of the inhibitory input elements there was little difference in the membrane potential with and without short-term depression. For high input frequencies, in contrast, the membrane potential was much more depolarized with short-term depression compared to control. Increasing the inhibitory input frequency caused actually little additional hyperpolarization at high frequencies. As a result the DCN neurons continued to spike at inhibitory input levels where they were completely silenced otherwise. Meanwhile, the spike timing precision on the other hand was not altered by short-term depression. It depends on the amplitude fluctuation of the inhibitory input conductance (Gauck and Jaeger, 2000, 2003) which in turn depends on changes in input frequency and on input synchronization. Short-term depression has no effect whatsoever on input synchronization and its consequences. Its effect on momentary frequency changes as present in Poisson-like input patterns is also negligible as the unaltered spike timing precision suggests. Based on paired pulse depression experiments (Pedroarena and Schwarz, 2003) one might have expected otherwise. But such an argument would hold only on a superficial level. Paired pulse stimulation overestimates the depression occurring during ongoing activity because it relates high input frequencies, the reverse of the interval between paired pulses, to an unphysiologically low input frequency close to zero, the reverse of pauses between stimulation pairs.

Taking into consideration that Purkinje cells can maintain high frequencies it is an open question how DCN neurons maintain an ongoing activity in the presence of such a barrage of inhibitory input. The finding presented here might provide an important aspect to answer this question. Spike rate and spike timing determine together the amount of information that can be transmitted via a spike train. The dynamic clamp experiments showed that short-term depression extended the range of information transmission for DCN neurons very effectively into the regime of high inhibitory input activity. On function of short-term depression would consequently be a progressive suppression of synaptic strength with

increasing inhibitory input frequencies such that DCN neurons are able to respond to incoming signals like brief changes in spike rate or pulses of synchronized input even at high inhibitory input frequencies.

Like short-term depression, 5-HT increased the spiking activity at hyperpolarized potentials. This effect was less robust for 5-HT then short-term depression but it acted in the same direction. At depolarized membrane potentials, where short-term depression had little impact, 5-HT caused a robust reduction in spike rate. Therefore, short-term depression and 5-HT acted together in changing the input-output characteristic of DCN neurons such that differences in baseline inhibitory input activity were filtered out to a large part but the effects of brief changes in frequency and input synchronization were transmitted effectively.

5-HT reduced also the strength of inhibitory synaptic inputs. This finding was not implemented in the dynamic clamp experiments but the results would have been identical except for one scaling factor valid for all input frequencies. A single scaling factor is sufficient because 5-HT changed the IPSC amplitude but left short-term depression unaltered. Therefore, DCN neurons would become further depolarized by 5-HT via its synaptic effect but in contrast to its intrinsic effects without a reduction in DCN excitability. The resulting DCN activity would exactly correspond to the recorded input-output frequency curves but shifted somewhat to the right corresponding to higher inhibitory input frequencies.

The level of 5-HT is elevated in the cerebellum during periods of increased motor activity (Mendlin et al., 1996). What effects might it have on DCN activity? Based on the results presented here, one can expect that 5-HT acts in concert with short-term depression such that DCN neurons are capable to transmit transient input signals over a much wider range of inhibitory input activity then it would be possible without these two adapting mechanisms.

4.4. Functional Consideration

4.4.1. serotonin: the functional role?

Is there a specific functional role of serotonin in the central nervous system? The serotonergic system has been suggested to serve many different functions such as motor activity, sleep cycle, stress and learning (Schweighofer et al., 2004; Jacobs and Fornal, 1999) and it regulates a variety of ionic currents in different brain regions. There seems to be no uniform action or effect of the serotonergic system in the brain (Glennon et al., 2000; Andrade, 1998). Based on its high heterogeneity regarding receptor subtypes and its widespread distribution, it has been suggested that the serotonergic system might be ideally suited to remodel membrane excitability in various brain regions rather independently from each other adjusting each region to its specific functional requirements (Andrade, 1998). The cooperation between 5-HT and other neuromodulatory transmitter systems, briefly described in the introduction, adds a further level of complexity but is likely to serve the same goal of adjusting various local networks to the momentary computational demands (Schweighofer et al., 2004; Andrade, 1998).

All parts of the cerebellum receive abundant serotonergic innervations. It is interesting to note that 5-HT has been reported to reset Purkinje cells *in vivo* to a preferred intermediate firing rate (Strahlendorf et al., 1984), a finding very similar to the activity-dependent effect of 5-HT on DCN neurons described in the present study. The exact functional role of 5-HT in the cerebellum remains to be resolved. The present study, however, provides evidence that the serotonergic input acts together with other adaptive mechanisms like short-term depression to adjust the working range of DCN neurons such that they can transmit transient signals for a wider range of inhibitory input levels. Similar functional roles are accomplished by mechanisms of adaptation in various sensory systems. The study by Strahlendorf et al. (1984) indicates that 5-HT might serve a similar function in the cerebellar cortex.

4.4.2. clinical consideration

Several possible causes for cerebellar ataxia have been reported including disturbances of the cerebellar serotonergic system (Trouillas, 1993), a loss of inhibitory input from the cerebellar cortex to the DCN (Sausbier et al., 2004; Orr, 2004) and an enhanced excitability of DCN neurons (Shakkottai et al., 2004). On the other hand it has been reported that treatment of ataxia with serotonergic substances might release symptoms (Trouillas et al.,

1993; Takei et al., 2005). The present study provides evidence that 5-HT might actually reduce hyper-activity within the DCN by reducing the slope of its input-output function and thereby making DCN activity less dependent on the baseline level of Purkinje cell input. Future therapeutical approaches might benefit from a more detailed mechanistic understanding of 5-HT actions on the cellular level.

Figure 1. Scheme of this project.

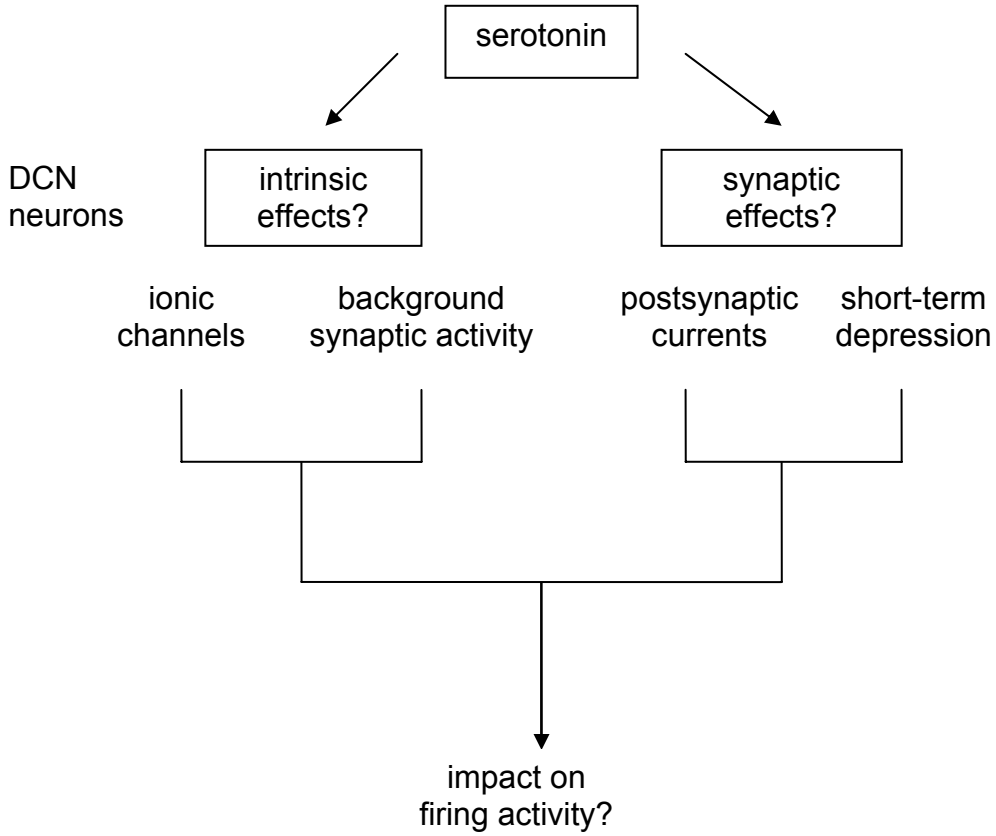

Figure 2. Gross anatomy and electrophysiological properties of DCN neurons. **A**, Gross features of three DCN nuclei. (Adapted from *Principle of Neuroscience*) **B**, Synaptic organization of cerebellar circuit. **C**, The response of DCN neuron at hyperpolarizing current injection. A depolarizing sag is developing after the onset of hyperpolarizing current injection, and a rebound depolarization after the offset of current injeciton.

A

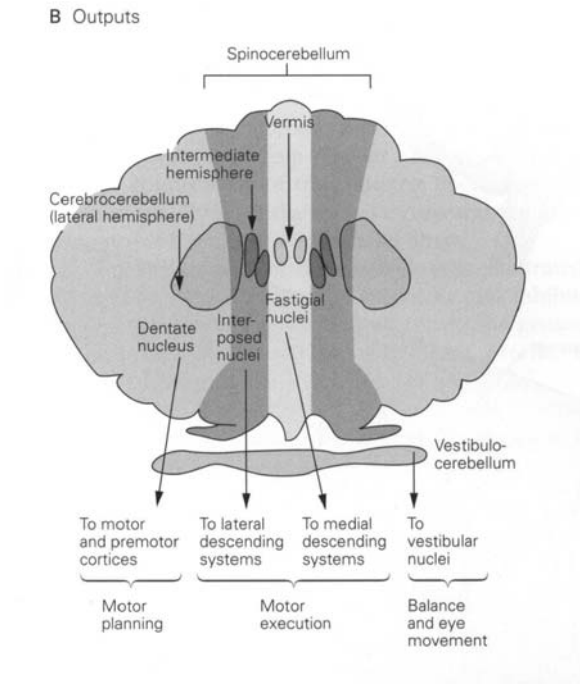

C

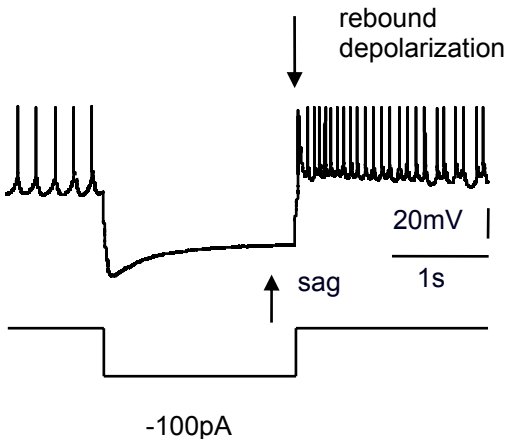

B

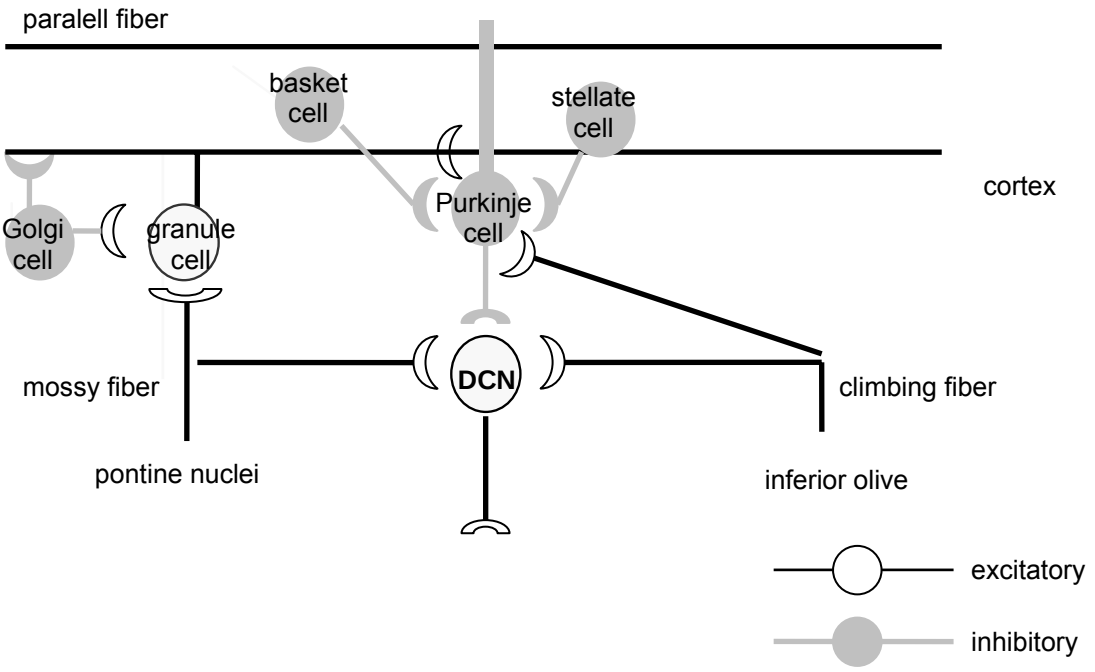

Figure 3. Dynamic current clamp. **A**, Main principle of dynamic current clamp. Based on the equation $I_{syn} = G_{ex}(t)*(E_{ex}-V_m) + G_{in}(t)* (E_{in}-V_m)$, an in-vivo like current (I_{syn}) is calculated from the driving force and the simulated conductance and injected into the recorded neuron. **B**, Construction of dynamic clamp stimulus. This example is with 100 inhibitory input elements each spiking at 35 Hz and 10 excitatory input elements spiking at 20 Hz. The total inhibitory conductance ($G_{in}(t)$) is the sum of all unitary conductances (g_{in}) that replace the poisson-distributed input spikes: $G_{in} = \Sigma\ [1/(\tau_{decay} - \tau_{rise})*(e^{-(t/\tau decay)} - e^{-(t/\tau rise)})]$. The same procedure was used for the excitatory conductance ($G_{ex}(t)$).

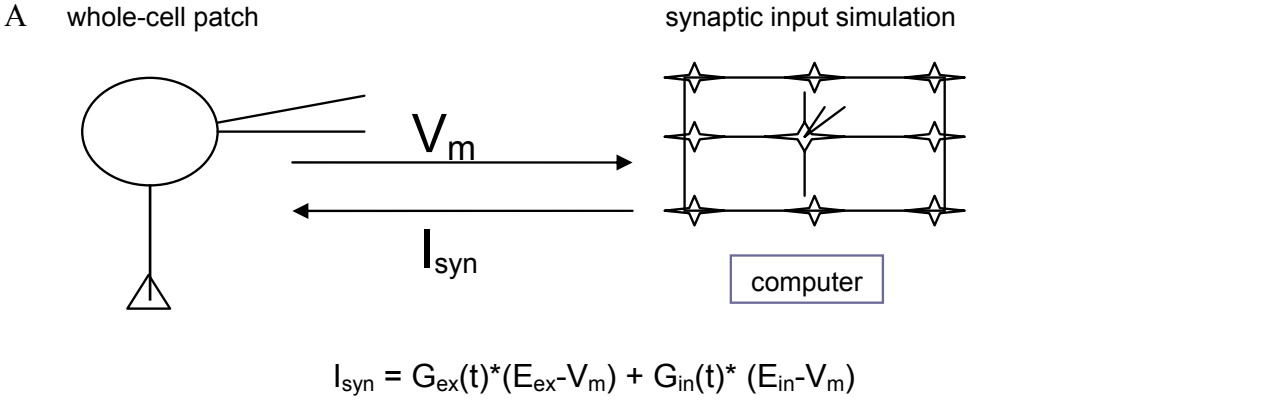

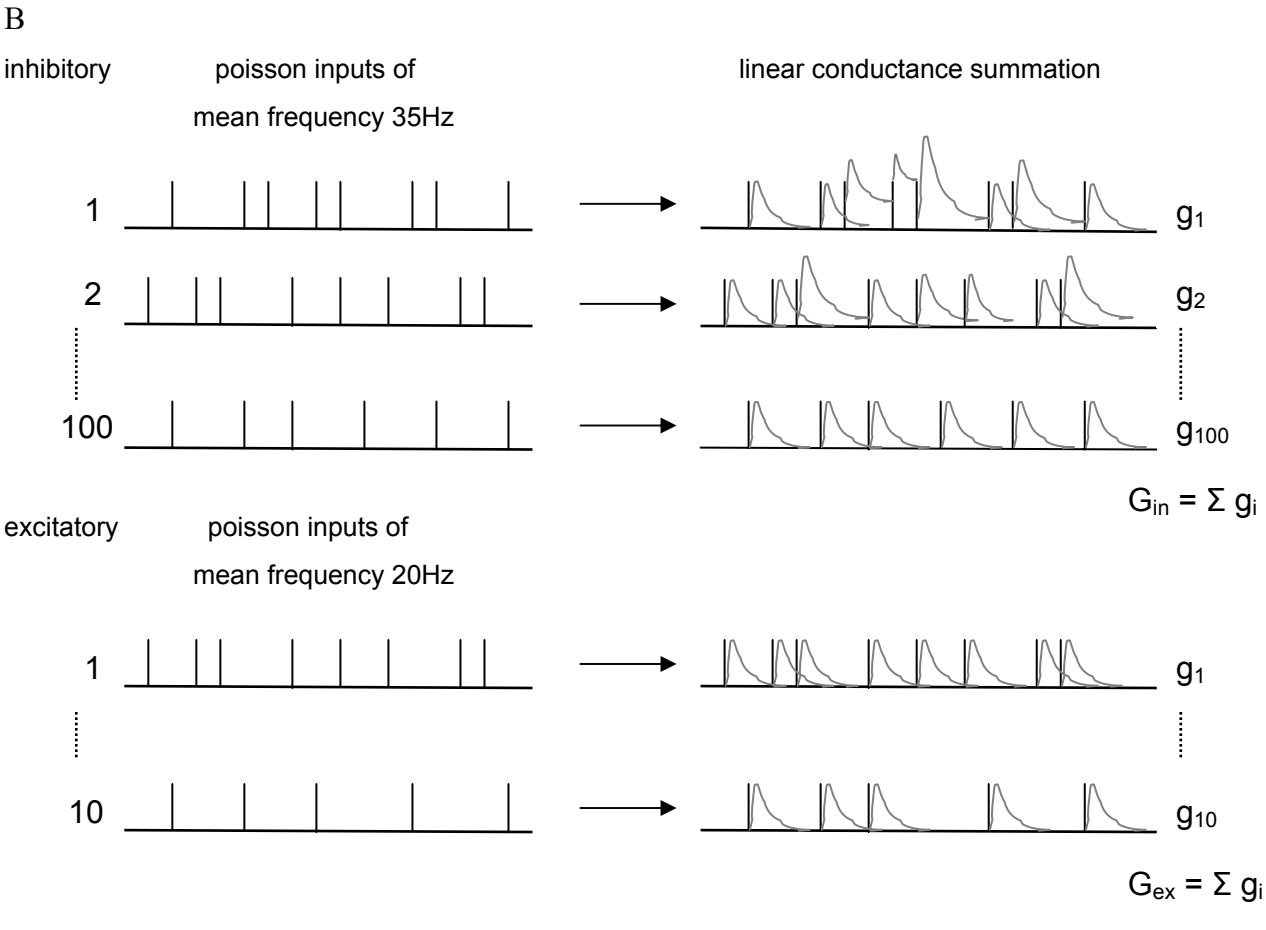

Figure 4. Effect of 5-HT on the firing activity of DCN neurons at current clamp. **A**, The voltage trace of one typical neuron, before (black line), during (dark gray) 10 μM 5-HT application and after long time wash (light gray). **B**, The relation between mean firing rate and injected current, before (black filled circle), during (open circle) 10 μM 5-HT application and after long time washout (gray filled circle), averaged from 27 neurons. **C**, Depolarization block induced by depolarizing current injection, from one typical neuron.

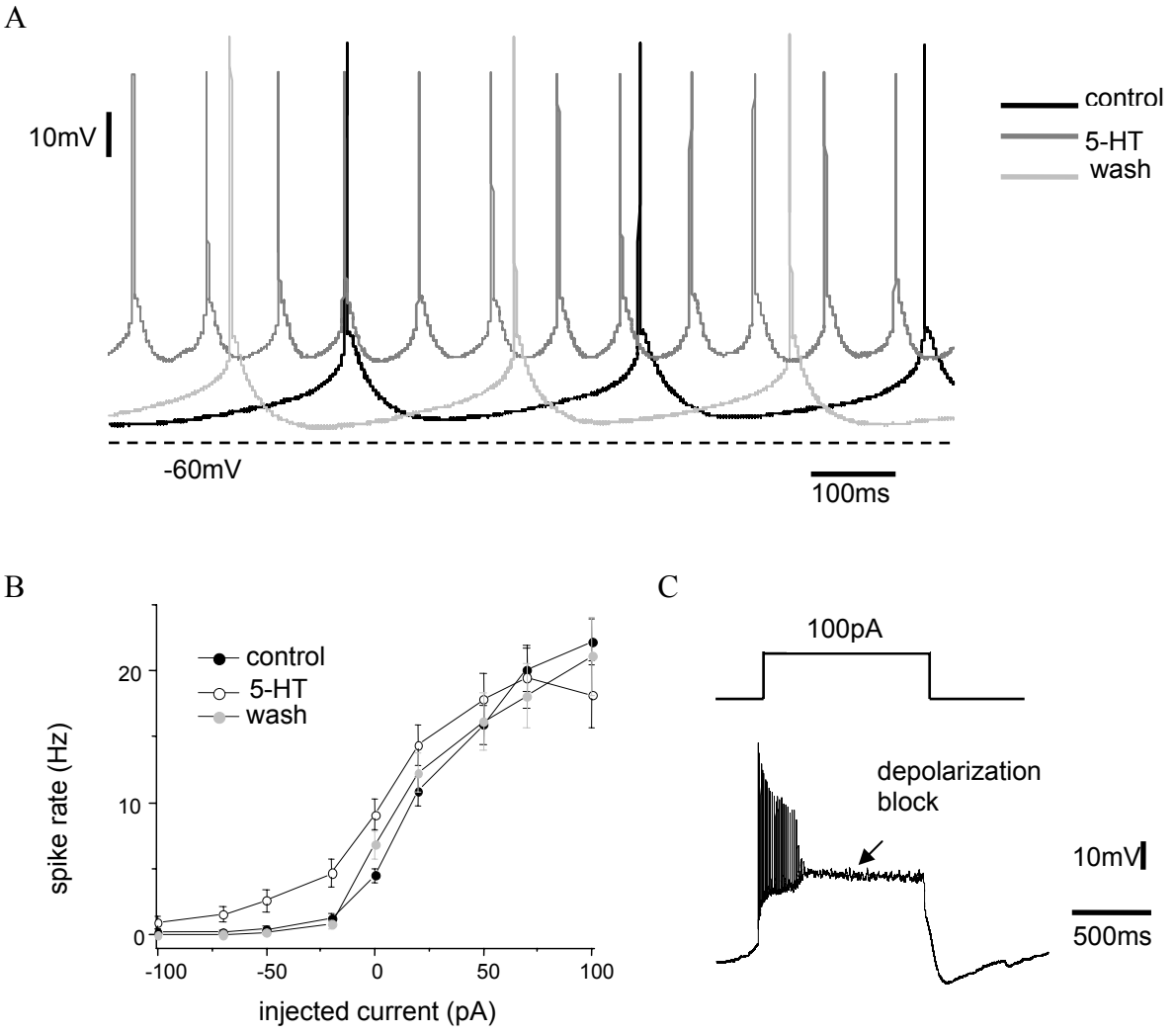

Figure 5. Effect of 5-HT on current-voltage relation (IV-curves) at voltage clamp, in the presence of TTX, TEA, 4-AP, Co^{2+}. Control (black), 5-HT (gray). **A**, The holding current trace corresponding to the voltage step from -50 mV to -20 mV. **B**, Holding current in response to a voltage step from -50 mV to -80 mV. **C**, Parallel shift of IV-curve by 5-HT from one representative neuron. **D**, IV-curve after 5-HT application intersects with IV-curve under control at +5mV, from one representive neuron. **E-F**, The same analysis as in C and D after I_h current subtraction.

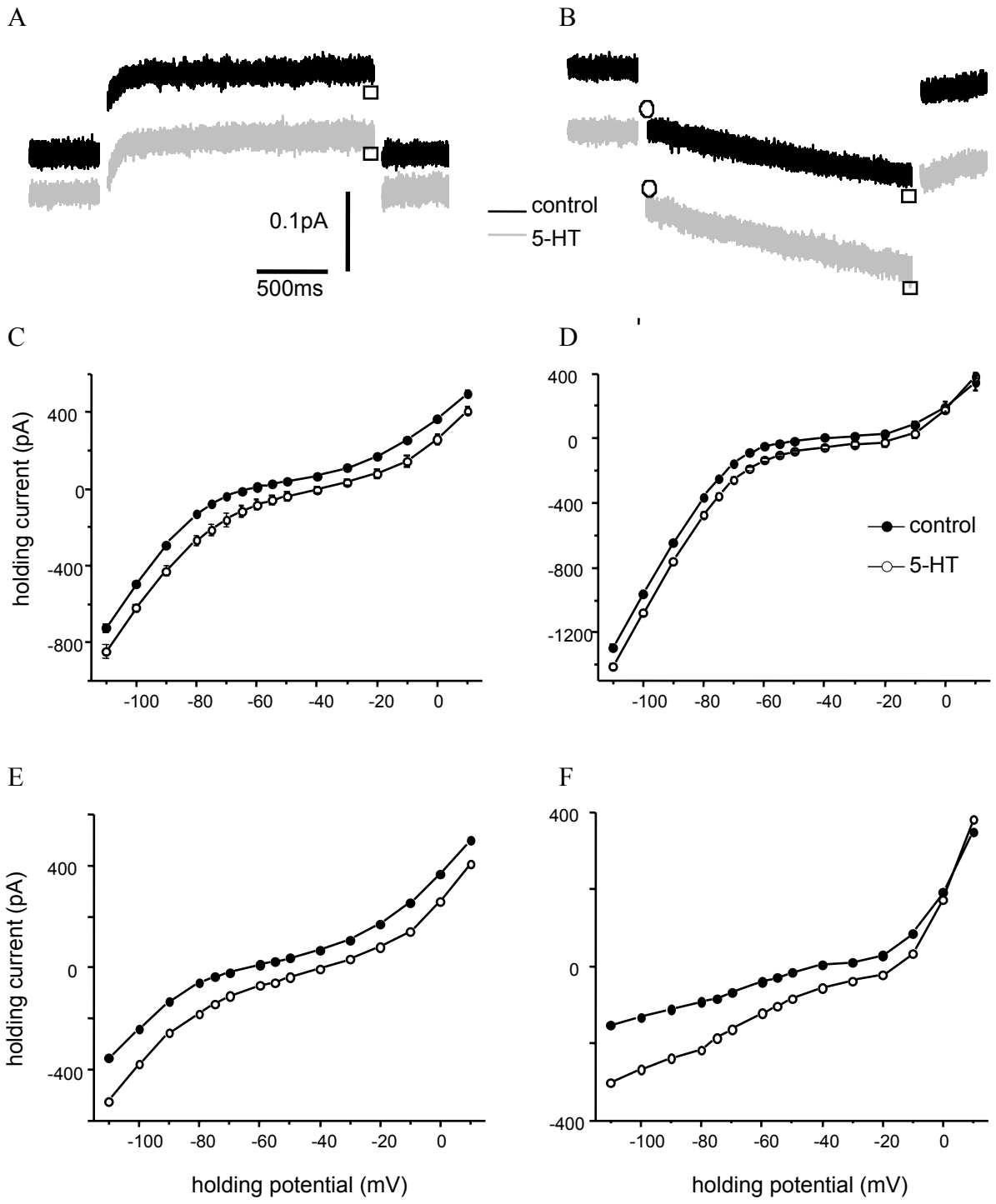

Figure 6. The effects of 5-HT on action potential waveform of DCN neurons in current clamp. **A**, Spike triggered average of voltage trace of one typical DCN neuron, before (black line), during (dark gray) 10 μM 5-HT application and after long time washout (light gray) under spontaneous spiking. **B**, Rate of depolarization (top) at current injection of 25, 50, 75 pA plotted as a function of the corresponding mean potential values, the same analysis for spike amplitude (middle) and spike threshold (bottom), averaged from 9 neurons. *P < 0.05, **P<0.01 with paired-t test.

A

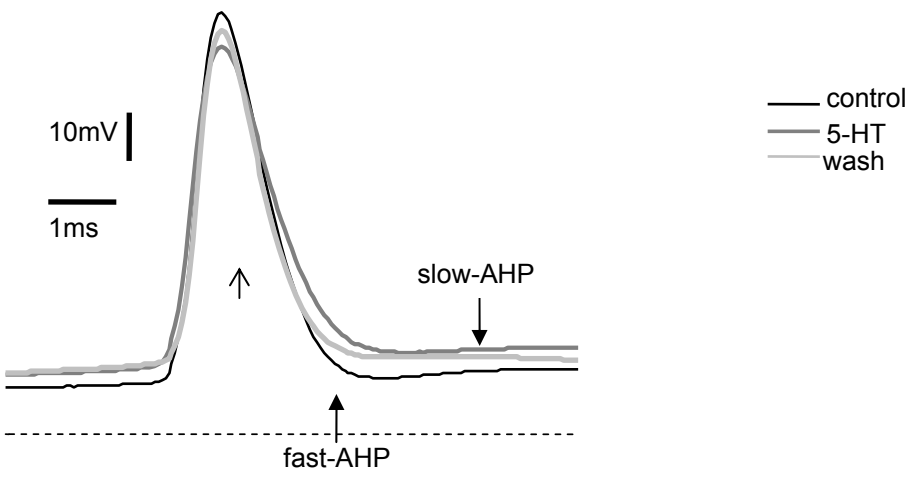

B

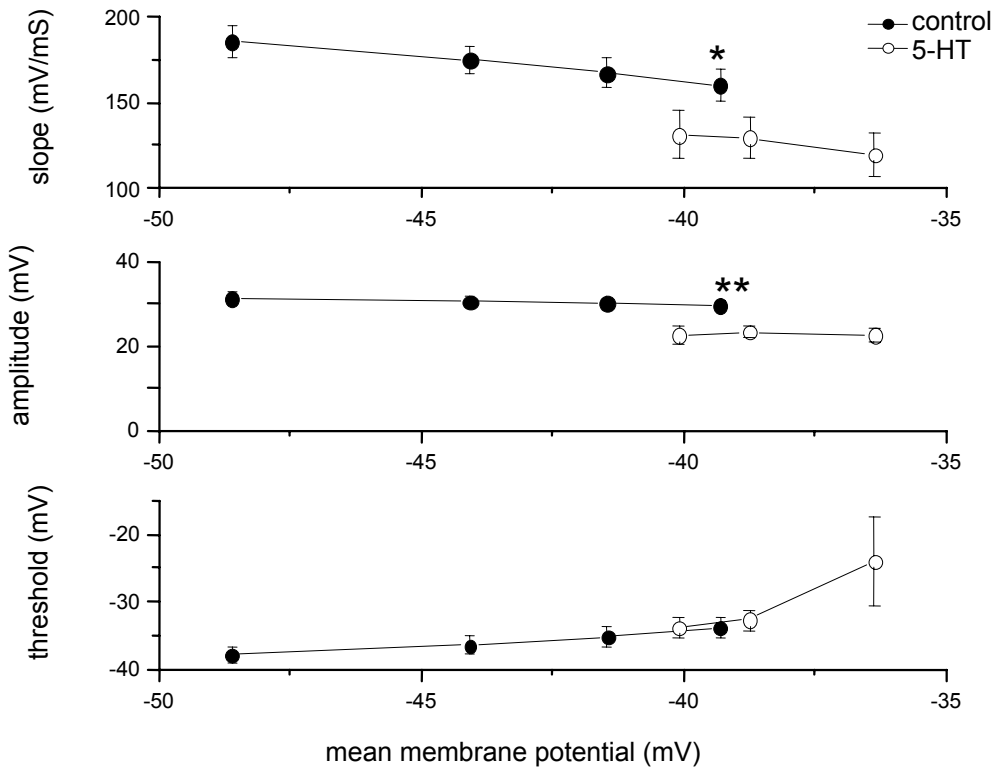

Figure 7. The effect of 5-HT on the spike rate under dynamic clamp at inhibitory input frequency of 35 Hz. **A**, Voltage trace and raster plot in response to synchronized inhibitory and constant excitatory inputs, from one typical neuron. **B**, Spike rate in response to four simulated stimuli: synchronized (syn) or unsynchronized (unsyn) inhibition (in) and voltage-dependent or constant excitation (ex) before (filled column) and during (open column) 5-HT application, averaged from 6 cells. *P < 0.05 with pair t-test.

A

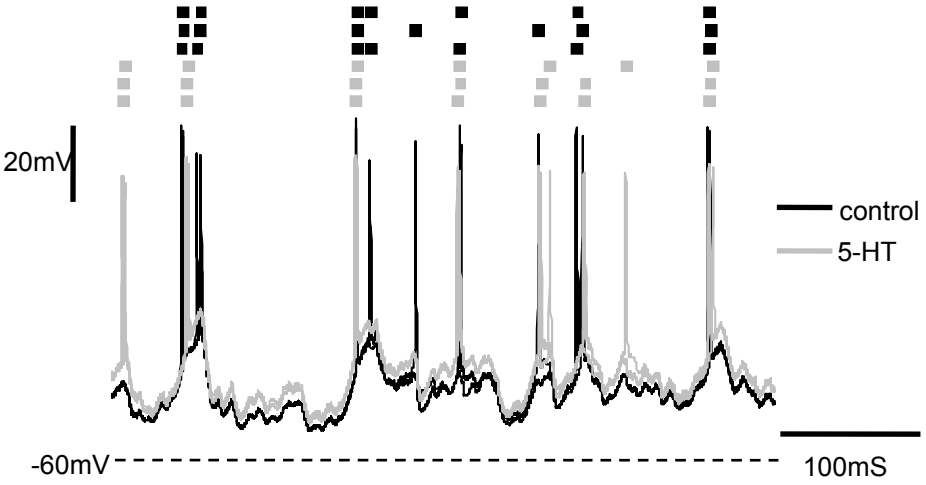

B

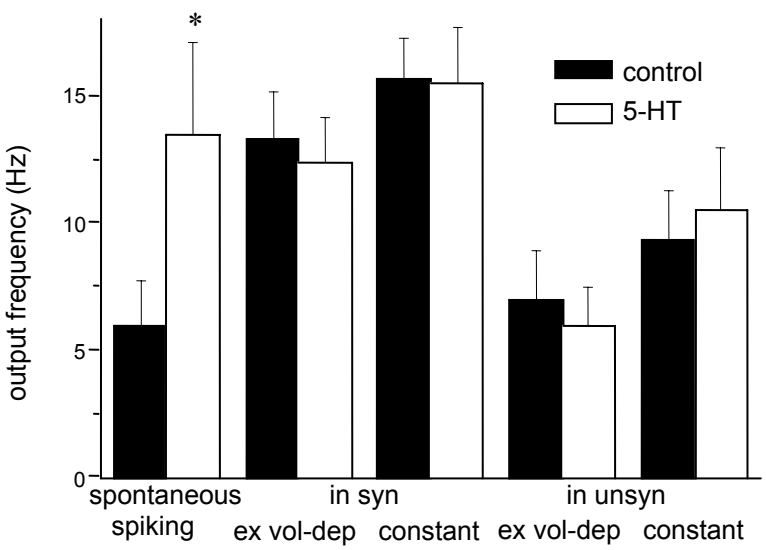

Figure 8. The effect of 5-HT is activity-dependent at dynamic clamp. **A**, Spike rate plotted as a function of inhibitory input frequency, in response to simulated stimuli of synchronized or unsynchronized inhibitory (G_{in}) inputs combining with voltage-dependent or constant excitatory (G_{ex}) inputs, before (filled circle) and during (open circle) application of 10 μM 5-HT, averaged from 9 cells. **B**, Spike precision against inhibitory input frequency, with a time window of ± 5 ms. *P < 0.05 with paired t-test.

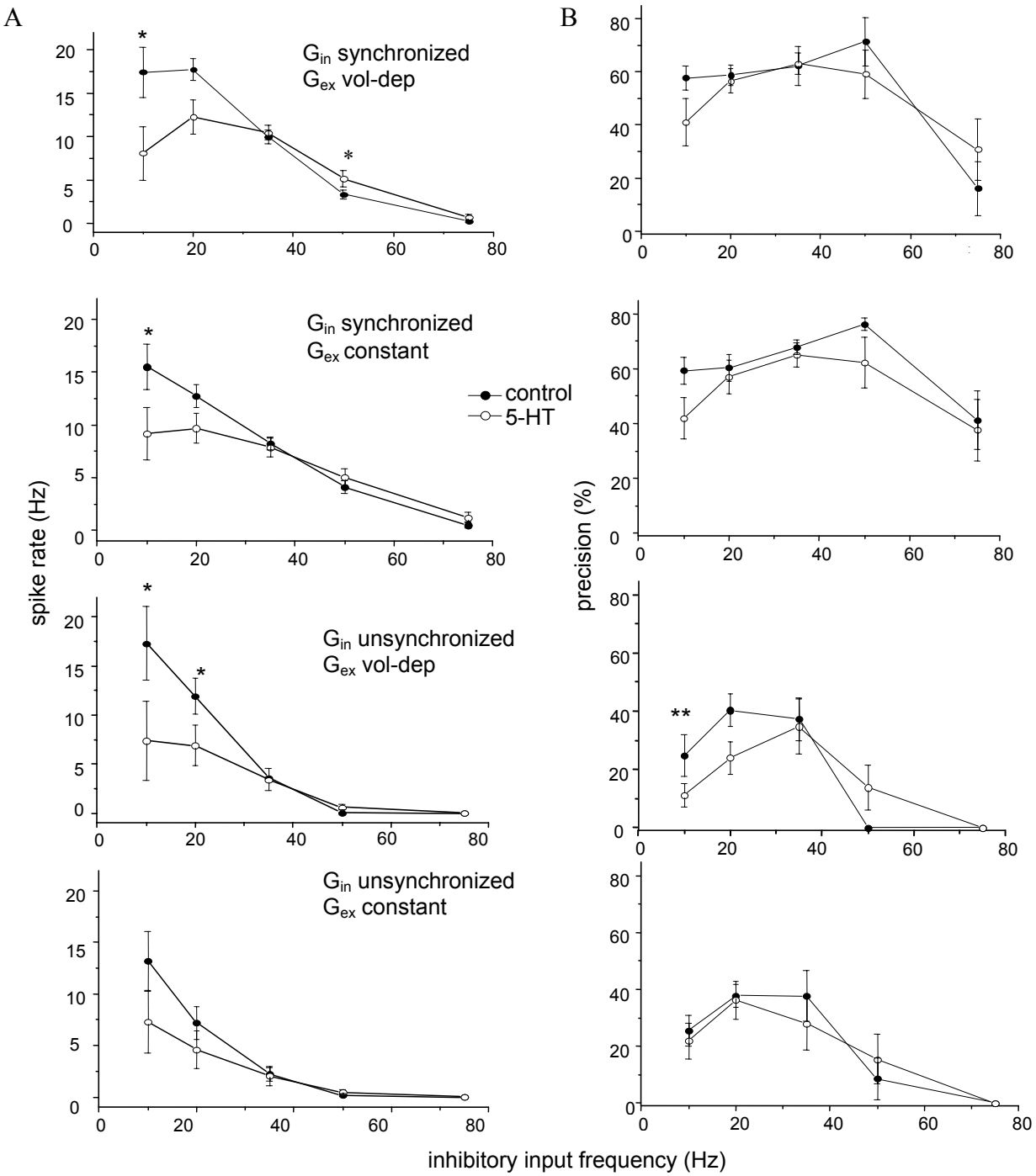

Figure 9. Synaptic shunting effect. Data were from one typical neuron in response to dynamic clamp stumulus of synchronized inhibitory inputs at 50 Hz and constant excitatory inputs, before (black) and during (gray) 10 μM 5-HT application. **A**, Spike triggered average (STA) of voltage trace. **B**, STA of injected current.

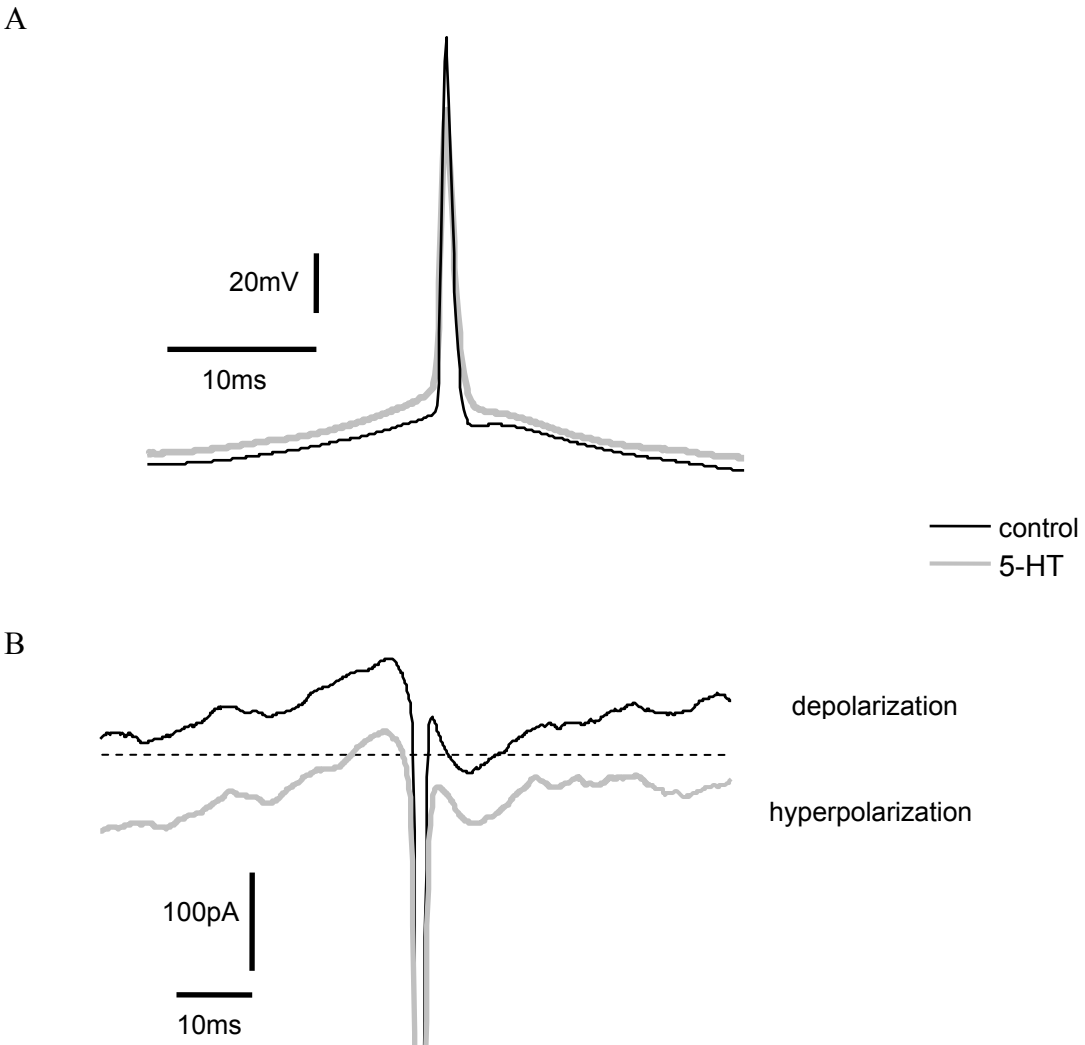

Figure 10. Synaptic shunting effect acts as a gain control factor, modulating the spike rate with 5-HT together. Data were from one representative neuron, before (filled circle) and during (open circle) 10 μM 5-HT application. **A**, Spike rate (top), mean membrane potential (middle) and action potential slope (bottom) plotted as a function of gain factor values at synchronized inhibitory frequencies of 35 Hz and voltage-dependent excitatory inputs. **B**, Spike rate plotted as a function of inhibitory input frequency at gain factor 0.5 (top), 1 (middle), 1.5 (bottom), at synchronized inhibition and voltage-dependent excitation.

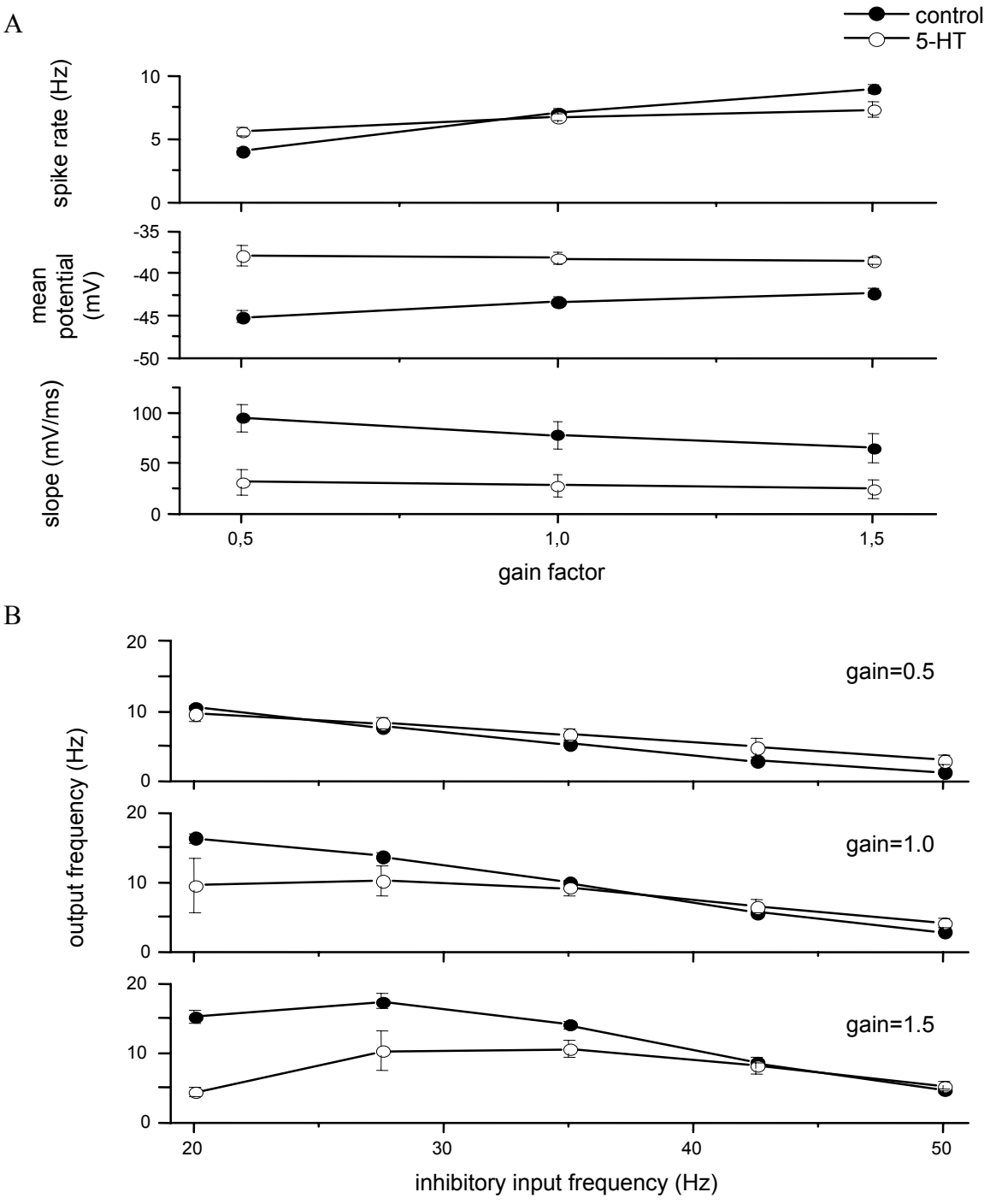

Figure 11. Multiple pulse depression of Purkinje-DCN compound IPSCs, in the presence of 100 μM AP5 and 25 μM DNQX. **A**, The evoked IPSCs in response to multiple spike trains of 1, 10, 20, 50 and 100 Hz brfore (left panel) and during (right panel) 10 μM 5-HT application, from one typical neuron. **B**, Depression pattern against time for different input frequencies, normalized by first evoked IPSC, before (filled circle) and during (open circle) 10 μM 5-HT application, averaged from 3 neurons. **C**, The rate of depression is frequency-dependent, as shown in plots of first IPSC (left), second to fifth IPSCs (middle) and steady-state IPSCs (right) against presynaptic input frequencies, averaged from 3 neurons. *P<0.05 with pair-t test.

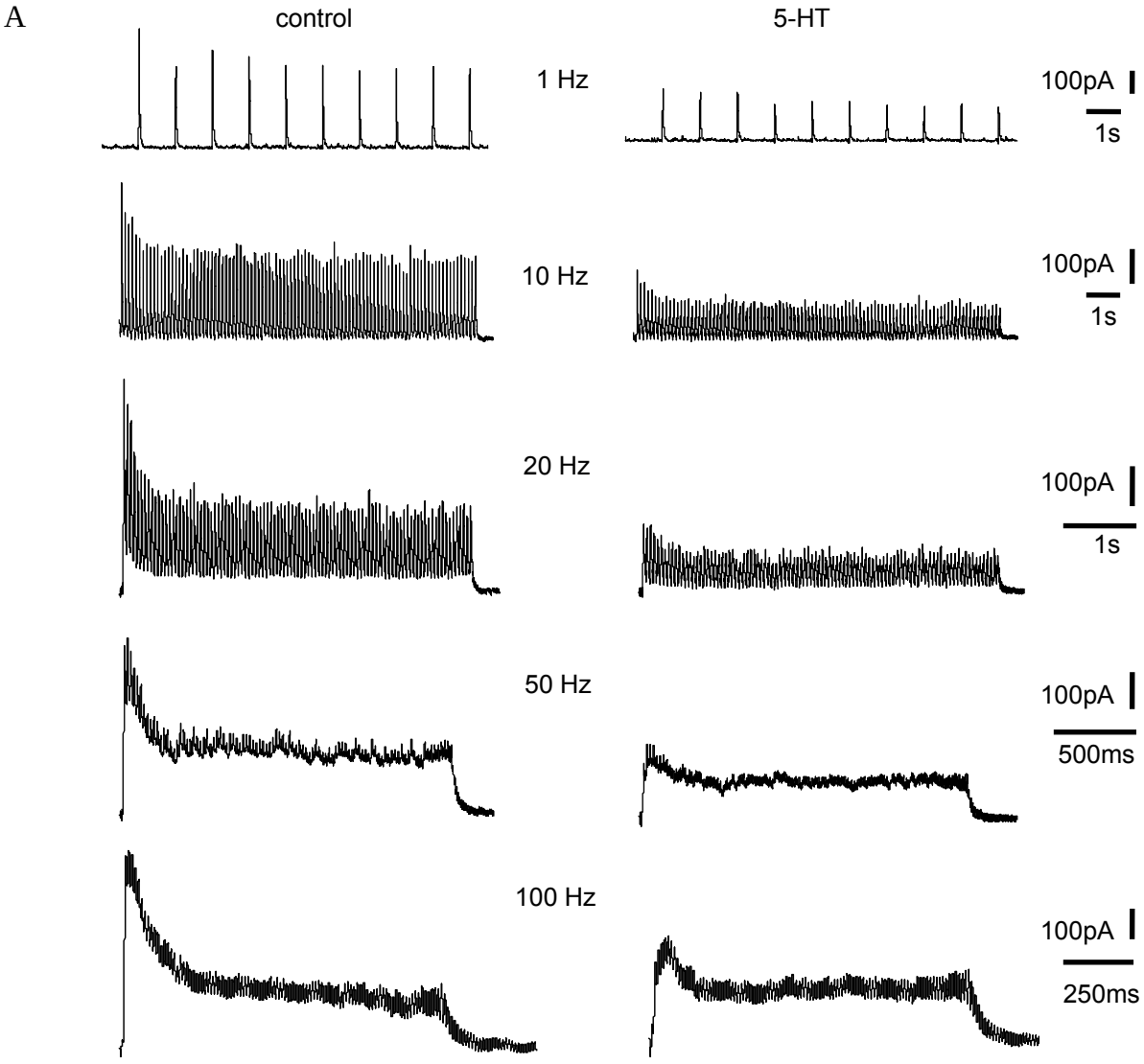

B

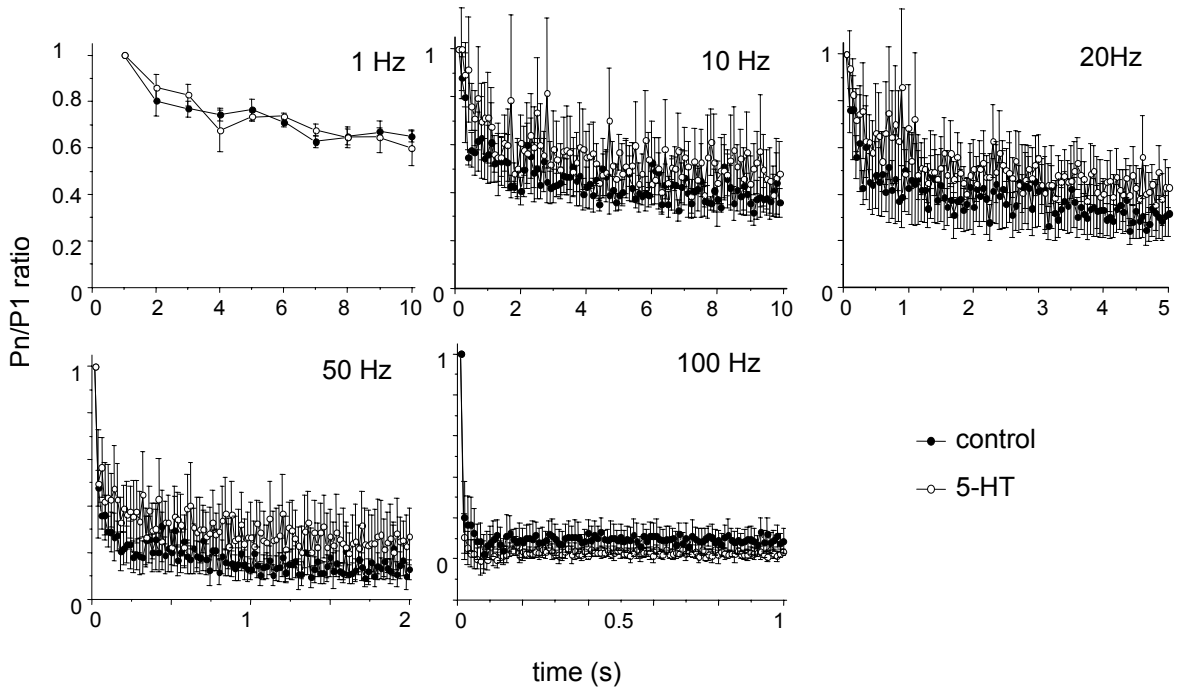
1 Hz
10 Hz
20Hz
50 Hz
100 Hz
Pn/P1 ratio
control
5-HT
time (s)

C

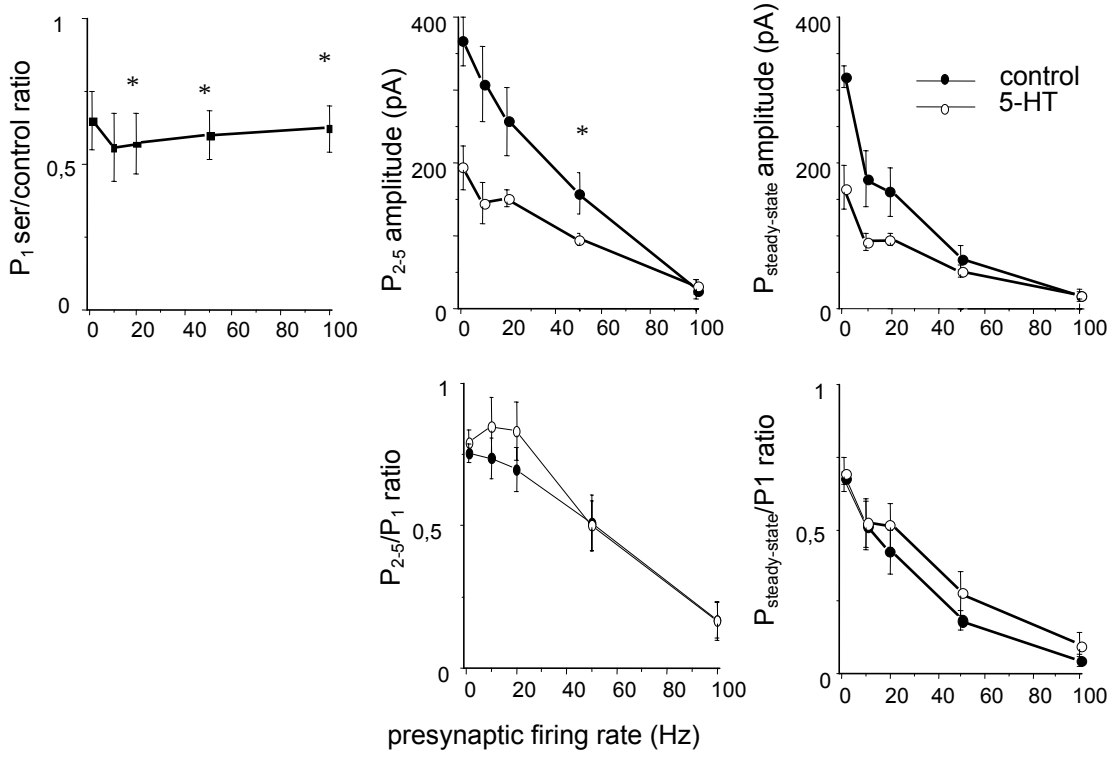
P1 ser/control ratio
P2-5 amplitude (pA)
Psteady-state amplitude (pA)
control
5-HT
P2-5/P1 ratio
Psteady-state/P1 ratio
presynaptic firing rate (Hz)

Figure 12. Changes in spontaneous IPSCs (sIPSCs) by 5-HT. They were recorded from DCN neurons clamped at 0 mV in the presence of 100 µM AP5 and 25 µM DNQX. **A**, Examples of consecutive traces of sIPSCs from one typical neuron (top), 30 minutes after 10 µM 5-HT application (middle), and after 10 µM bicuculline application (bottom). **B**, Inter-event interval cumulative probability of sIPSCs before and after 5-HT. **C**, sIPSCs amplitude cumulative probability distribution.

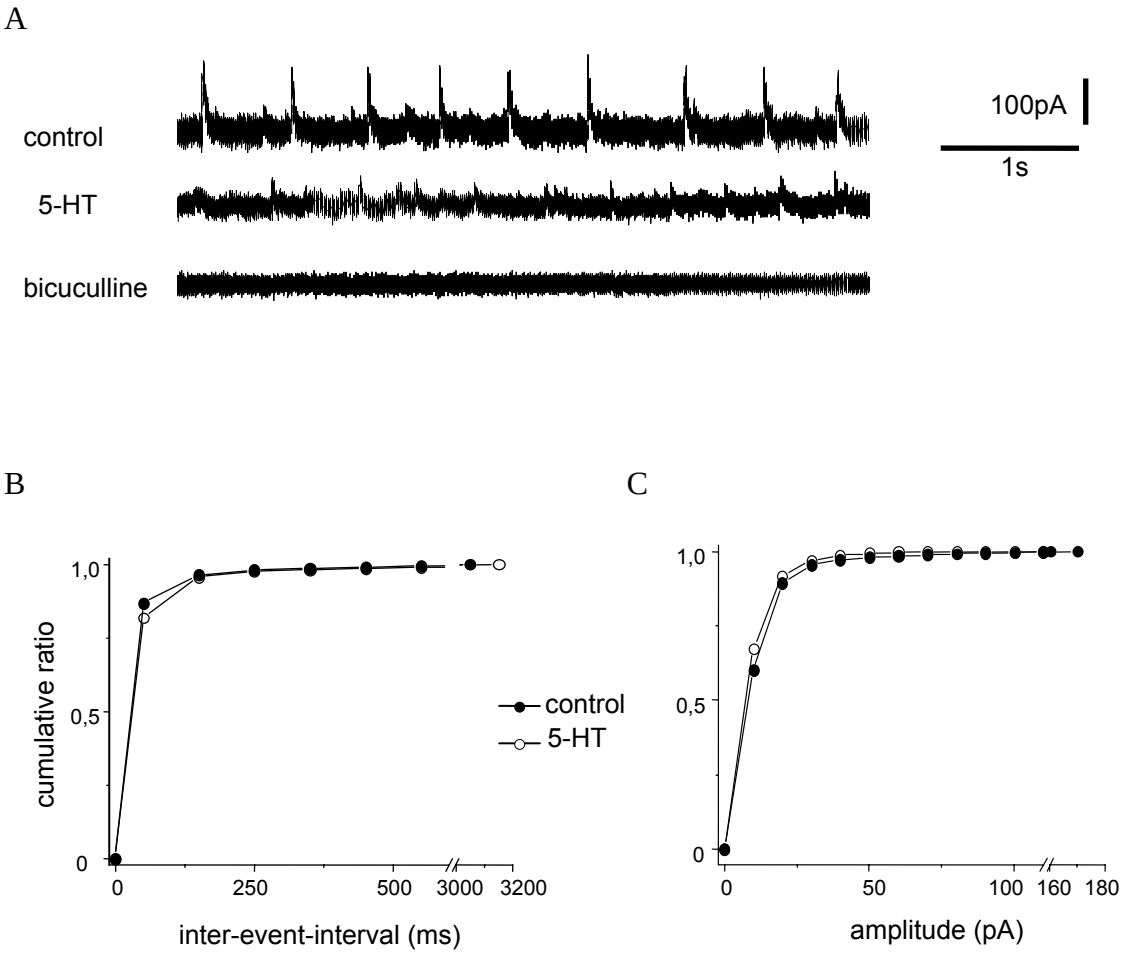

Figure 13. Recovery from short-term depression. **A**, IPSCs were evoked by the presynaptic firing frequency of 10, 50 and 100 Hz for 100 stimulation then followed by a 10 sec, 1 Hz recovery train, before (left) and during (right) 10 μM 5-HT application, from 1 typical neuron. **B**, time course of recovery train at 10, 20, 50, 100 Hz then a 10 sec, 1 Hz recovery train (left); at 20, 50, 100 Hz then a 10 sec, 10 Hz recovery train (middle); by 50, 100 Hz then a 5 sec, 20 Hz recovery train (right); normalized to first IPSC at depression train, averaged from 3 neurons. **C**, The same analysis as in B, during 10 μM 5-HT application. **D**, No significant difference in recovery time course by 5-HT.

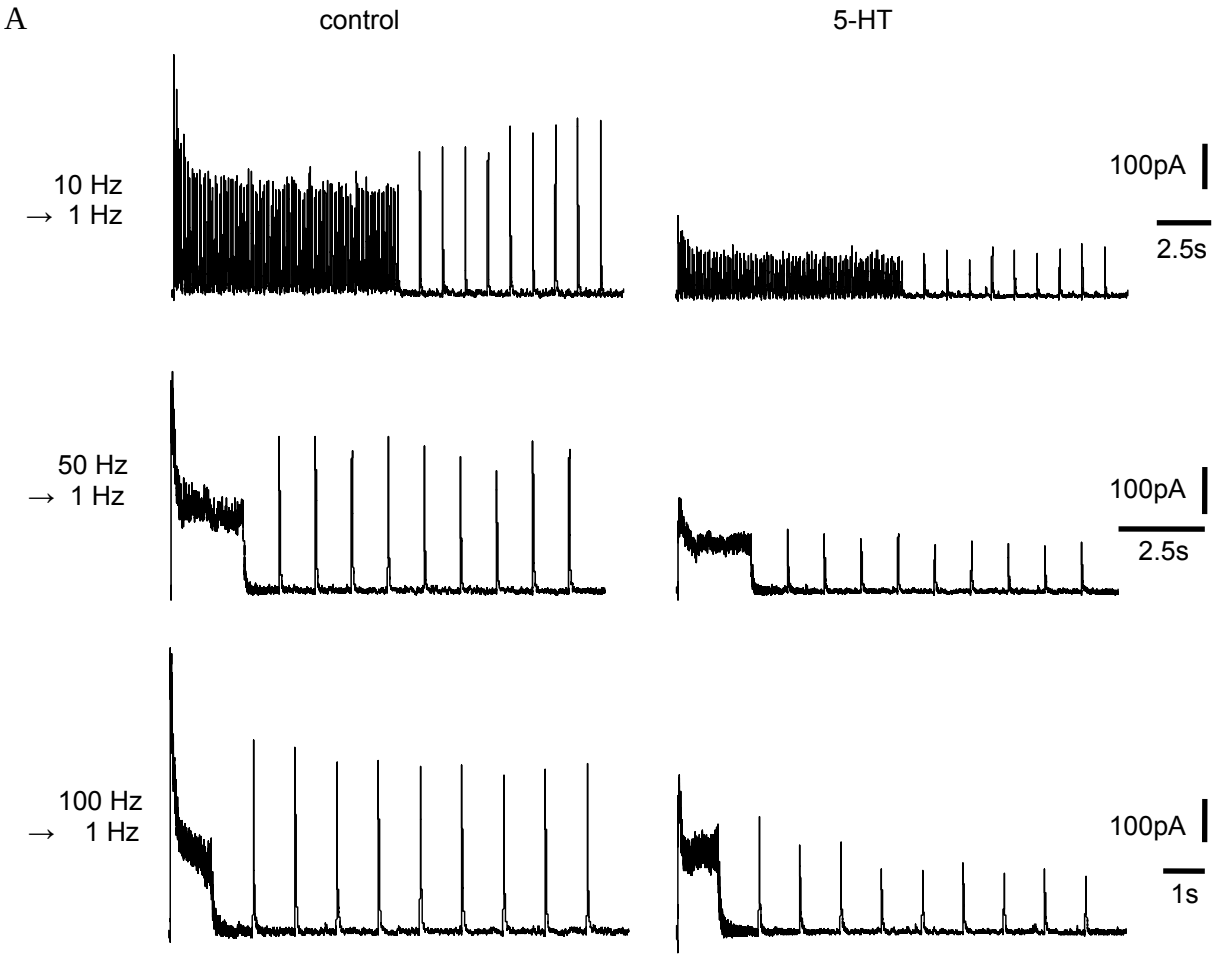

B

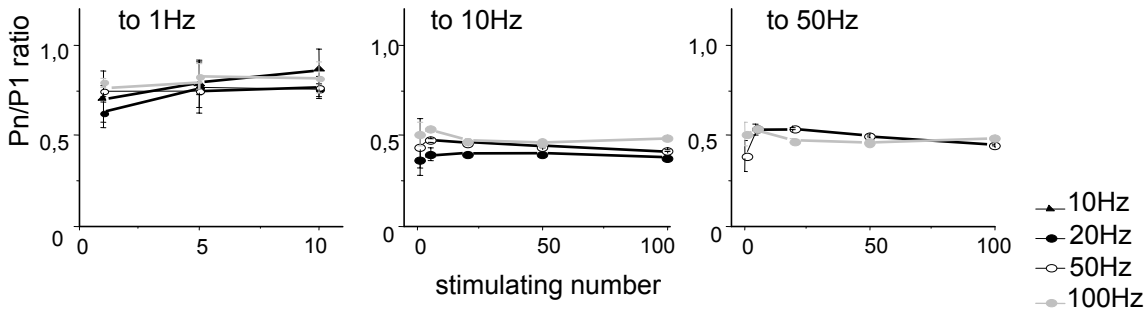
to 1Hz
to 10Hz
to 50Hz
Pn/P1 ratio
1,0
0,5
0
0
5
10
0
50
100
stimulating number
10Hz
20Hz
50Hz
100Hz

C

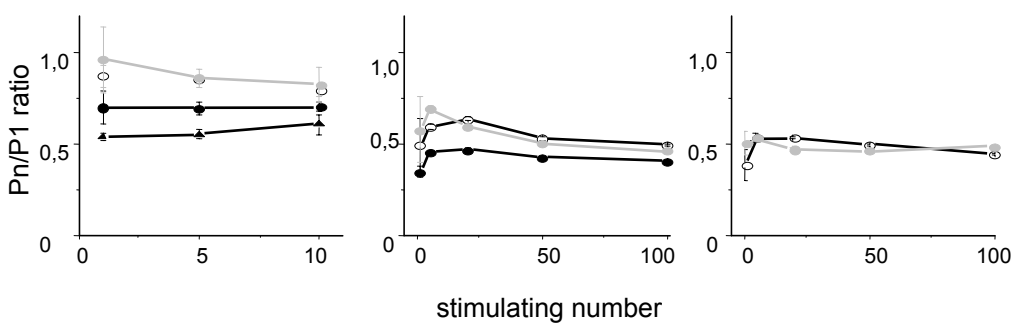
Pn/P1 ratio
1,0
0,5
0
0
5
10
0
50
100
stimulating number

D

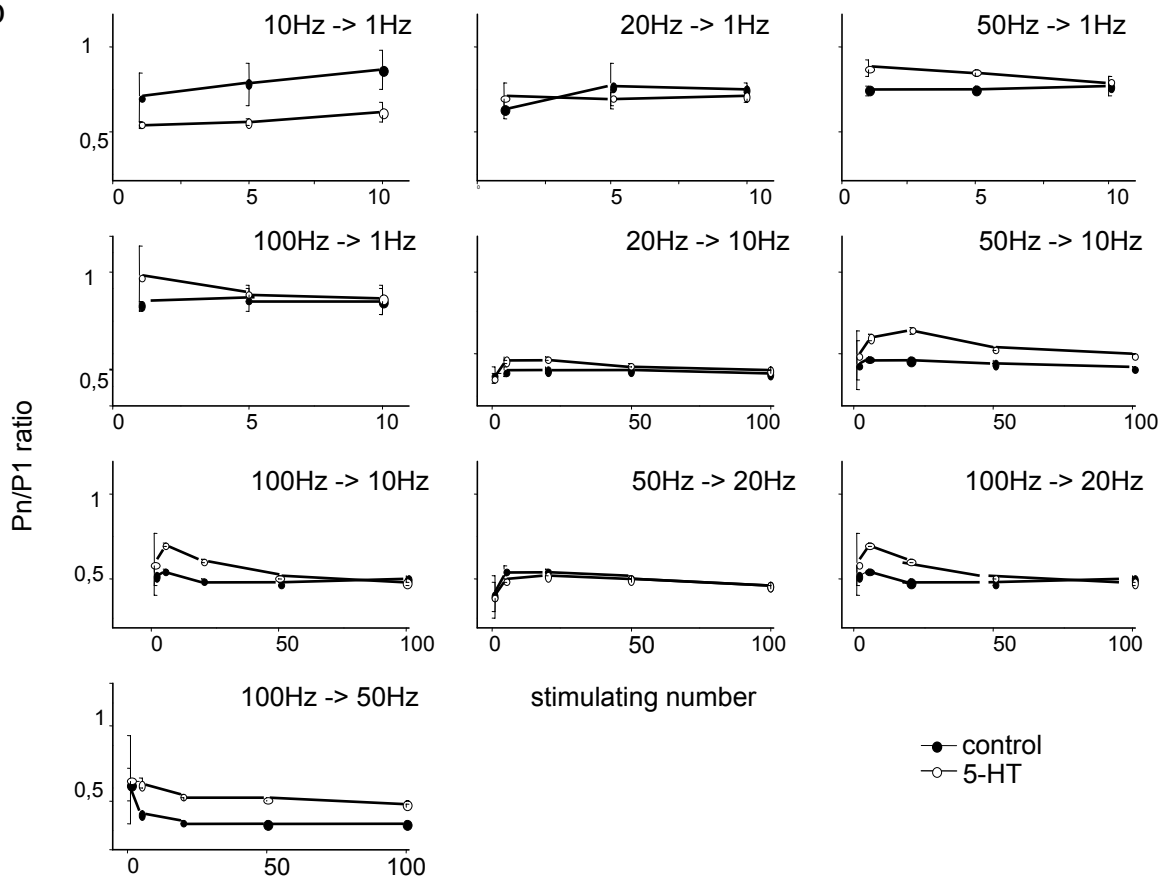
10Hz -> 1Hz
20Hz -> 1Hz
50Hz -> 1Hz
100Hz -> 1Hz
20Hz -> 10Hz
50Hz -> 10Hz
100Hz -> 10Hz
50Hz -> 20Hz
100Hz -> 20Hz
100Hz -> 50Hz
Pn/P1 ratio
1
0,5
0
5
10
50
100
stimulating number
control
5-HT

Figure 14. The impact of short-term depression in inhibitory inputs on firing activity in DCN neurons, averaged from 5 cells. Spike rate was plotted as a function of inhibitory input frequency, under different simulated synaptic inputs with and without short-term depression in inhibitory components before and during application of 10 μM 5-HT. The followings are the tested simulated synaptic inputs. **A**, Synchronized inhibitory inputs and voltage-dependent excitatory inputs. **B**, Synchronized inhibitory inputs and constant excitatory inputs. **C**, Unsynchronized inhibitory inputs and voltage-dependent excitatory inputs. **D**, Unsyn-chronized inhibitory inputs and constant excitatory inputs. **P < 0.01, ***P < 0.001 with pair-t test.

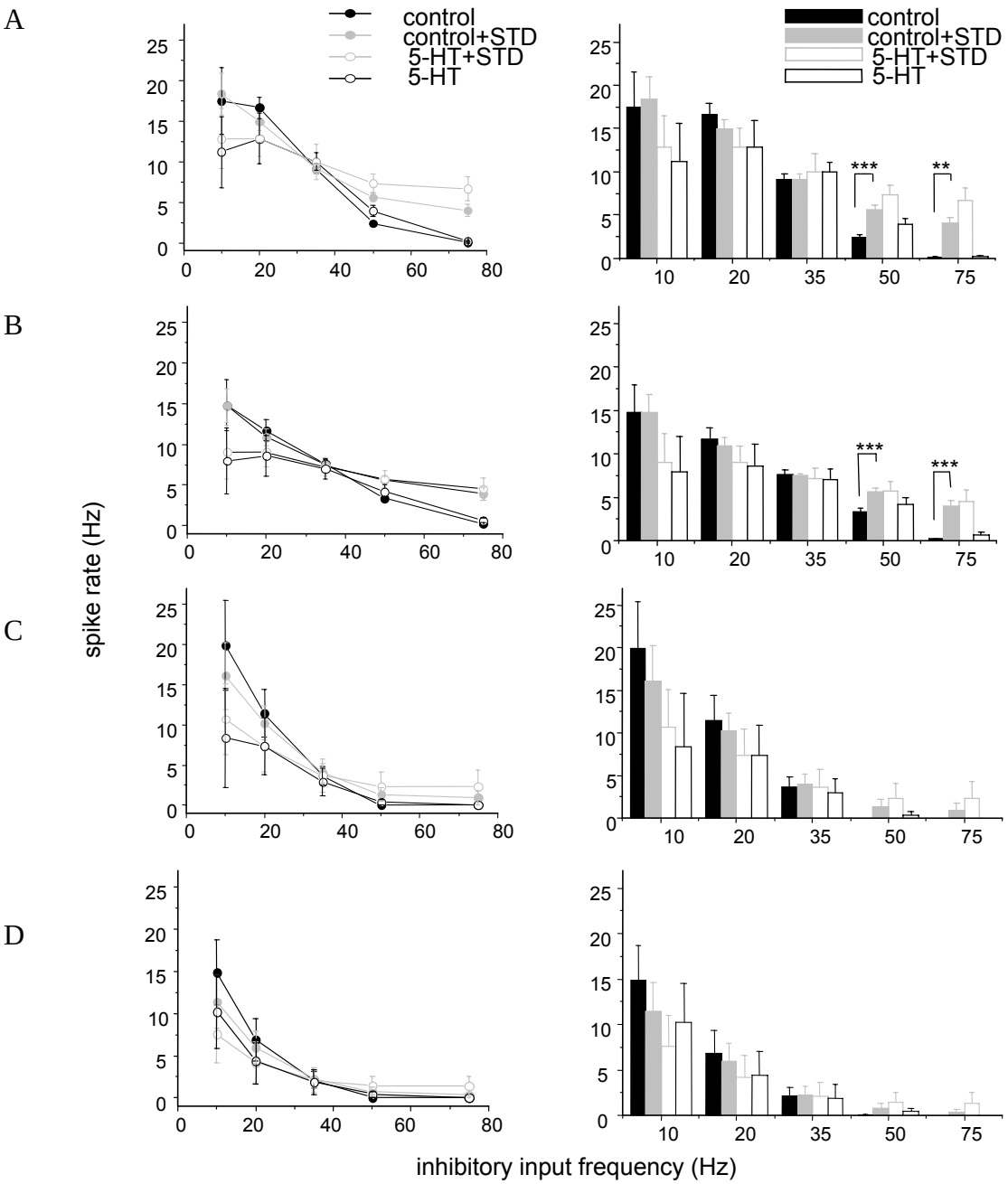

Figure 15. Stabilization of membrane potential in DCN neurons by short-term depression in inhibitory inputs. Mean membrane potential was plotted as a function of inhibitory input frequency, under the same stimulations in Figure 13. *P < 0.05, **P < 0.01, ***P < 0.001 with pair-t test.

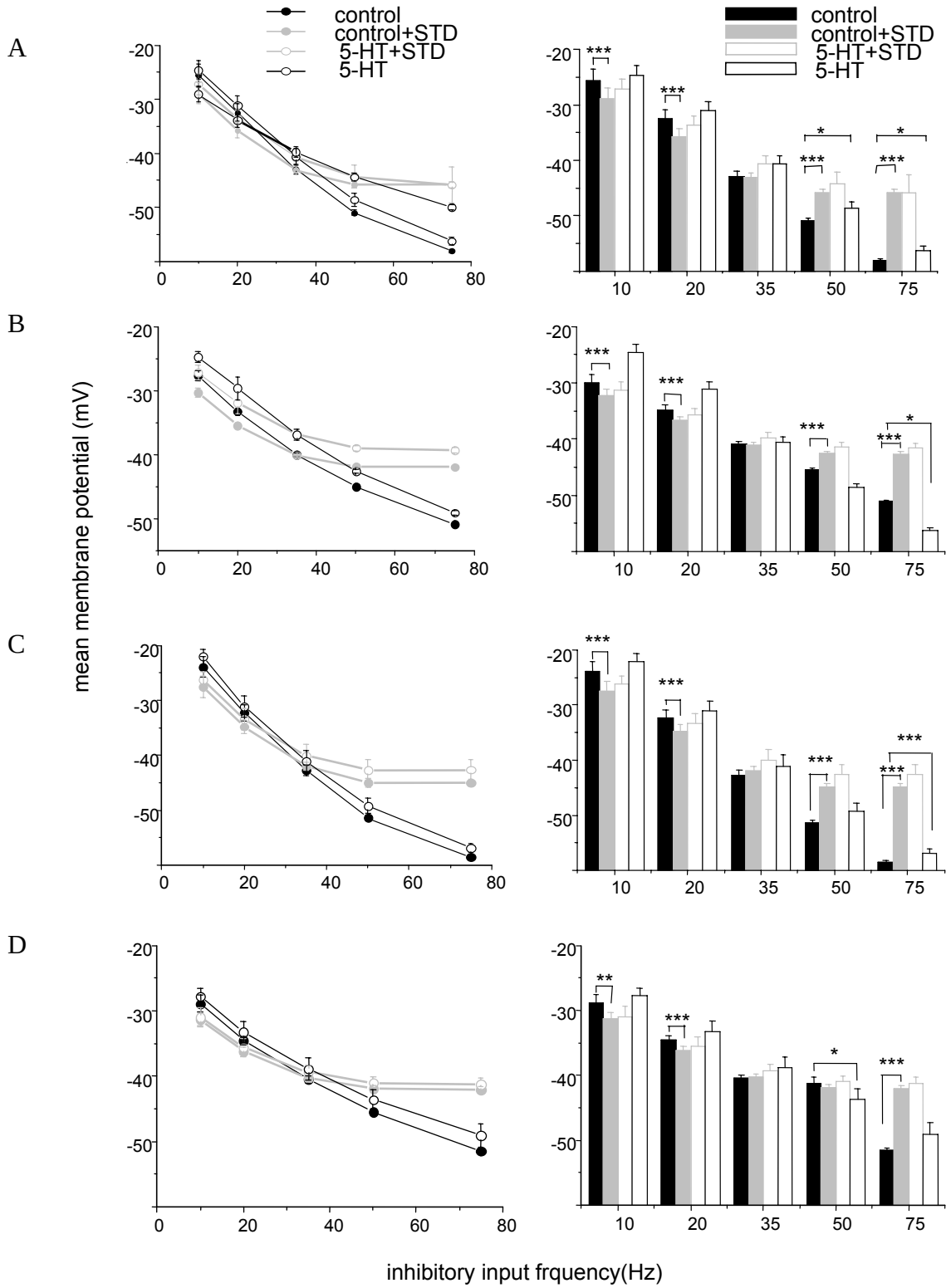

Figure 16. Spike timing precision was not significantly altered by short-term depression in inhibitory inputs. Spike precision was plotted as a function of inhibitory input frequency, with a time window of ± 5 ms, under the same stimulations in Figure 13. *P < 0.05, **P < 0.01, ***P < 0.001 with pair-t test.

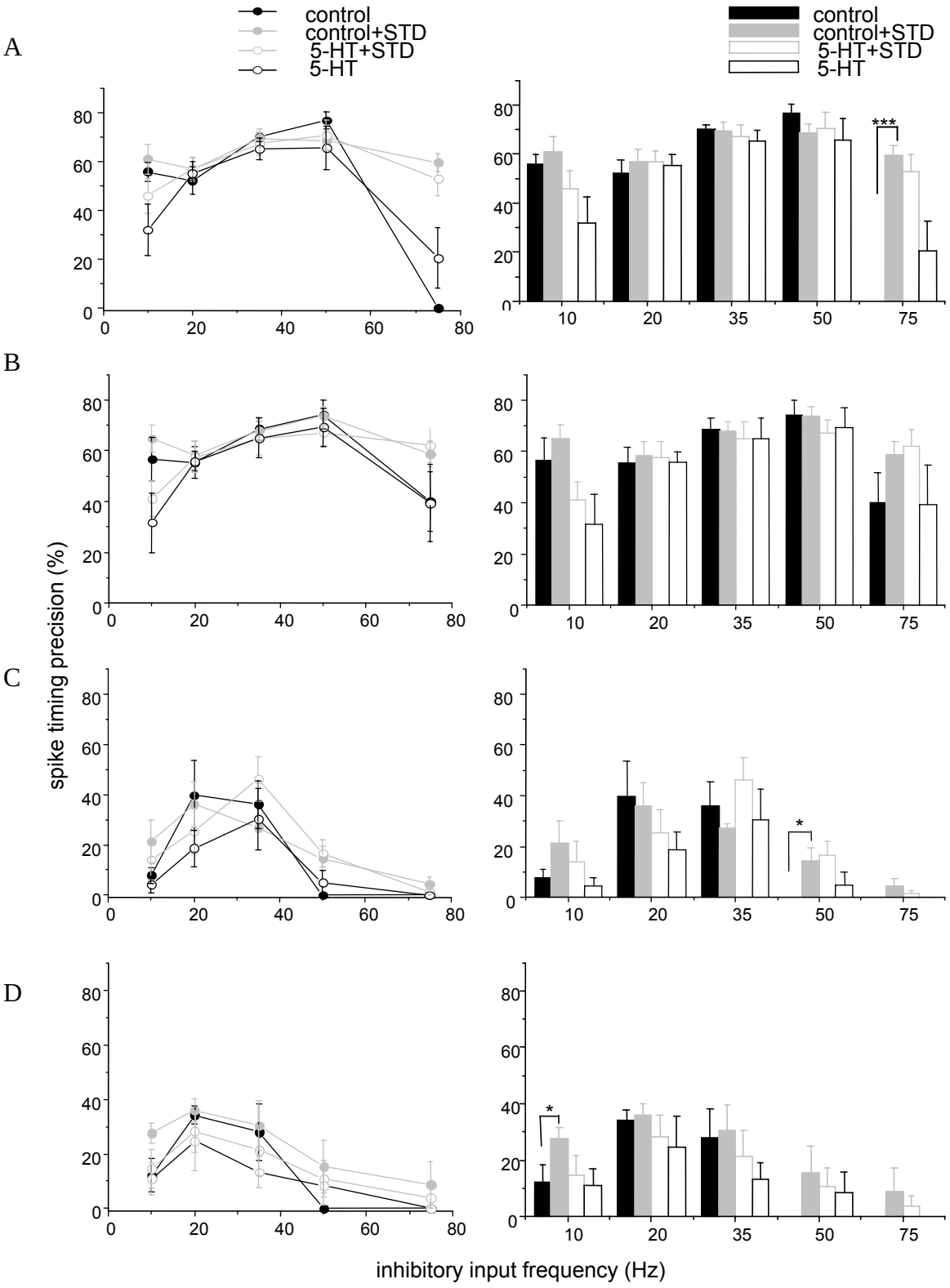

Figure 17. Depolarization by 5-HT was mediated via 1 and 5 receptors. **A**, depolarization was mimicked by application of RU-24269 (1 μM), the agonist of 5-HT1 receptor, from one representive neuron. **B,** the same effect by 5-CT (5 μM), the agonist of 5-HT5 receptor, from one representive neuron.

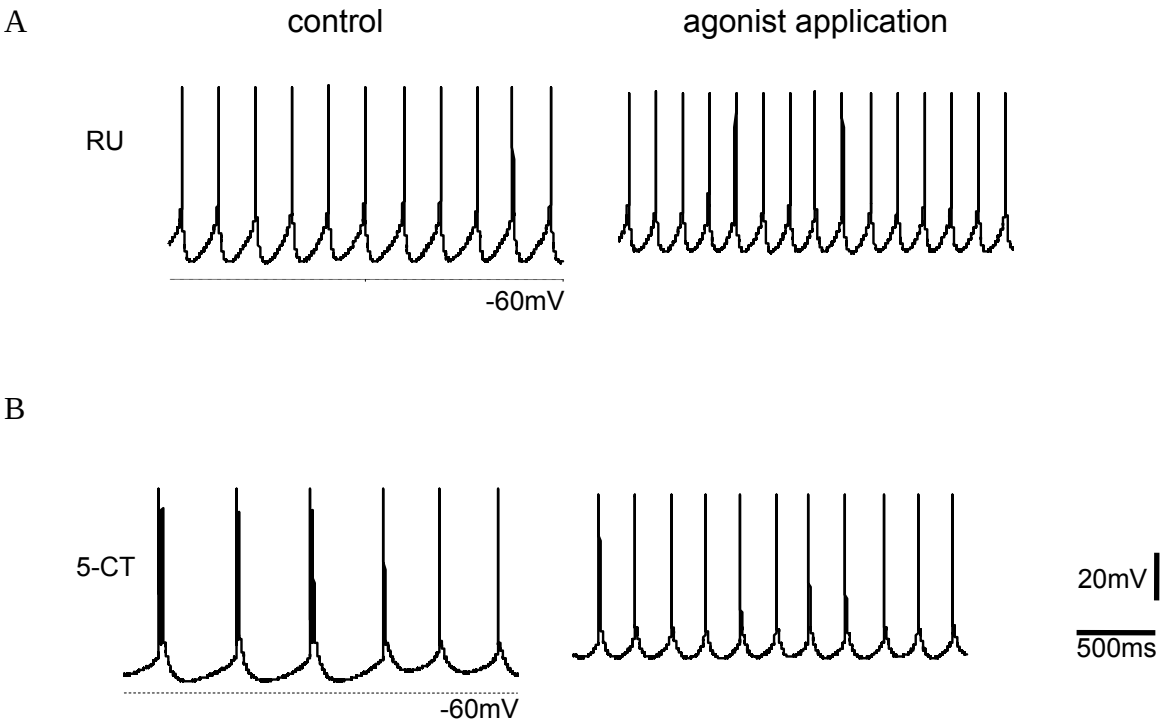

Figure 18. Firing performance is determined by the interaction between background synaptic activity and dominant intrinsic effect by 5-HT

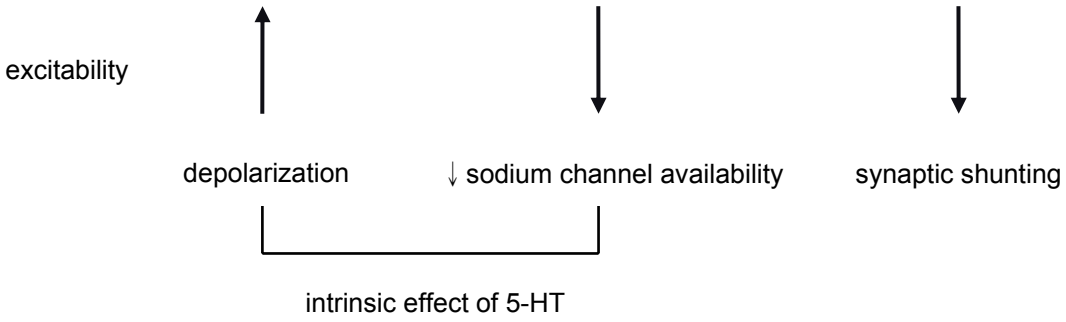

Table 1. Classification of recorded nuclei neurons at current clamp experiments by soma size and the response to 5-HT.

cell category	soma size (µm)	Vm (mV)		spike rate (Hz)	
		control	5-HT	control	5-HT
insensitive to 5-HT	cell 1: 13.33	-42.28 ± 0.9	-45.45 ± 1.2	6.50 ± 0.7	1.75 ± 0.4
N = 2	cell 2: 16.67	-46.89 ± 0.6	-46.98 ± 1.6	6.90 ± 0.7	6.90 ± 0.7
N = 17	15 - 20				
enhanced spike rate	18.21 ± 0.5	-47.18 ± 1.3	-40.57 ± 1.3	3.90 ± 0.7	8,46 ± 0.9
by 5-HT in 14 cells					
reduced spike rate	cell 1: 15.56	-44.86 ± 0.2	-39.20 ± 0.2	9.75 ± 0.4	9.5
by 5-HT in 2 cells	cell 2: 20	-51,57 ± 2.6	-45.90 ± 1.8	8.59 ± 2.1	7.44 ± 2.4
1 silent cell	20	-43.1 ± 1.3	-39.15 ± 0.2	0	0
N = 13	> 20				
	24.7 ± 0.9	-46.77 ± 1.5	-38.17 ± 2.1	4.62 ± 0.6	11.06 ± 2

Table 2. Classification of recorded neurons at voltage-clamp experiments by the response to 5-HT.

neuron	IV relationship	conductance change (pS)	soma size (µm)
1	Parallel	-91	15.56
2	parallel	1342.3	24
3	Parallel	-405.3	31.11
4	cross at +10mV	-24.8	17.78
5	cross at +5mV	-280.1	18.89
6	cross at +5mV	-231.3	18.89
7	cross at +5mV	291	20

Table 3. The effect of 5-HT on time course of recovery from depression, normalized to the first IPSC in depression train, averaged from 3 cells. Steady-state phase is the averaged IPSCs amplitude following the first 5 recovery events for recovery train of 1 Hz, and following the first 50 recovery events for recovery train of 10, 20 and 50 Hz.

frequency (Hz)		P_1 (%)		steady-state phase (%)	
from	to	control	5-HT	control	5-HT
10	1	70.15 ± 15.3	54.2 ± 1.8	86.11 ± 11.4	61.28 ± 5.5
20	1	62.8 ± 5.6	70.35 ± 8.7	74.15 ± 3	70.28 ± 3.1
50	1	74.4 ± 2.7	87.64 ± 5.7	75.96 ± 4.9	83.09 ± 1.7
100	1	79.03 ± 2.5	96.56 ± 17.9	82.16 ± 8.5	86.07 ± 6.1
20	10	37.1 ± 5.2	35.21 ± 3.1	39.24 ± 0.3	42.65 ± 0.4
50	10	43.71 ± 15.3	49.48 ± 14.8	43.23 ± 0.4	53.32 ± 0.7
100	10	50.98 ± 6.7	58.12 ± 18.2	47.92 ± 0.4	49.89 ± 0.7
50	20	39.01 ± 8.8	38.17 ± 12.1	47.99 ± 0.5	47.13 ± 0.4
100	20	51.04 ± 12.3	57.71 ± 11.4	36.59 ± 0.4	48.1 ± 0.4
100	50	51.43 ± 7.2	53.85 ± 20.7	32.72 ± 0.2	43.64 ± 0.3

5. Acknowledgement

The current project was supported by the *Hermann and Lilly Schilling Foundation* (TS013/01.184/98), the *Federal Ministry of Education and Research* (Fo: 01KS9602) and the *Interdisciplinary Center of Clinical Research Tübingen*.

I am sincerely grateful to *Professor Hans-Peter Thier* for giving me this precious chance to pursue my doctoral study at Department of Cognitive Neurology, University Tübingen and for the kind support in the last year of my study. I am thankful to my supervisor, *Dr. Volker Gauck,* for all discussions and support for the experiments and the careful correction of this manuscript. Thanks to *Dr. Fahard Sultan* for the inspiring discussion in anatomical and *Dr. Martin Möck* in pharmacological aspects.

Thanks to all my colleagues, *Thomas Berge, Sacha Melon, Sebastian Bundeschuhe, Christoph Zrenner, Christoph Linnemann,* for all the support during these together-working days. Thanks to other colleagues in the department for all warm help in the past 4 years. Thanks to the lab management, *Ute Großhenning,* and the program coordinator of graduate school of Neuronal and Behavioral Science, *Prof. Dr. Horst Herbert,* for so much help in all aspects in the past 4 years.

Special thank to all sacrificed animals for this project.

At last, thanks to my *family* and *friends* for the forever support and encouragement when I was frustrated and depressed during these alone-abroad days. And thanks to *Life,* who gives everyone the best years in youth.

6. References

Abbott LF, Varela JA, Sen K, Nelson SB (1997) Synaptic depression and cortical gain control. Science 275: 220-223.

Aghajanian GK (2000) Electrophysiology of serotonin receptor subtypes and signal transduction pathways. http://www. acnp.org/g4/GN401000043/Ch43.html

Aizenman CD, Linden DJ (1999) Regulation of the rebound depolarization and spontaneous firing patterns of deep cerebellar nuclear neurons in slices of rat cerebellum. J Neurophysiol 82: 1697-1709.

Aizenman CD, Manis PB, Linden DJ (1998) Polarity of long-term synaptic gain change is related to postsynaptic spike firing at a cerebellar inhibitory synapse. Neuron 21: 827-835.

Aksenov DP, Serdyukova NA, Bloedel JR, Bracha V (2005) Glutamate neurotransmission in the cerebellar interposed nuclei: involvement in classically conditioned eyeblinks and neuronal activity. J Neurophysiol 93: 44-52.

Anchisi D, Scelfo B, Tempia F (2001) Postsynaptic currents in deep cerebellar nuclei. J Neurophysiol 85: 323-331.

Andrade R (1998) Regulation of membrane excitability in the central nervous system by serotonin receptor subtypes. Ann N Y Acad Sci 861:190-203.

Azouz R, Gray CM (2000) Dynamic spike threshold reveals a mechanism for synaptic coincidence detection in cortical neurons in vivo. Proc Natl Acad Sci 97(14): 8110-8115.

Batini C, Compoint C, Buisseret-Delmas C, Daniel H, Guegan M (1992) Cerebellar nuclei and the nucleocortical projections in the rat: retrograde tracing coupled to GABA and glutamate immunohistochemisty. J Comp Neurol 315: 74-84.

Beas-Zarate C, Sandoval ME, Feria-Velasco A (1984) Serotonin uptake and release from rat cerebellum in vitro. J Neurosci Res 12: 129-136.

Bickmeyer U, Heine M, Manzke T, Richter DW (2002) Differential modulation of I_h by 5-HT receptors in mouse CA1 hippocampal neurons. Eur J Neurosci 16(2):209-218.

Brenowitz S, Trussell LO (2001) Minimizing synaptic depression by control of release probability. J Neurosci 21(6): 1857-1867.

Carr DB, Michelle D, Cantrell AR, Held J, Scheuer T, Catterall WA, Surmeier DJ (2003) Transmitter modulation of slow, activity-dependent alterations in sodium channel availability endows neurons with a novel form of cellular plasticity. Neuron 39: 793-806.

Chance FS, Abbott F, Reyes AD (2002) Gain modulation from background synaptic input. Neuron 35:773-782.

Chance FS, Nelson SB, Abbott LF (1998) Synaptic depression and the temporal response characteristics of V1 cells. J Neurosci 18(12): 4785-4799.

Chan-Palay V (1977) Cerebellar dentate nucleus. Organization, cytology and transmitters. Springer: Berlin.

Chen S, Hillman DE (1993) Colocalization of neurotransmitters in the deep cerebellar nuclei. J Neurocytol 22: 81-91.

Chung SY, Li XG, Nelson SB (2002) Short-term depression at thalamocortical synapses contribute to rapid adaptation of cortical sensory responses in vivo. Neuron 34: 437-446.

Cook DL, Schwindt PC, Grande LA, Spain WJ (2003) Synaptic depression in the localization of sound. Nature 421: 66-70.

Cooper JR, Bloom FE, Roth RH (2003) Serotonin, histamine, and adenosine. In: The biochemical basis of neuropharmacology (8th ed.), pp. 271-320. New York: Oxford Uiversity Press.

Cordero-Erausquin M, Changuex JP (2000) Tonic nicotinic modulation of serotonergic modulation in the spinal cord. Proc Natl Acad Sci 98(5): 2803-2807.

Crochet S, Fuentealba P, Cissé Y, Timofeev I, Steriade M (2005) Synaptic plasticity in local cortical network in vivo and its modulation by the level of neuronal activity. Cerebral Cortex 16(5): 618-631.

Cumming-Hood PA, Strahlendorf HK, Strahlendorf JC (1993) Effects of serotonin and the 5-HT2/1C receptor agonist DOI on neurons of the cerebellar dentate/interpositus nuclei: possible involvement of a GABAergic interneuron. Eur J Pharmacol 236(3): 457-465.

Czubayko U, Sultan F, Thier P, Schwarz C (2001) Two types of neurons in the rat cerebellar nuclei as distinguished by membrane potentials and intracellular fillings. J Neurophysiol 85: 2017-2029.

Desai NS, Walcott E (2006) Synaptic bombardment modulates muscarinic effects in forelimb motor cortex. J Neurosci 26(8): 2215-2226.

Destexhe A, Rudolph M, Paré D (2003) The high-conductance state of neocortical neurons in vivo. Nat Rev Neurosci 4: 739-751.

De Zeeuw CI, Berrebi AS (1995) Postsynaptic targets of purkinje cell terminals in the cerebellar and vestibular nuclei of the rat. Eur J Neurosci 7: 2322-2333.

Dieudonné S, Dumoulin A (2000) Serotonin-driven long-range inhibitory connections in the cerebellar cortex. J Neurosci 20(5): 1837-1848.

Di Matteo V, Cacchio M, Di Giulio C, Esposito E (2002) Role of serotonin (2C) receptors in the control of brain dopaminergic function. Pharmacol Biochem Behav 71(4): 727-734.

Di Mauro M, Fretto G, Caldera M, Li Volci G, Licalta F, Ciranna L, Santangero F (2003) Noradrenaline and 5-hydroxytryptamine in cerebellar nuclei of the rat: functional effects on neuronal firing. Neurosci Lett 347(2): 101-105.

Esposito E (2006) Serotonin-dopamine interaction as a focus of novel antidepressant drugs. Curr Drug Targets 7(2): 177-185.

Fellous JM, Rudolph M, Destexhe A, Sejnowski TJ (2003) Synaptic background noise controls the input/output characteristics of single cells in an in vitro model of in vivo activity. Neurosci 122(3): 811-829.

Fuhrmann G, Cowan A, Segev I, Tsodyks M, Stricker C (2004) Multiple mechanisms govern the dynamics of depression at neocortical synapses of young rats. J Physiol 557.2: 415-438.

Gardette R, Krupa M, Crepel F (1987) Differential effects of serotonin on the spontaneous discharge and on the excitatory amino acid induced responses of deep cerebellar nuclei neurons in rat cerebellar slices. Neurosci 23(2): 491-500.

Gauck V, Jaeger D (2000) The control of rate and timing of spikes in the deep cerebellar nuclei by inhibition. J Neurosci 20(8): 3006-3016.

Gauck V, Jaeger D (2003) The contribution of NMDA and AMPA conductances to the control of spiking in neurons of the deep cerebellar nuclei. J Neurosci 23(22): 8109-8118.

Geurts (2002) Localization of 5-HT2A, 5-HT3, 5-HT5A and 5-HT7 receptor-like immunoreactivity in the rat cerebellum. J Chem Neuroanat 24: 65-74.

Ghez C, Thach WT (1991) The cerebellum. In: Principles of Neuroscience (4th ed.), pp 832-852. USA: McGraw-Hill companies.

Giovannini MG, Ceccarelli I, Molinari B, Cecchi M, Goldfarb J, Blandina P (1998) Serotonergic modulation of acetylcholine release from cortex of freely moving rats. J Pharmacol Exp Ther 85(3):1219-1225.

Glennon RA, Dukat M, Westkaemper RB (2000) Serotonin receptor subtypes and ligands. http://www.acnp.org/g4/GN401000039/Ch39.html

Hasuo H, Matsuoka T, Akasu T (2002) Activation of presynaptic 5-Hydroxytryptamine 2A receptors facilitates excitatory synaptic transmission via protein kinase C in the dorsolateral septal nucleus. J Neurosci 22(17): 7509-7517.

Holdefer RN, Houk JC, Miller LE (2005) Movement-related discharge in the cerebellar nuclei persists after local injections of $GABA_A$ antagonists. J Neurophysiol 93: 35-43.

Izumi J, Washizuka M, Miura N, Hiraga Y, Ikeda Y (1994). Hippocampal serotonin 5-HT_{1A} receptor enhances acetylcholine release in conscious rats. J Neurochem 62(5): 1804-1808.

Jacobs BL, Fornal CA (1999) Activity of serotonergic neurons in behaving animals. Neuropsychopharmacol 21: 9S-15S.

Johnson SW, Mercuri NB, North RA (1992) 5-HT1B receptor blocks the GABAB synaptic potential in rat dopamine neurons. J Neurosci 12(5): 2000-2006.

Kang J, Huguenard JR, Prince DA (2000) Voltage-gated potassium channels activated during action potentials in layer V neocortical pyramidal neurons. J Neurophysiol 83: 70-80.

Kay AR, Miles R, Wong RKS (1986) Intracellular fluoride alters the kinetic properties of calcium currents facilitating the investigation of synaptic events in hippocampal neurons. J Neurosci 6(10): 2915-2920.

Kerr CW, Bishop GA (1992) The physiological effects of serotonin are mediated by the 5-HT1A receptor in the cat's cerebellar cortex. Brain Res 591: 253-260.

Kerr CWH, Bishop GA (1991) Topographical organization in the origin of serotonergic projections to different regions of the cat cerebellar cortex. J Comp Neurol 304: 502-515.

Kia HK, Brisorgueil MJ, Daval G, Langlois X, Hamon M, Verge D (1996) Serotonin1A receptors are expressed by a subpopulation of cholinergic neurons in the rat medial septum and diagonal band of Broca--a double immunocytochemical study. Neurosci 74(1): 143-54.

Kitzman PH, Bishop GA (1997) The physiological effects of serotonin on spontaneous and amino acid-induced activation of cerebellar nuclear cells: an in vivo study in the cat. Prog Brain Res 114: 219-223.

Kitzman PH, Bishop GA (1994) The origin of serotoninergic afferents to the cat's cerebellar nuclei. J Comp Neurol 340: 541-550.

Kreitzer AC, Regehr WG (2000) Modulation of transmission during trains at a cerebellar synapses. J Neurosci 20(4): 1348-1357.

Laurent A, Goaillard JM, Cases O, Lebrand C, Gaspar P, Ropert N (2002) Activity-dependent presynaptic effect of serotonin 1B receptors on the somatosensory thalamocortical transmission in neonatal mice. J Neurosci 22(3): 886-900.

Lee MY, Strahhlendorf JC, Strahlendorf HK (1986) Modulation action of serotonin on glutamate-induced excitation of cerebellar Purkinje cells. Brain Res 361: 107-113.

Li SJ, Wang Y, Strahlendorf HK, Strahlendorf JC (1993) Serotonin alters an inward rectifying current (I_h) in rat cerebellar Purkinje cells under voltage clamp. Brain Res 617: 87-95.

Malinina E, Druzin M, Johansson S (2005) Fast neurotransmission in the rat medial preoptic nucleus. Brain Res 1040(1-2): 157-168.

Marek JG, Wright RA, Schoepp DD, Monn JA, Aghajanian GK (2000) Physiological antagonism between 5-Hydroxytryptamine$_{2A}$ and group II metabotropic glutamate receptors in prefrontal cortex. Pharmacol 192(1): 76-87.

Matsumura M, Cope T, Fetz E.E. (1988) Sustained excitatory synaptic input to motor cortex neurons in awake animals revealed by intracellular recording of membrane potentials. Exp Brain Res 70: 463-469.

Mauk MD (1997) Roles of cerebellar cortex and nuclei in motor learning: contradictions or clues? Neuron 18: 343-346.

Melena J, Chidlow G, Osborne NN (2000) Blockade of voltage-sensitive Na(+) channels by the 5-HT(1A) receptor agonist 8-OH-DPAT: possible significance for neuroprotection. Eur J Pharmacol 406(3): 319-324.

Mendlin A, Martin FJ, Rueter LE, Jacobs BL (1996) Neuronal release of serotonin in the cerebellum of behaving rats: an in vivo microdialysis study. J Neurochem 67: 617-622.

Miles GB, Dai Y, Brownstone RM (2005) Mechanisms underlying the early phase of spike frequency adaptation in mouse spinal motoneurons. J Physiol 566.2: 519-532.

Mitchell SJ, Silver RA (2003) Shunting inhibition modulates neuronal gain during synaptic excitation. Neuron 38: 433-445.

Mitoma H, Kobayashi T, Song SY, Konishi S (1994) Enhancement by serotonin of GABA-mediated inhibitory synaptic currents in rat cerebellar Purkinje cells. Neurosci Lett 173(1-2): 127-130.

Mitoma H, Konishi S (1999) Monoaminergic long-term facilitation of GABA-mediated inhibitory transmission at cerebellar synapses. Neuroscience 88(3): 871-883.

Möck M, Schwarz C, Thier P (2002) Serotonergic control of cerebellar mossy fiber activity by modulation of signal transfer by rat pontine nuclei neurons. J Neurophysiol 88: 549-564.

Moncton JE, McCormick DA (2002) Neuromodulatory role of serotonin in the ferret thalamus. J Neurophysiol 87: 2124-2136.

Morishita W, Sastry BR (1995) Pharmacological characterization of pre- and postsynaptic $GABA_B$ receptors in the deep nuclei of rat cerebellar slices. Neuroscience 68: 1127-1137.

Mouginot D, Gähwiler BH (1996) Presynaptic $GABA_B$ receptors modulate IPSPs evoked in neurons of deep cerebellar nuclei in vitro. J Neurophysiol 75: 894-901.

Orr HT (2004) Into the depth of ataxia. J Clin Invest 113:505-507.

Ouardouz M, Sastry BR (2000) Mechanisms underlying LTP of inhibitory synaptic transmission in the deep cerebellar nuclei. J Neurophysiol 84: 1414-1421.

Palkovits M, Mezey É, Hámori J, Szentágpthai J (1977) Quantitative histological analysis of the cerebellar nuclei in the cat. I. Numerical data on cells and on synapses. Exp Brain Res 28: 189-209.

Pedroarena CM, Schwarz C (2003) Efficacy and short-term plasticity at GABAergic synapse between Purkinje and cerebellar nuclei neurons. J Neurophysiol 89: 704-715.

Perrier JF, Alaburda A, Hounsgaard J (2003) $5\text{-}HT_{1A}$ receptors increase excitability of spinal motoneurons by inhibiting a TASK-1-like K^+ current in the adult turtle. J Physiol 548.2: 485-492.

Placantonakis DG, Schwarz C, Welsh JP (2000) Serotonin suppresses subthreshold and suprathreshold oscillatory activity of rat inferior olivary neurons in vitro. J Physiol 524.3: 833-851.

Pugh JR, Raman IR (2005) $GABA_A$ receptor kinetics in the cerebellar nuclei: evidence for detection of transmitter from distant release sites. Biophy J 88: 1740-1754.

Raman IM, Gustafson AE, Padgett D (2000) Ionic currents and spontaneous firing in neurons isolated from the cerebellar nuclei. J Neurosci 20(24): 9004-9016.

Reig R, Gallego R, Nowak LG, Sanchez-Vives MV (2006) Impact of cortical network activity on short-term synaptic depression. Cerebral Cortex 16: 688-695.

Robinson HP, Kawai N (1993) Injection of digitally synthesized synaptic conductance transients to measure the integrative properties of neurons. J Neurosci Methods 49: 157-165.

Rowland NC, Jaeger D (2005) Coding of tactile response properties in the rat deep cerebellar nuclei. J Neurophysiol 94: 1236-1251.

Rueter LE, Jacobs BL (1996) A microdialysis examination of serotonin release in the rat forebrain induced by behavioral/environmental manipulations. Brain Res 739: 57-69.

Sakaba T, Neher E (2001) Calmodulin mediates rapid recruitment of fast-releasing synaptic vesicles at a calyx-type synapse. Neuron 32: 1119-1131.

Sausbier M, Hu H, Arntz C, Feil S, Kamm S, Adelsberger H, Sausbier U, Sailer CA, Feil R, Hofmann F, Korth M, Shipston MJ, Knaus HG, Wolfer DP, Pedroarena CM, Storm JF, Ruth P (2004) Cerebellar ataxia and purkinje cell dysfunction caused by Ca^{2+}-activated K^{+} channel deficiency. Pro Natl Acad Sci 101(25): 9474-9478.

Savio T, Tempia F (1985) On the Purkinje cell activity increase induced by suppression of the inferior olive activity. Exp Brain Res 57: 456-463.

Schweighofer N, Doya K, Kuroda S (2004) Cerebellar aminergic neuromodulation: towards a functional understanding. Bran Res Reviews 44: 103-116.

Shakkottai VG, Chou CH, Oddo S, Sailer CA, Knaus HG, Gutman GA, Barish ME, LaFerla FM, Chandy KG (2004) Enhanced neuronal excitability in the absence of neurodegeneration induces cerebellar ataxia. J Clin Invest 113: 582-590.

Sharp AA, O'Nell MB, Abbott LF, Marder E (1993) Dynamic clamp: computer-generated conductances in real neurons. J Neurophysiol 69: 992-995.

Shu YS, Hasenstaub A, Badoual M, Bal T, McCormick DA (2003) Barrages of synaptic activity control the gain and sensitivity of cortical neurons. J Neurosci 23(32): 10388-10401.

Stanford IM, Kantaria MA, Chahal HS, Loucif KC, Wilson CL (2005) 5-Hydroxytryptamine induced excitation and inhibition in the subthalamic nucleus: action at 5-HT(2C), 5-HT(4) and 5-HT(1A) receptors. Neuropharmacol 49(8): 1228-1234.

Steriade M, Timofeev I, Grenier F. (2001) Natural waking and sleep states: a view from inside neocortical neurons. J. Neurophysiol 85: 1969-1985.

Steuber V, De Schutter E, Jaeger D (2004) Passive models of neurons in the deep cerebellar nuclei: the effect of reconstruction errors. Neurocomputing 58-60: 563-568.

Strahhlendorf JC, Lee M, Strahhlendorf HK (1989) Modulatory role of serotonin on GABA-elicited inhibition of cerebellar Purkinje cells. Neurosci 30(1): 117-125.

Strahhlendorf JC, Lee M, Strahhlendorf HK (1984) Effects of serotonin on cerebellar purkinje cells are dependent on the baseline firing rate. Exp Brain Res 56: 50-58.

Stratton SE, Lorden JF, Mays LE, Oltmans GA (1988) Spontaneous and harmaline-stimulated purkinje cell activity in rats with a genetic movement disorder. J Neurosci 8: 3327-3336.

Sugihara I, Lang EJ, Llinas R (1995) Serotonin modulation of inferior olivary oscillations and synchronicity: a multiple-electrode study in the rat cerebellum. Eur J Neurosci 7: 521-534.

Takei A, Hamada T, Yabe I, Sasaki H (2005) Treatment of cerebellar ataxia with 5-HT1A agonist. Cerebellum 4(3): 211-215.

Tan HB, Zhong P, Yan Z (2004) Corticotropin-releasing factor and acute stress prolongs serotonergic regulation of GABA transmission in prefrontal cortical pyramidal neurons. J Neurosci 24(21): 5000-5008.

Telgkamp P, Padgett DE, Ledoux VA, Woolley CS, Raman IM (2004) Maintenance of high-frequency transmission at Purkinje to cerebellar nuclear synapses by spillover from boutons with multiple release sites. Neuron 41: 113-126.

Telgkamp P, Raman IM (2002) Depression of inhibitory transmission between Purkinje cells and neurons of the cerebellar nuclei. J Neurosci 22(19): 8447-8457.

Thellung S, Barzizza A, Maura G, Raiteri M (1993) Serotonergic inhibition of the mossy fiber-granule cell glutamate transmission in rat cerebellar slices. Naunyn Schmiedebergs Arch Pharmacol 348(4): 347-351.

Trouillas P (1993) The cerebellar serotoninergic system and its possible involvement in cerebellar ataxia. Can J Neurol Sci suppl 3: S78-82.

Trouillas P, Xie J, Adeleine P (1997) Buspirone, a serotonergic 5-HT1A agonist, is active in cerebellar ataxia. A new fact in favor of the serotonergic theory of ataxia. Prog Brain Res 114: 589-599.

Tsodyks MV, Markram H (1997) The neuroal code between neocortical pyramidal neurons depends on neurotransmitter release probability. Proc Natl Acad Sci 94: 719-723.

Ulrich D, Stricker C (2000) Dendrosomatic voltage and charge transfer in rat neocortical pyramidal cells in vitro. J Neurophysiol 84: 1445-1452.

Varela JA, Sen K, Gibson J, Fost J, Abbott LF, Nelson SB (1997) A quantitative description of short-term plasticity at excitatory synapses in layer 2/3 of rat primary visual cortex. J Neurosci 17: 7926-7940.

Veasey SC, Fornal CA, Metzler CW, Jocobs BL (1995) Response of serotonergic caudal raphe neurons in relation to specific motor activities in freely moving cats. J Neurosci 15: 5346-5359.

Wang LY, Kaczmarek LK (1998) High-frequency firing helps replenish the readily releasable pool of synaptic vesicles. Nature 394(6691): 384-388.

Weis S, Schneggenburger R, Neher E (1999) Properties of a model of ca++-dependent vesicle pool dynamics and short term synaptic depression. Biophys J 77: 2418-2429.

Williams SR (2004) Spatial compartmentalization and functional impact of conductance in pyramidal neurons. Nat Neurosci 7(9): 961-967.

Wolfart J, Debay D, Le Masson G, Destexhe A, Bal T (2005) Synaptic background activity controls spike transfer from thalamus to cortex. Nat Neurosci 8(12): 1760-1767.

Wu LG, Borst JG (1999) The reduced release probability of releasable vesicles during recovery from short-term synaptic depression. Neuron 23: 821-832.

Zhao Y, Klein M (2006) Modulation of the readily releasable pool of transmitter and of excitation-secretion coupling by activity and by serotonin at Aplysia sensorimotor synapses in culture. J Neurosci 22(24): 20671-20679.

Zsiros V, Hestrin S (2005) Background synaptic conductance and precision of EPSP-spike coupling at pyramidal cells. J Neurophysiol 93: 3248-3256.

Zucker RS, Regehr WG (2002) Short-term synaptic plasticity. Annu Rev Physiol 64: 355-405.

Appendix: animal care statement

All animnal procedures followed the guidelines set by the NIH and national law and were approved by the local comitte supervising the handling of experimetnal animals.